

QC852
v. C6
no. 464
ARCHIVE

WINTERTIME LOCAL CIRCULATIONS IN NORTHWESTERN COLORADO



RICHARD L. GRAW

**Colorado
State
University**

**DEPARTMENT OF
ATMOSPHERIC SCIENCE**

PAPER NO. 464



U18401 1577484

WINTERTIME LOCAL CIRCULATIONS IN NORTHWESTERN COLORADO

By

Richard L. Graw

This report was prepared with support provided by National Science
Foundation Grants ATM-8407543, ATM-8519370, ATM-8704776, ATM-8813345
Principal Investigator, Lewis O. Grant
and the Bureau of Reclamation

Department of Atmospheric Science
Colorado State University
Fort Collins, Colorado

May 1990

Atmospheric Science Paper

QC852
.C6
no. 464
ARCHIVE

ABSTRACT OF THESIS

WINTERTIME LOCAL CIRCULATIONS OF NORTHWESTERN COLORADO

Using two months of wintertime meteorological data, surface flows and thermal structure within the Yampa Valley of Northwestern Colorado have been investigated. The primary goals of this study were: 1) describe the climatology of these local circulations, 2) associate synoptic scale weather patterns with regional airflow patterns and 3) present case studies of observed airflow patterns.

Three different procedure were chosen to meet each of the three objectives. A climatological analysis of the two month data set was performed in which statistical methods were used to help define the mean flow and the associated variability. The data set was then stratified into synoptically defined subsets. A climatological analysis was conducted on each subset in which the mean flow and variability were defined. Finally, case studies are presented in which detailed descriptions of the regional flow are shown. One case study is presented for each synoptically defined subset.

Several interesting findings resulted from this research. The climatological analysis of the complete two month wintertime data set revealed interesting horizontal and vertical variations in the airflow existed. The airflow in the portion of the Yampa Valley floor lying east of the topographic constriction between Hayden and Milner remained

decoupled from the flow aloft 80% of the time. West of the constriction, down valley flows occurred most of the time with the exception of early afternoon at which time regional westerly flows extended down to the valley floor. Up valley flows as such did not occur during the study period. Above the valley floor regional westerly flows occurred greater than 90% of the study period.

The synoptic stratification and subsequent climatological analysis of these synoptically defined subsets revealed differing local circulations with each synoptically defined category. Local circulations during periods dominated by a synoptic high pressure system were essentially the same as the local circulations described in the climatological analysis of the entire two month data set. During periods marked by an approaching cold front, the regional flows were stronger and were observed on the western valley floor for longer periods of time than during high pressure periods. The onset of down valley flows did not occur until much later in the evening. After the passage of a cold front, down valley flows were not observed and the valley floor was dominated by regional westerly flows.

The same physical principles operated during each category but the strength of each factor varied with each synoptic category to affect a different local circulation associated with the respective categories. Thus airflow within a high mountain valley is a function of thermally forced pressure gradients and the turbulent mixing of kinetic energy from aloft. The thermally forced pressure gradient is a function of terrain, and the local energy budget. Seasonal variations in precipitation and local terrain will modify the thermally structure of the valley. In this study, the absence of up valley flows may be attributed to the cold

surface associated with unusually heavy snow fall in the upper portion of the Yampa Valley. Synoptic variations in wind speed was the biggest factor affecting the turbulent transfer of kinetic energy. After the passage of a cold front regional westerlies observed throughout the valley floor can be attributed to the strong winds aloft, but during synoptic high pressure systems with weak winds aloft, thermally forced flows are more common within the valley atmosphere.

Richard L. Graw
Atmospheric Science Department
Colorado State University
Fort Collins, Colorado 80523
Spring 1990

ACKNOWLEDGEMENTS

I would like to express my appreciation to a few individuals whose help made my experience at CSU a little more pleasant and more fulfilling. Professor Lew Grant's love for atmospheric science is contagious and inspiring. He is a role model of the applied scientist who I try to mimic each day. Without his guidance and belief in me, I would not have had an opportunity to pursue a career in atmospheric science.

I would also like to express my gratitude to Dr. Dave Rogers and Dr. Randy Borys whose constant encouragement was a source of energy. Dave was always there for my persistent questions with genuine care and technical guidance. Randy encouraged me to reach for my full potential without fear of failure. These two individuals illustrated, through their love of "field work", the fun of science. I will never forget my experiences which I shared with these two at Beaver, Utah and at the Storm Peak Laboratory in Steamboat Springs, Colorado.

Finally, I would like to thank Jan Davis and Lucy McCall for all their support. Jan was very helpful in preparing this manuscript in its final format. Lucy's artistic talents are illustrated throughout this thesis in each figure. But most of all I thank Jan and Lucy for their youthfulness and laughter which always made the office an enjoyable place to be. I am proud to be associated with all of these outstanding individuals.

This research was sponsored by the National Science Foundation. The Bureau of Reclamation provided the PROBE network which was a key component to this analysis.

TABLE OF CONTENTS

I.	INTRODUCTION.....	1
II.	BACKGROUND.....	3
III.	OBJECTIVE.....	14
IV.	DATA BASE.....	16
	A. COLORADO OROGRAPHIC SEEDING EXPERIMENT.....	16
	1. General Purpose.....	16
	2. Location and Topography.....	16
	B. INSTRUMENTATION.....	19
V.	PROCEDURE.....	22
VI.	ANALYSIS AND RESULTS.....	29
	A. CLIMATOLOGICAL CHARACTERISTICS OF VALLEY BOUNDARY LAYER.....	29
	1. Slope Flows.....	29
	2. Valley Flow.....	31
	B. METEOROLOGICAL CONTROLS ON VALLEY BOUNDARY LAYER.....	41
	1. Meteorological Categories.....	41
	2. Airflow for Respective Categories.....	44
	C. CASE STUDIES.....	86
	1. 8 December 1981.....	86
	2. 15 December 1981.....	96
	3. 16 December 1981.....	106
VII.	DISCUSSION AND CONCLUSIONS.....	116

VIII.	APPLICATIONS AND SUGGESTIONS FOR FUTURE RESEARCH.....	122
A.	AIR POLLUTION.....	122
B.	WEATHER MODIFICATION.....	123
C.	SUGGESTIONS FOR FUTURE RESEARCH.....	124
IX.	SUMMARY.....	126
	REFERENCES.....	129
	APPENDIX: STATISTICAL SUMMARY OF WEST TO EAST COMPONENT OF THE HORIZONTAL WIND.....	131

LIST OF TABLES

Table 1. Summary of the mean (for all days during the study period) diurnal variation of the component of the wind parallel to the slope for selected PROBE stations. Elevations are listed in feet. Wind speed units are knots. Standard deviations are listed in parenthesis. All times are Mountain Standard..... 30

Table 2. Overview of air quality aspects of the five synoptic Categories illustrated in Figure 12 (reproduced from Yu and Pielke, 1986)..... 45

Table 3. Listing of synoptic stratification results. Dates and times are listed with the assigned synoptic Category for that time period. Asterisk indicates that weather maps were unavailable for this time period..... 46

Table 4. Summary of the mean (for all days in which synoptic Category #1 was present) diurnal variation of the component of the wind parallel to the slope for selected PROBE stations. Elevations are listed in feet. Wind speed units are knots. Standard deviations are listed in parenthesis. All times are Mountain Standard..... 48

Table 5. Summary of the mean (for all days in which synoptic Category #3 was present) diurnal variation of the component of the wind parallel to the slope for selected PROBE stations. Elevations are listed in feet. Wind speed units are knots. Standard deviations are listed in parenthesis. All times are Mountain Standard..... 61

Table 6. Summary of the mean (for all days in which synoptic Category #4 was present) diurnal variation of the component of the wind parallel to the slope for selected PROBE stations. Elevations are listed in feet. Wind speed units are knots. Standard deviations are listed in parenthesis. All times are Mountain Standard..... 74

LIST OF FIGURES

Figure 1. Schematic illustration of the normal diurnal variations of the air currents in valley.....	6
Figure 2. Schematic illustration of energy to volume relationships between valley and plain.....	8
Figure 3. Typical wind system development at mid morning during inversion breakup.....	10
Figure 4. COSE field program instrumentation network.....	17
Figure 5. Topographic map of PROBE station network. Station names are represented by three letter abbreviations above the dot.....	18
Figure 6. Average west to east component of the wind (knots, shown as wind barbs), average potential temperature (kelvin, shown above the dots), and percent decoupled flow (shown below the dots) at 0700 MST for all days within the study period.....	32
Figure 7. Average vertical profile of potential temperature (kelvin) constructed from selected PROBE station data for all days within the study period.....	34
Figure 8. Average west to east component of the wind (knots, shown as wind barbs), average potential temperature (kelvin, shown above the dots), and percent decoupled flow (shown below the dots) at 1100 MST for all days within the study period.....	36
Figure 9. Average west to east component of the wind (knots, shown as wind barbs), average potential temperature (kelvin, shown above the dots), and percent decoupled flow (shown below the dots) at 1400 MST for all days within the study period.....	38
Figure 10. Average west to east component of the wind (knots, shown as wind barbs), average potential temperature (kelvin, shown above the dots), and percent decoupled flow (shown below the dots) at 1700 MST for all days within the study period.....	39
Figure 11. Average west to east component of the wind (knots, shown as wind barbs), average potential temperature (kelvin, shown above dots), and percent decoupled flow (shown below the dots) at 2200 MST for all days within the study period.....	40

Figure 12. Example of a surface analysis chart (for January 9, 1964) showing the application of the synoptic climatological model for the five synoptic classes listed in Table 2.....	43
Figure 13. Monthly averaged frequencies of occurrences of each synoptic climatological category during the study period.....	47
Figure 14. Average west to east component of the wind (knots, shown as wind barbs), average potential temperature (kelvin, shown above the dots), and percent decoupled flow (shown below the dots) at 0700 MST for all days in which synoptic Category #1 was present.....	50
Figure 15. Average vertical profile of potential temperature (kelvin) constructed from selected PROBE station data for all days in which synoptic Category #1 was present.....	53
Figure 16. Average west to east component of the wind (knots, shown as wind barbs), average potential temperature (kelvin, shown above the dots), and percent decoupled flow (shown below the dots) at 1100 MST for all days in which synoptic Category #1 was present.....	54
Figure 17. Average west to east component of the wind (knots, shown as wind barbs), average potential temperature (kelvin, shown above the dots), and percent decoupled flow (shown below the dots) at 1400 MST for all days in which synoptic Category #1 was present.....	56
Figure 18. Average west to east component of the wind (knots, shown as wind barbs), average potential temperature (kelvin, shown above the dots), and percent decoupled flow (shown below the dots) at 1700 MST for all days in which synoptic Category #1 was present.....	58
Figure 19. Average west to east component of the wind (knots, shown as wind barbs), average potential temperature (kelvin, shown above the dots), and percent decoupled flow (shown below the dots) at 2200 MST for all days in which synoptic Category #1 was present.....	60
Figure 20. Average west to east component of the wind (knots, shown as wind barbs), average potential temperature (kelvin, shown above the dots), and percent decoupled flow (shown below the dots) at 0700 MST for all days in which synoptic Category #3 was present.....	63
Figure 21. Average vertical profile of potential temperature (kelvin) constructed from selected PROBE station data for all days in which synoptic Category #3 was present.....	65
Figure 22. Average west to east component of the wind (knots, shown as wind barbs), average potential temperature (kelvin, shown above the dots), and percent decoupled flow (shown below the dots) at 1100 MST for all days in which synoptic Category #3 was present.....	67
Figure 23. Average west to east component of the wind (knots, shown as wind barbs), average potential temperature (kelvin, shown above the dots), and percent decoupled flow (shown below the dots) at 1400 MST for all days in which synoptic Category #3 was present.....	69

Figure 24. Average west to east component of the wind (knots, shown as wind barbs), average potential temperature (kelvin, shown above the dots), and percent decoupled flow (shown below the dots) at 1700 MST for all days in which synoptic Category #3 was present..... 70

Figure 25. Average west to east component of the wind (knots, shown as wind barbs), average potential temperature (kelvin, shown above the dots), and percent decoupled flow (shown below the dots) at 2200 MST for all days in which synoptic Category #3 was present..... 72

Figure 26. Average west to east component of the wind (knots, shown as wind barbs), average potential temperature (kelvin, shown above the dots), and percent decoupled flow (shown below the dots) at 0700 MST for all days in which synoptic Category #4 was present..... 76

Figure 27. Average vertical profile of potential temperature (kelvin) constructed from selected PROBE station data for all days in which synoptic Category #4 was present..... 78

Figure 28. Average west to east component of the wind (knots, shown as wind barbs), average potential temperature (kelvin, shown above the dots), and percent decoupled flow (shown below the dots) at 1100 MST for all days in which synoptic Category #4 was present..... 80

Figure 29. Average west to east component of the wind (knots, shown as wind barbs), average potential temperature (kelvin, shown above the dots), and percent decoupled flow (shown below the dots) at 1400 MST for all days in which synoptic Category #4 was present. M=missing data..... 81

Figure 30. Average west to east component of the wind (knots, shown as wind barbs), average potential temperature (kelvin, shown above the dots), and percent decoupled flow (shown below the dots) at 1700 MST for all days in which synoptic Category #4 was present..... 83

Figure 31. Average west to east component of the wind (knots, shown as wind barbs), average potential temperature (kelvin, shown above the dots), and percent decoupled flow (shown below the dots) at 2200 MST for all days in which synoptic Category #4 was present..... 85

Figure 32a. 500 mb upper level map depicting synoptic conditions of December 8, 1981 at 0500 MST..... 87

Figure 32b. 700 mb upper level map depicting synoptic conditions of December 8, 1981 at 0500 MST..... 88

Figure 32c. Surface map depicting synoptic conditions of December 8, 1981 at 0500 MST..... 89

Figure 33. PROBE wind histories for 7 December 1981 at 1900 MST through 8 December 1981 at 1800 MST..... 90

Figure 34. Potential temperature (kelvin) for selected PROBE stations [STP (10330 feet), BLK (9900 feet), HAR (7380 feet) and DIV (7130 feet)] from 7 December 1981 at 1900 MST to 8 December 1981 at 1800 MST.....	91
Figure 35. Vertical profile of potential temperature (kelvin) constructed from selected PROBE station data for 7 December 1981 at 1700 MST and 2200 MST to 8 December 1981 at 0700 MST, 1100 MST and 1400 MST. This time period is representative of synoptic Category #4.....	93
Figure 36. Time series of potential temperature (kelvin) for selected PROBE stations along the valley floor. Elevations are listed on the ordinate in feet (ASL). Distances west of the Barrier are listed along the abscissa in miles; the Barrier is located on the far right. Five hourly values are shown from 1700 MST on 7 December 1981 to 1400 on December 8 1981.....	95
Figure 37a. 500 mb upper level map depicting synoptic conditions of 15 December 1981 at 1700 MST.....	97
Figure 37b. 700 mb upper level map depicting synoptic conditions of 15 December 1981 at 1700 MST.....	98
Figure 37c. Surface map depicting synoptic conditions of 15 December 1981 at 1700 MST.....	99
Figure 38. PROBE wind histories for 14 December 1981 at 1700 MST through 15 December 1981 at 1700 MST.....	101
Figure 39. Potential temperature (kelvin) for selected PROBE stations [(STP (10330 feet), BLK (9900 feet), HAR (7380 feet) and DIV (7130 feet)] from 14 December 1981 at 1700 MST to 15 December 1981 at 1700 MST.....	102
Figure 40. Vertical profile of potential temperature (kelvin) constructed from selected PROBE station data for 14 December 1981 at 1700 MST and 2200 MST to 15 December 1981 at 0700 MST, 1100 MST and 1400 MST. This time period is representative of synoptic Category #1.....	104
Figure 41. Time series of potential temperature (kelvin) for selected PROBE stations along the valley floor. Elevations are listed on the ordinate in feet (ASL). Distances west of the Barrier are listed along the abscissa in miles; the Barrier is located on the far right. Five hourly values are shown from 1700 MST on 14 December 1981 to 1400 MST on 15 December 1981.....	105
Figure 42a. Surface map depicting synoptic conditions of 16 December 1981 at 0200 MST.....	107
Figure 42b. 700 mb upper level map depicting synoptic conditions of 16 December 1981 at 0200 MST.....	108

Figure 42c. 500 mb upper level map depicting synoptic conditions of 16 December 1981 at 0200 MST.....109

Figure 43. PROBE wind histories for 15 December 1981 at 1800 MST through 16 December 1981 at 1700 MST.....111

Figure 44. Potential temperature (kelvin) for selected PROBE stations (STP (10330 feet), BLK (9900 feet), HAR (7380 feet) and DIV (7130 feet)) from 15 December 1981 at 1700 MST to 16 December 1981 at 1700 MST.....112

Figure 45. Vertical profile of potential temperature (kelvin) constructed from selected PROBE station data for 15 December 1981 at 2200 MST to 15 December 1981 at 0700 MST, 1100 MST, 1400 MST and 2200 MST. This time period is representative of synoptic Category #3.....113

Figure 46. Time series of potential temperature (kelvin) for selected PROBE stations along the valley floor. Elevations are listed on the ordinate in feet (ASL). Distances west of the Barrier are listed along the abscissa in miles; the Barrier is located on the far right. Five hourly values are shown from 2200 MST on 15 December 1981 to 1700 MST on 16 December 1981.....114

I. INTRODUCTION

As the world population continues to grow, ever increasing numbers of people will inhabit mountainous regions. For many mountain towns, specifically in the Colorado Rockies, tourism and ranching are two major economic sources. Local weather, particularly a winter storm which can deposit several feet of snow during one event, is a concern to ranchers, motorists, and skiers. In addition, the quality of life within the Rockies is potentially threatened by coal burning power plants, auto emissions, wood burning stoves and fireplaces; all which add to an ever increasing air pollution problem. Unfortunately, public weather forecasts are focused upon synoptic scale events, not upon mesoscale phenomenon such as those listed above. Thus a need arises to forecast local pollution episodes, orographic storms, and other such local weather phenomenon.

However, before one can forecast such events, an understanding of the controlling factors must be grasped. This thesis presents an investigation of one of these factors, the local circulations of the Yampa Valley of Northwestern Colorado. It focuses upon the local winds and thermal structure as observed by a network of 24 automated surface weather stations located in the valley and on the adjacent peaks and ridges. A climatological summary of the wind and temperature structure is presented for the two-month study period in which diurnal trends were examined. Then the data set is stratified into synoptically defined subsets in which a climatological analysis is performed on each. Finally, three case

studies are presented, one for each synoptically defined subset. The first case focuses upon the valley circulations during a period dominated by a synoptic high-pressure system. The second case study is used to illustrate surface flows during a period marked by an approaching cold front. The third case study is used to demonstrate surface flows immediately after the passage of a cold front. A discussion of the relevant findings are then presented as they relate to previous studies. Suggestions are made for future research, as well as suggestions for air pollution and weather modification applications.

II. BACKGROUND

Early works in the study of local circulations in mountain valleys were reported by Burger and Ekhardt (1937), who focused on the Austrian Alps, and in separate studies along the east slope of the Rocky Mountains, by Wagner (1938) and Ekhardt (1940). Defant (1951) summarized observations from Austria's Inn Valley with the following theoretical model. Under weak gradient conditions at the synoptic scale, local flows were observed. The first of the local flows described is the thermal slope wind, which air rises due to a temperature difference between the air over the inclined slope and the air over the adjacent valley floor, at the same elevation. Soon after sunrise the air over the inclined slope, with this flow type, begins to warm, creating a relative area of low pressure. This drives an upslope wind with an average velocity of 2-4 m/s and 100-200 m thick, according to measurements. These flows are especially well developed on the southern slopes because of the stronger insolation, and are weaker or almost nonexistent on northern slopes. Shortly after sunset, a reversal in flow occurs producing the less intense downslope wind.

Mountain and valley winds blow parallel to the valley axis. Beginning about 0900 LT the wind blows up the valley axis, continuing after sunset. It reaches its maximum intensity approximately at 1500 LT, about the time of maximum temperature. At night, the air drains down the valley axis and continues after sunrise, referred to as the mountain wind.

These winds are best developed during the summer months on clear, synoptically weak gradient days. Defant, following Wagner, explained valley winds as being thermally forced. Observations of diurnal temperature ranges over the valley were more than twice as large as diurnal temperature ranges over the adjacent plain. As a consequence, a horizontal pressure gradient is established toward the valley during the day and away from the valley at night.

In his own work, Defant (1951) explained the interaction between the mountain valley and slope winds, as illustrated in Figure 1. The theory behind this interaction is based upon Prandtl's (1942) discussion of turbulent heat conduction and turbulent friction. Defant's model is a generalized working model but as discussed by Whiteman (1980) several researchers have found only parts of this model apply to their particular valleys of study.

Vergeiner and Drieseitl (1987) make several alterations to Defant's model. After their studies in Austria's Inn Valley, they redefined slope winds as spontaneous and intermittent, not continuous, but rather a succession of thermal bubbles. Secondly, and of primary significance to this paper, they discussed seasonal variations of these thermally forced flows. They observed in winter, drainage of cold air out of the valley was the seasonal norm, as opposed to summer when cold air drainage primarily occurred during the late night and early morning hours. They also recognized Steinacker (1984) as the first to adequately explain how valley winds are a function of pure geometry. Comparing a column of air over a mountain valley and a column of air over a plain surface, the column over the plain has a greater volume than the column over the mountain valley. The mountain slopes and ridges occupy the difference in

Fig. 1. Schematic illustration of the normal diurnal variations of the air currents on a valley. (After F. Defant)

(a) Sunrise; onset of upslope winds (white arrows), continuation of mountain wind (black arrows). Valley cold, plains warm.

(b) Forenoon (about 0900); strong slope winds, transition from mountain wind to valley wind. Valley temperature same as plains.

(c) Noon and early afternoon; diminishing slope winds, fully developed valley wind. Valley warmer than plains.

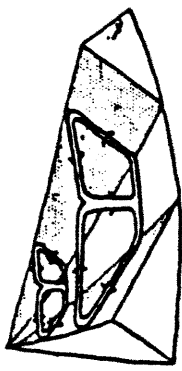
(d) Late afternoon; slope winds have ceased, valley wind continues. Valley continues warmer than plains.

(e) Evening; onset of downslope winds, diminishing valley wind. Valley only slightly warmer than plains.

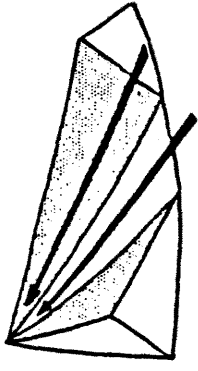
(f) Early night; well-developed downslope winds, transition from valley wind to mountain wind. Valley and plains at same temperature.

(g) Middle of night; downslope winds continue, mountain wind fully developed. Valley colder than plains.

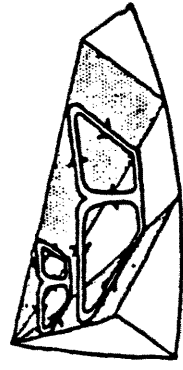
(h) Late night to morning; downslope winds have ceased, mountain wind fills valley. Valley colder than plains.



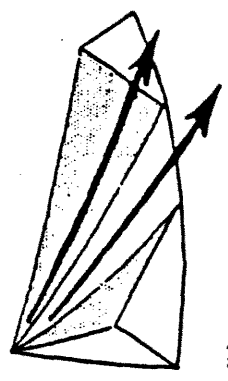
(b)



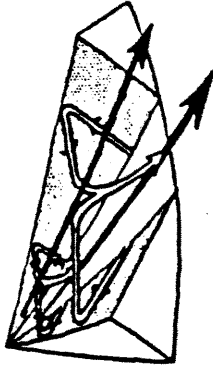
(d)



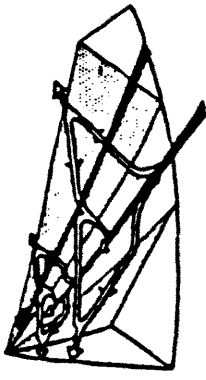
(e)



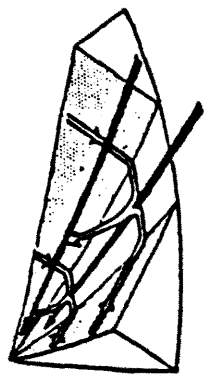
(h)



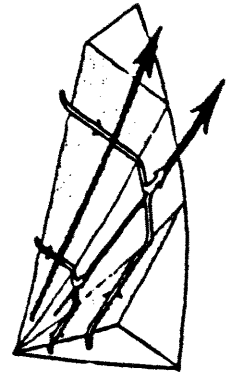
(a)



(c)



(e)



(g)

volume (see Figure 2). The difference in diurnal temperature range is not only due to less volume of air to heat and cool through sensible processes by the surface of the column but also the valley has the added advantage of the slope surfaces also providing sensible heating and cooling.

Regional flows are forced by large scale pressure gradients but modified by the terrain and atmospheric stability. Regional flows are frequently observed at levels below the blocking level of the continental divide but typically lie above the more stable layers in the valley below. In wintertime, the valley atmosphere is frequently stably stratified and blocked flows often result; this exemplifies one type of regional flow. Specifically, the barrier obstructs the flow, but only horizontal deflection occurs in the stable atmosphere.

Synoptic flows are associated with large scale pressure gradients and are identified as free atmospheric flows as distinct from flows primarily originating from or controlled by the underlying terrain.

Temperature inversions are a phenomenon frequently observed in mountain valleys and are primarily responsible for the trapping of a haze layer within these valleys. Whiteman (1980) investigated the cause for the buildup and destruction of temperature inversions in seven Colorado mountain valleys in all seasons. He concluded that the sensible heat flux from the valley surface provides the energy to cause the growth of the convective boundary layer (CBL). As the CBL grows, mass is removed from the base of the inversion layer provided by the diverging upslope flows. This allows the inversion layer to sink and warm. Whiteman (1981) cited similar mechanisms for the buildup of temperature inversions in Colorado mountain valleys. Soon after the time of maximum solar insolation, cooler downslope flows converge at the valley bottom. If the air does not drain

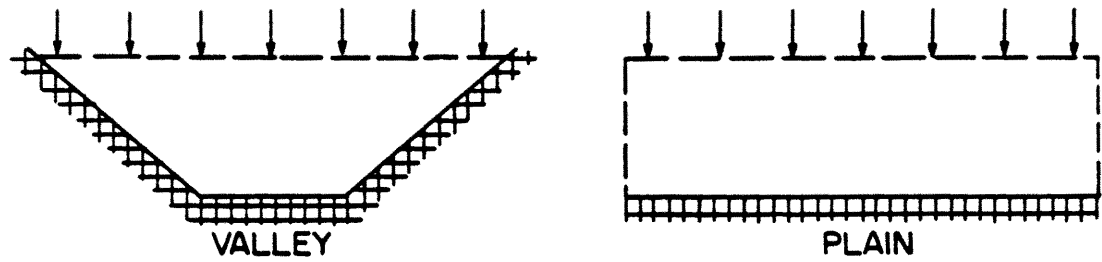


Figure 2. Schematic illustration of energy to volume relationships between valley and plain.

out the valley, it becomes trapped, building a cool stagnant layer of air, the top of which marks the top of the inversion layer.

Whiteman also presented a conceptual model which described five distinct layers of airflow within the valley environment (see Figure 3) during inversion breakup. The five layers include the gradient wind, the incline wind, the stable core, the slope wind, and the valley floor wind. These winds were observed from tether soundings in which a wind shift in speed and direction is correlated with a unique vertical sector of the temperature sounding. The gradient wind responds to synoptic scale pressure gradients. The along-incline wind is a local, diurnally forced wind that blows up and down the mesoscale slope of a mountain range. The along-valley wind system is also local and diurnally forced. It blows up and down the valley axis in the central region of the valley volume. The along-floor wind system is a diurnal wind system that blows up or down the valley in a shallow boundary layer over the valley floor. The slope wind is a diurnal wind system that blows up or down the valley sidewalls in a boundary layer that forms above them.

Not only is temperature structure (specifically, the change of temperature as a function of height) important for trapping inversions but also is related to valley flows as explained. "Blocking is a process in which air can neither go over nor go around because it is too stable and the terrain feature too elongated, the influence of the mountain propagates rapidly upwind" (Pielke, 1984). Blocking will occur when a critical Froude number, F_c , is exceeded.

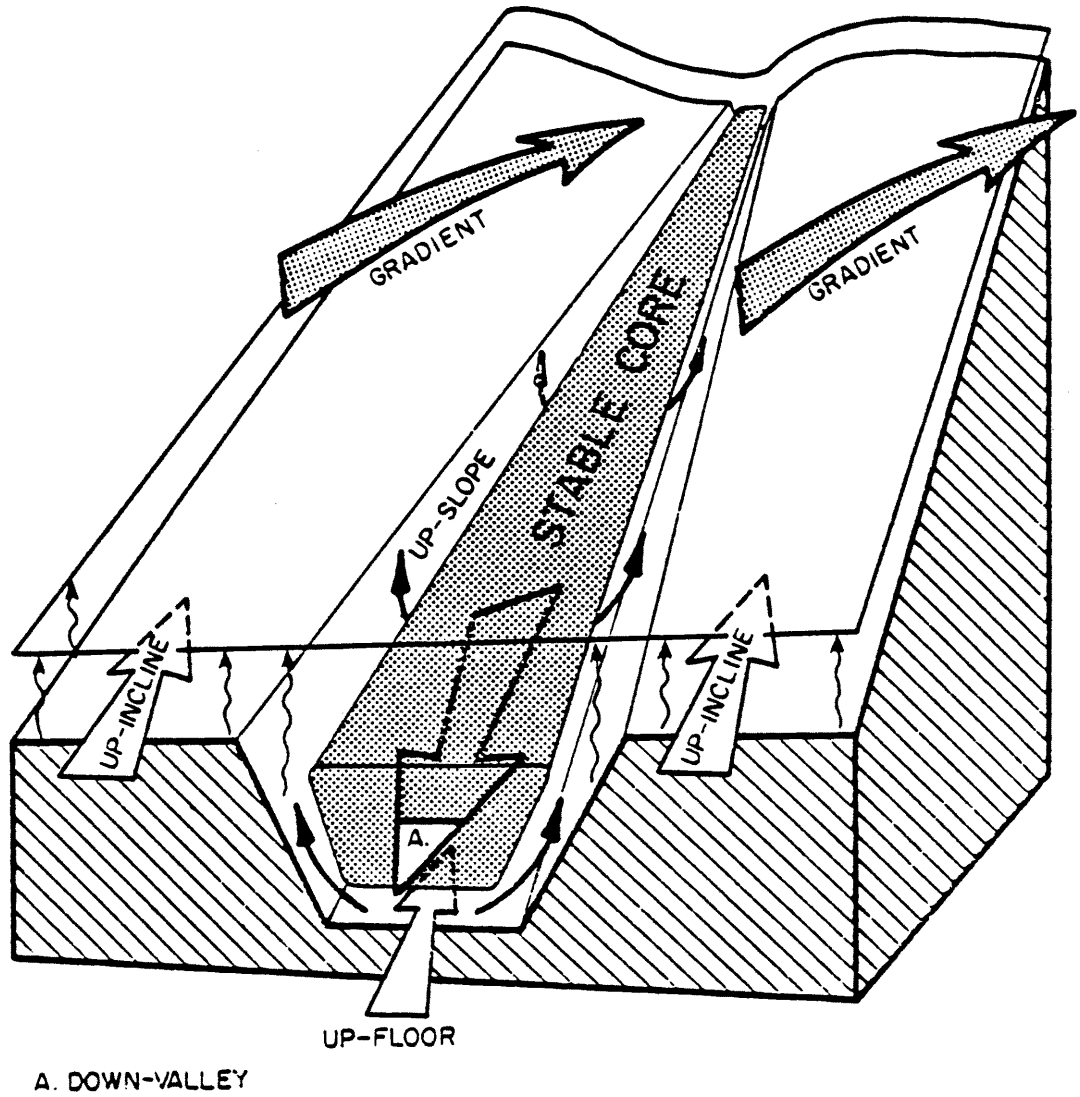


Figure 3. Typical wind system development at mid morning during inversion breakup.

$$F = U / (gH\Delta\theta/\theta_r)^{1/2}$$

F = Froude number

U = upstream ambient wind

g = gravitational acceleration

H = height of the ridge above the upstream surface

θ_r = a representative potential temperature

$\Delta\theta$ = change in air temperature from near surface to above ridge height upwind of the ridge

The square of the Froude number expresses the relative magnitudes of kinetic energy of the ambient wind to potential energy change required to lift a parcel from near the surface to a height to clear the ridge. If this ratio is larger than a critical Froude number (F_c) then the stagnant airmass within the valley will be dynamically swept out. If the ratio is less than F_c , then blocking will occur. The critical Froude number is determined by empirical study of each individual valley.

Manins and Sawford (1982) studied upwind blocked flows in the Latrobe Valley of Southeastern Australia in which they observed a critical Froude number of 1.6. They also were unable to correlate the height of the blocked layer to the Froude number as was hoped. They identified the blocked layer to exist as one of four distinct layers within the valley environment. In the lowest 20 m they observed katabatic flows. Above this layer, extending up to 80 m was the blocked flow layer. Interestingly, the flow was not calm but actually had a katabatic component to it, which the authors suggested as being turbulently influenced by the katabatic layer below. Above the region of blocked flow existed the sweeping region from 80 m (ridge tops were at 100 m) to 160

m. This layer was defined by its transition to the ambient layer in which wind speeds gradually increased to ambient speeds, wind direction gradually transitioned from blocked to ambient direction, and the virtual potential temperature gradient steadily weakened. Above this sweeping region, ambient conditions existed beyond 160 m above the valley floor, 60 m above ridge tops.

Several numerical studies have been conducted to investigate the complex interactions within the mountain valley. Manins and Sawford (1978) employed a hydraulic approach to develop a model of katabatic winds. It emphasizes the importance of mixing between the ambient and cooled layers. Whiteman (1980) attempted to numerically simulate the breakup of temperature inversions in his Colorado mountain valleys with some success. Bader (1985) using a two and three dimensional model was also somewhat successful at reproducing the development of the mesoscale boundary layer for a western Colorado valley. He noted the significance of a synoptic scale wind field which provided the necessary shearing to deepen the nocturnal boundary layer. McNider and Pielke (1984) simulated slope and mountain flows using a three dimensional model and compared it with actual observations from an existing data set with qualitative success. Counter to intuition, their model showed that cooling of the valley atmosphere occurred due to upward vertical motion over the center of the valley, not due to direct downslope flow from the slopes. Also stressed, was the importance of turbulence in reproducing the dynamics of flows in mountain valleys.

The occurrence of thermally forced flows within mountain valleys is typically a phenomenon of clear, synoptically weak gradient conditions. Vergeiner and Driesietl studied the variability of these flows under all

synoptic conditions. They only observed mountain valley flows 43% of the time under weak gradient flows and only 29% of the time for all days. However, the method of synoptic classification used by Vergeiner and Driesietl was based solely upon observed wind direction and speed, ignoring other such factors as stability and cloud cover. Perhaps a more encompassing synoptic classification system based upon the relative position within an extratropical cyclone is presented by Yu and Pielke (1986) which is based upon the work of Lindsey (1980). It relates predominate mesoscale phenomenon to synoptics. A detailed explanation of this system is presented later within this paper.

To date, this author was not able to find any description of flows within mountain valleys during periods when thermally forced slope and valley flows were not observed with the exception of Marwitz (1980). He described the flow as it evolved through four distinct stages during a winter storm in the San Juan Mountains of Southern Colorado. Each stage was related to thermodynamic stability. "The stages in sequence are stable, neutral, unstable, and dissipation. During the stable stage, much of the flow below mountain top level is blocked and diverted away from the barrier. During the neutral stage, the storm is deep; it typically extends throughout much of the troposphere. During the unstable stage, a zone of horizontal convergence appears to form near the surface at the base of the mountain on the upwind side and a convective cloud line is often present over this convergence zone. Subsidence at mountain top height causes dissipation."

III. OBJECTIVE

The objective of this study is to better understand airflows in a high mountain valley. This objective is divided into three categories: 1) describe the climatology of these local circulations, 2) associate synoptic scale weather patterns with regional airflow patterns and 3) present case studies of observed airflow patterns.

In order to enhance the general characterization of local circulations in a high mountain valley, the climatology must be described in detail. To achieve this goal, descriptions of the mean slope and valley flow must be addressed. Variations of these flows should also be stated. To enhance the description further, spatial and temporal characteristics of these regional flows must be depicted, including descriptions of decoupled flows between the valley air and the atmosphere immediately above.

Once the climatology is described adequately, the objective is to stratify the data set such that a physical understanding of these flows is possible. This objective is focused further by concentrating on interactions of scales of motion, specifically, the relationship between regional airflow patterns and the synoptic scale meteorological patterns. The goal is to illustrate any relationship between these two scales of motion, within the confinements of the available data set. With good fortune, this work will lead to identifying a predictive indicator in the

synoptic scale atmosphere such that details of the valley airflow can be more accurately forecast.

More precise relationships can be observed in specific examples than in the climatology, hence the need for case studies. The increase in precision can be attributed to variability. Variability is greatly reduced when examining one day of data compared to the variability that occurs during several weeks. Hence, the goal is to examine and describe specific case studies of airflow in a high mountain valley, one for each type of synoptic scale weather pattern that occurs. In this manner, physical relationships between the different scales of motion may appear more readily than in the climatological analysis.

In addition to an enhanced understanding of regional flows in a high mountain valley, the investigation is intended to have several practical applications. Applications of this study pertain to the transport of point source releases in complex terrain. These sources may include artificial nuclei from ground based cloud seeding generators or particulates introduced from wood burning fireplaces and stoves. After reading this thesis, the reader should be able to answer such questions as 1) Where is the best location for ground based cloud seeding generators for effective transport to cloud? 2) Under what meteorological conditions, if any, should regulations regarding the banning of wood burning stoves be enforced? Etc...

IV. DATA BASE

A. COLORADO OROGRAPHIC SEEDING EXPERIMENT

1. General Purpose

The third Colorado Orographic Seeding Experiment (COSE III) was conducted during the winter of 1981-1982, as part of a continuing study of the clouds in the Northern Colorado River Basin. The specific objectives of experiment were to : 1) Describe the microphysical processes governing the growth and development of precipitation in northern Colorado orographic systems. 2) Quantitatively define the dispersion and transport of seeding materials in complex terrain. 3) Identify atmospheric covariants (predictors) needed for analyses of weather modification programs. 4) Establish a baseline for air quality measurements in the Yampa Valley. The project was conducted during the months of December, 1981 and January, 1982, although some measurements were taken during February, 1982. This particular study concentrated on the second of these objectives: quantitative description of the dispersion and transport of seeding materials in complex terrain.

2. Location and Topography

COSE III was carried out in the Yampa Valley of northwestern Colorado. The Yampa Valley is essentially an east-west valley, extending some 44 miles westward from the Park Range (see Figures 4 and 5). It varies in width from approximately 0.5 miles to 20 miles with an average width of about 12.5 miles. The Park Range, at the head of the valley,

COSE FIELD PROGRAM INSTRUMENTATION DEC 81-JAN 82

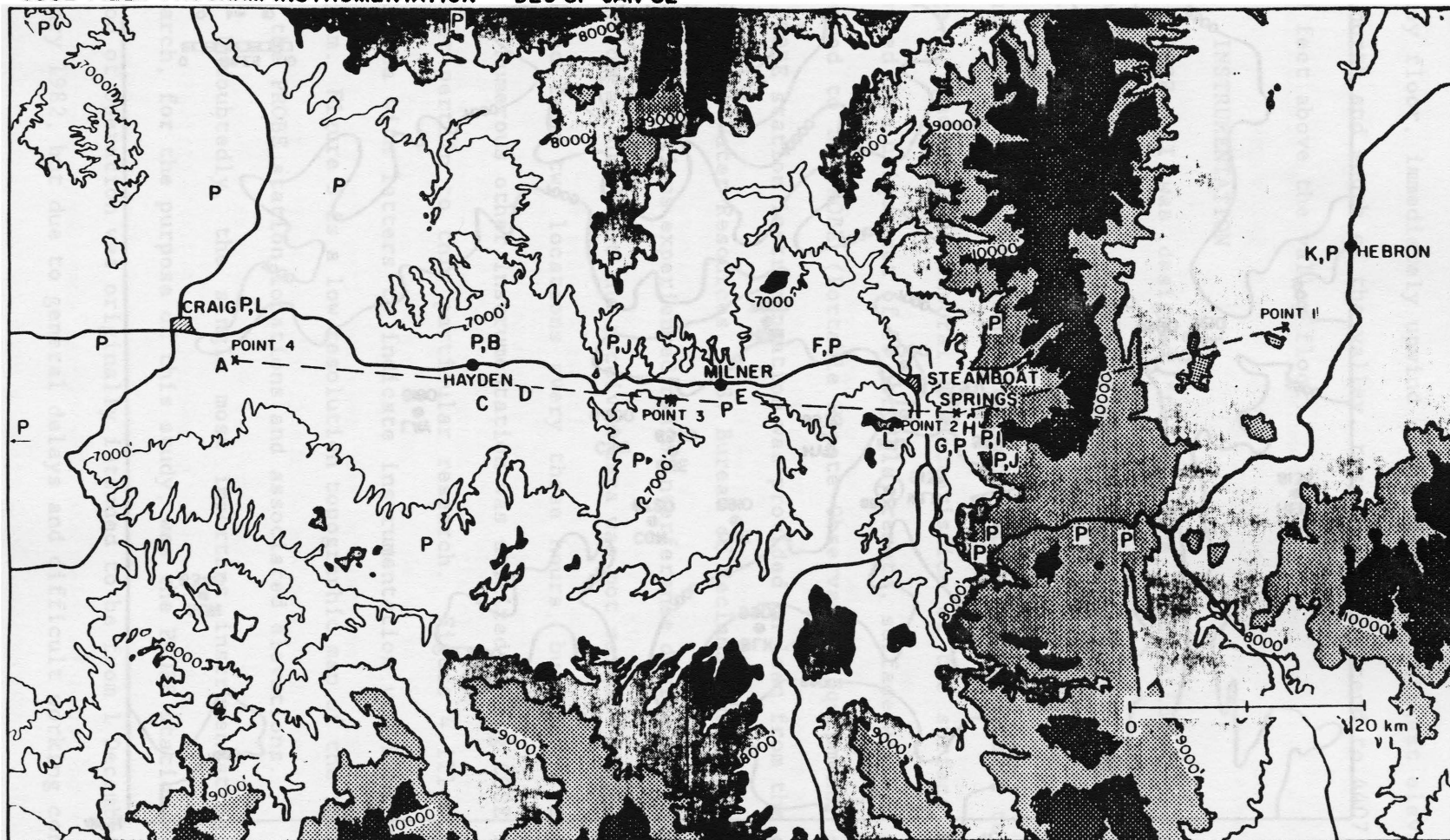


Figure 4. COSE field program instrumentation network.

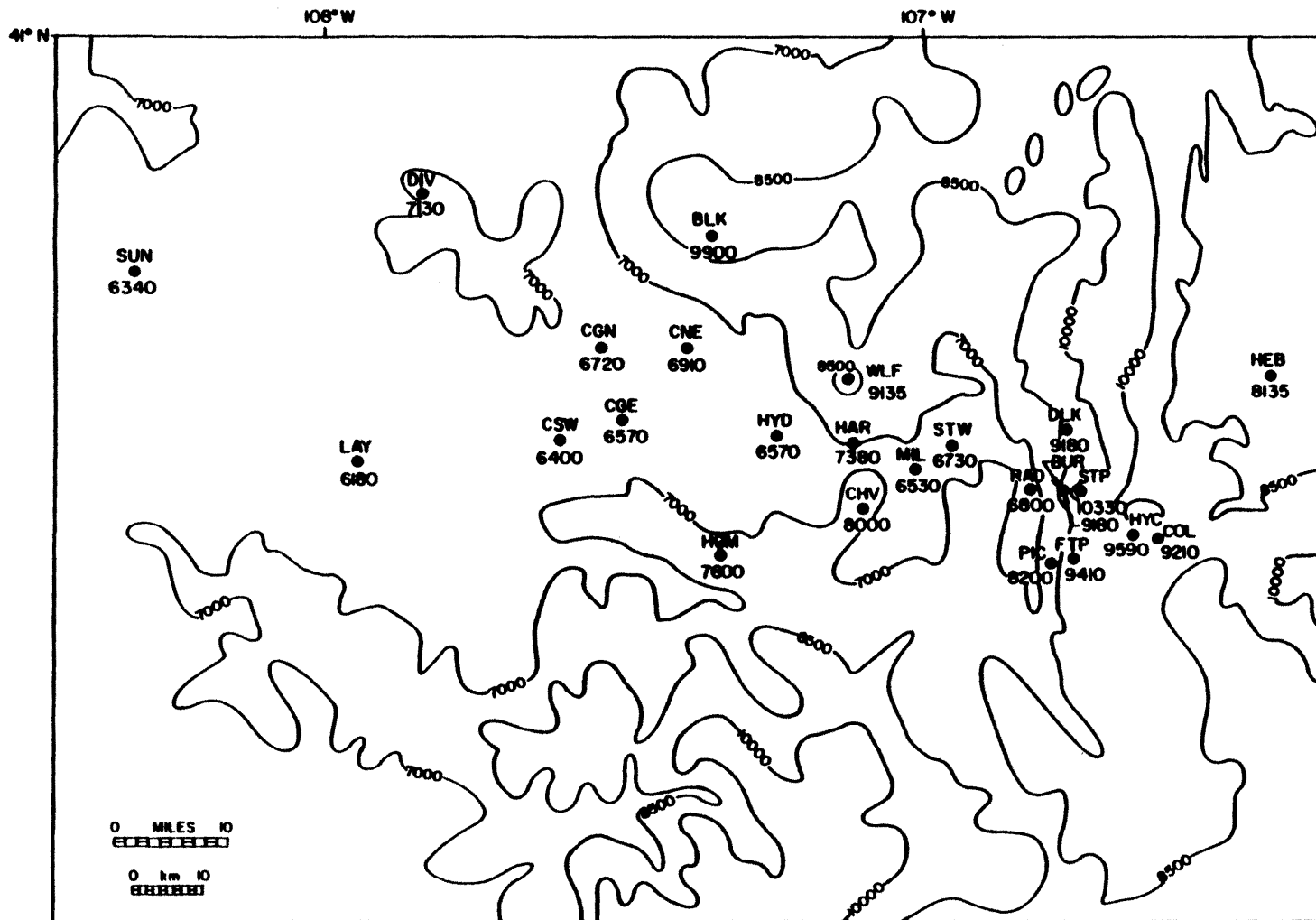


Figure 5. Topographic map of PROBE station network. Station names are represented by three letter abbreviations above the dot.

extends to about 11,000 feet above sea level, some 4755 feet above the valley floor, immediately upwind of the barrier. Highest elevations to the north and south of the valley, respectively, extend to 4407 feet and 5569 feet above the valley floor.

B. INSTRUMENTATION

COSE III was designed "to maximize information concerning the changes which occur in cloud systems as air passes over a mountain barrier". To achieve this goal effectively, instrumentation was installed along an west-east line along the Yampa Valley, perpendicular to the Park Range. Spacial and temporal characteristics of the surface flow were measured by a unique set of 25 portable, remote, surface weather stations, referred to as PROBE (Portable Remote Observation Equipment) stations. The PROBE station instrumentation was provided on loan from the office of Atmospheric Water Resources, U.S. Bureau of Reclamation. Unfortunately, one of the stations experienced radio interference during the transmission of the data, such that the received data was not valid. Rawinsondes were launched from two locations every three hours, but during experiments only. Numerous other instrumentation was utilized during COSE III which did not pertain to this particular research. Figure 4 illustrates the COSE area with letters to indicate instrumentation utilized during the program. Figure 5 is a low resolution topographic map of the Yampa Valley with the PROBE station locations and associated elevations.

Undoubtedly, the single most important instrumentation in this research, for the purpose of this study, was the PROBE station data. The period of operation was originally intended to be from 1 December 1981 to January 1982, but due to general delays and difficult working conditions,

it was 10 December before the entire array of stations was operational. The PROBE network was located throughout the valley and on the adjacent slopes and ridges. It extended 100 miles east-west and 31 miles north-south, yielding an average spacial density of one station for every 124 square miles or 11 mile spacing.

The PROBE array was designed to fulfill a number of objectives including: 1) classification of surface airflow for use in diffusion, transport, and local circulation studies; 2) precipitation measurements for verification of conceptual and numerical models; 3) pressure measurements to verify existence of certain dynamical factors; 4) temperature measurements for the study of radiatively induced flows. The performance of the network was considered excellent for the extreme conditions encountered. For a rough evaluation of station performance, refer to the PROBE station summaries in the COSE III Operation Log compiled by Rauber and Grant (1982), Colorado State University.

Measurements of pressure, temperature, humidity, winds and precipitation were made every fifteen minutes for a five minute average. Pressure was recorded with a pressure transducer located in the DCP housing at three to six feet above the ground. Pressure was accurate only to within ± 3 or 4 mb as limited by the accuracy of the calibration procedure. Temperature was measured five to six feet AGL with a thermistor; accuracy was within $\pm 1.0^{\circ}\text{C}$, determined by laboratory testing of the thermistor. Humidity was measured with a humidity capacitor in which the capacitance was converted to 0-100 millivolts to represent relative humidity. This too was located at five to six feet AGL. Winds were recorded in speed and directional components then converted to the u and v components. Most sensors were placed sixteen feet AGL, but in

areas where expected heavy snowfall and accumulation was anticipated, sensors were placed 20 - 30 feet AGL. Winds were measured with an anemometer and wind vane. Precipitation was measured using a Belfort weighing bucket which varied in height between three and seven feet above the ground, depending on how much snow accumulation was expected at each site.

Potential temperature was a calculated parameter computed from two measured parameters; temperature and pressure. Equation 2 shows the relationship between temperature, pressure, and potential temperature.

$$\theta = T \left(1000 \text{ mb} / P \text{ mb} \right)^{0.286} \quad (2)$$

where

θ = Potential temperature (kelvin)

T = Temperature (kelvin)

P = Pressure

Given a realistic temperature range between -30°C and 15°C and varying the pressure by ± 4 mb, the potential temperature can be considered accurate to a little better than $\pm 1.0^{\circ}\text{K}$.

V. PROCEDURE

There are three stages within this investigation. In sequence, they are 1) a climatological analysis of the two month data set, 2) a climatological type analysis of synoptically defined subsets of the complete data set and, 3) case study analysis of synoptically defined subset airflow patterns. Within the climatological analysis, statistical methods are utilized to help define the mean flow and the associated variability. The data set is then stratified into subsets. Each subset is associated with a region within an extratropical cyclone. The association between regional airflow and synoptic scale meteorological conditions is investigated using the same analysis techniques utilized in the climatological analysis. Finally, case studies are included in which detailed descriptions of the air flows are presented. One case study is presented for each synoptically defined subset of the extratropical cyclone.

For ease of discussion, the PROBE network is divided into six different regions containing specific stations within the study area. Grouping the stations allows one to utilize the most appropriate station locations to observe specific airflows including: slope flows, valley flows, barrier effects, and effects of elevation and exposure. The criteria used to group the PROBE station network is chosen to take advantage of the west to east orientation of the valley axis and the existing format of the data.

The criteria for selecting PROBE stations for use in investigating slope flows is as follows. First, the orientation of the slope must be perpendicular to the valley axis in order to easily distinguish between a valley and a slope flow. This also minimizes the amount of data processing necessary. Second, the station must lie on a slope and not lie on top of a ridge in order to eliminate the confusion of determining the individual effect of each slope on the slope flow. In addition, this criteria minimizes the ambiguities that may arise due to the expected enhanced turbulence in these regions. The orientation of the slope must be closely aligned to either north-south or east-west in order to minimize the amount of data processing necessary. Two of the PROBE stations meet these criteria, LAY (6180 ft) and HYD (6570 ft) are the stations used to investigate slope flows and are referred to as slope stations.

To investigate valley flows, the valley is divided into three horizontal categories. The valley is divided into Down Valley, Middle Valley, and Upper Valley. Down Valley is defined as that portion of the Yampa Valley that lies far enough west such that the difference in elevation between the valley floor and the adjacent slopes and ridges is less than 1000 feet. This describes the area west of Craig. Down valley stations may be further divided into those stations where the river valley axis lies west to east and those stations where the river valley axis is not well defined. Those stations lying where the river flows east to west include LAY (6180 ft) and CSW (6400 ft). Stations in the Down Valley where the valley axis is not as well defined include SUN (6340 ft) and DIV (7130 ft).

The Middle Valley is defined as that portion of the valley west of the constriction in width between Hayden and Milner that is surrounded by

adjacent peaks and ridges which rise greater than 1000 feet above the valley floor. Middle valley stations may be further divided into those stations where the river valley axis lies west to east and those stations where the river valley axis is not well defined. Stations located in this region in which the valley axis clearly lies east to west include HYD (6570 ft) and CGE (6570 ft). Stations located in this region of the valley where the valley axis is not as well defined include CNE (6910 ft) and CGN (6720 ft). In addition, two stations in the Middle Valley lie above the valley floor, one on the ridge to the north, BLK (9900 ft) and one on a smaller ridge to the south, HGM (7600 ft).

There are three stations that lie on the slopes and ridges near the constriction in width between Hayden and Milner. Unfortunately, there are no station measurements on the valley floor within this constriction in width. HAR (7380 ft) and WLF (9135 ft) lie on the north side of the valley, and CHV (8000 ft) lies on the south side of the valley.

The Upper Valley is defined as that portion of the valley east of the constriction and west of the barrier (the Park Range). At the extreme eastern end of the Upper Valley, the valley axis turns north-south within a few kilometers of the barrier. Stations located on the valley floor in the east-west region of the valley include MIL (6530 ft) and STW (6730 ft). Only RAD (6800 ft) is located on the valley floor in the north-south portion of the Upper Valley.

The final section of the valley is the barrier itself. Only those stations on the barrier which lie windward of the continental divide are used to examine airflow characteristics on the barrier. These stations include DLK (9180 ft), BUR (9180 ft), FTP (9410 ft) and STP (10330 ft).

The slope flows are defined by the v (south to north) component wind for those stations identified as slope stations. Because the slope stations are situated on slopes perpendicular to the valley axis, the v component of the wind is parallel to the slope of the terrain. By presenting the v component of the wind for the slope stations at five different time periods throughout the day, the temporal characteristics of the slope flows are illustrated.

Because the valley's axis is aligned west to east, valley flows are defined by the u component of the wind. Spatial characteristics of valley flows are illustrated by presenting PROBE station observations on a surface map of the region. In this manner, Down Valley flows are easily compared to Middle and Upper Valley flows, as well as comparing the valley floor airflow to the airflow on the adjacent slopes and ridge tops. Presenting the data at various times throughout the day allows for depiction of the temporal characteristics of the valley flow.

Once the PROBE network is partitioned, the climatological analysis is organized to facilitate a discussion of the spatial and temporal distribution of the airflow. The spatial characteristics of the airflow are presented at five different time periods (0700, 1100, 1400, 1700 and 2200 MST) to represent the temporal distribution of airflow. For each hour, the data is analyzed for values occurring only during that hour, for all days within the two month period. As an example, at 0700 MST, only the west to east component of the wind occurring at 0700 MST on each day for Storm Peak (PROBE station STP) is utilized in calculating the average west to east component of the wind for STP at 0700 MST.

The airflow analysis is based upon the mean u (west to east) component and the mean v (south to north) component of the vector wind.

All values reported are the magnitude (knots) of the wind while direction is held constant (either 270 or 180 degrees). First, a discussion of the spatial distribution of the mean (for all days) u component of the wind is presented. This is followed by a presentation of the variability associated with the mean airflow for each station.

The thermal structure of the valley is then presented. Potential temperature is chosen as the parameter to analyze because it is a conserved property of a dry airmass. The horizontal distribution of the mean (for all days) potential temperature is presented; the purpose of which is to quantify the horizontal temperature gradient along the valley which drives the thermally forced valley flows. A vertical profile of mean potential temperature is presented to obtain an idea of the vertical thermal structure. Unfortunately, sounding data from storm episodes is all that is available. However, by using the PROBE station data plotted as a function of elevation, temperature discontinuities are revealed.

Finally, the frequency and spatial distribution of decoupled flows are investigated for each time period. Decoupled flows are identified by noting where the surface wind direction varies from the ambient airflow direction. Ratios of the number of u component winds from the east to the total number of observations are presented for each station for five different diurnal periods. In addition potential temperature observations are presented to help identify differing airmasses.

In order to understand the necessary meteorological conditions in which particular flow phenomenon appear (e.g., drainage flow), the two months of data need to be stratified. The chosen method is based upon the interaction between scales of motion within the atmosphere. Therefore,

it is presupposed that the observed regional flows are related to the overlying, larger scale, synoptic weather patterns.

The synoptic weather patterns are divided into three categories based upon the relative position of the associated extratropical cyclone to the study area (Yu, 1986). From a LaGrangian perspective, each region within the extratropical cyclone has a unique climate associated with it. The appropriate synoptic categories are determined for each twelve hour period for the entire two month data period. This is accomplished by referring to the facsimile surface and 500 mb weather maps and identifying which region of the extratropical cyclone the study area is located in, every twelve hours. Additional local weather information was gained by referring to the COSE III log book (Rauber and Grant, 1982). The regional observations are divided into one of three categories determined by the day and time of the observation.

According to Yu, based upon a location's relative position within an extratropical cyclone, several regional atmospheric characteristics are disclosed. Examples of these characteristic parameters include surface winds, vertical motion, temperature inversions, dominant mesoscale systems, ventilation, deposition, and transport. Based upon this association, mountain-valley flows do not usually occur under all synoptic classes. The percentage of days of each observed synoptic category is presented.

Once the data is stratified, the approach is similar to the two month climatological analysis. The PROBE network is divided into the same groups of stations as defined previously (upper valley, middle valley, etc). Then, using statistical analysis, the mean flow and variability is presented. The objective is to investigate the variability of the mean

flow pattern for each synoptic category. A decrease in the variability indicates a more precise relationship between the synoptic and mesoscale atmospheric conditions.

Case study analysis for differing synoptic weather patterns and the associated regional flows are presented in detail. The first case study provides an example of regional airflows in which a polar high is the dominant synoptic scale feature. The second case study is used to examine the regional airflows during a synoptic scale pre-frontal condition. The third case study is used to present details of the regional airflow that occurred in a synoptic scale post-frontal environment. In each case study, the spacial distribution of the winds and potential temperature are presented along with the variations throughout the day. Vertical profiles of both these parameters are illustrated for different hours of the day. Finally, the relationship between the regional and synoptic meteorological conditions are discussed.

VI. ANALYSIS AND RESULTS

A. CLIMATOLOGICAL CHARACTERISTICS OF VALLEY BOUNDARY LAYER

1. Slope Flows

By presenting the v (south to north) component of the wind for the slope stations at five different time periods throughout the day, the temporal characteristics of the slope flows are illustrated.

Table 1 presents the mean (for all days) component of the wind parallel to the local slope of the terrain for LAY (6180 ft) and HYD (6570 ft); the standard deviation of the mean airflow for all days is shown in parenthesis. Both these stations are located on south facing slopes. PROBE station LAY was located in the wider, lower portion of the Yampa Valley while HYD was located in the more narrow, middle portion of the Yampa Valley.

The v component wind at LAY (6180 feet) always exhibited an upslope flow. While values were greatest during the day, and were less during the afternoon and evening hours, classic slope flows as those described by Defant (1951) were not observed.

The mean v component wind at HYD (6570 feet) did exhibit upslope flows during the day and downslope flows at night. Downslope flows were slightly larger in magnitude than upslope flows and all mean values were less than 1.5 knots.

Table 1

Summary of the mean (for all days during the study period) diurnal variation of the component of the wind parallel to the slope for selected PROBE stations. Elevations are listed in feet. Wind speed units are knots. Standard deviations are listed in parenthesis. All times are Mountain Standard.

Station (elev.)	0700	1100	1400	1700	2200
LAY (6180)	1.2 (4.3)	3.5 (5.4)	4.7 (6.8)	1.4 (5.2)	1.9 (6.2)
HYD (6570)	-0.6 (2.3)	0.6 (2.5)	0.6 (3.9)	-1.4 (3.5)	-0.8 (2.9)

In each time period for both stations, standard deviations were always greater than the mean slope flow. Thus, slope flows were highly variable within the two month sample.

2. Valley Flow

a. 0700 MST

The results of the valley flow climatological analysis are illustrated on a map of the PROBE station network. West to east component of the wind are illustrated with wind barbs. Using the nomenclature of the National Weather Service, speeds are represented with barbs. Potential temperatures are plotted above the station and the frequency of decoupled flow is plotted below the station in percent.

Figure 6 illustrates the average u (west to east) component of the surface wind (knots), potential temperature (K), and percent decoupled flow for the entire two month data set, as observed by the PROBE array at 0700 MST. Appendix A presents the average, standard deviation, minimum, maximum, 75th, 50th, 25th percentiles and the number of observations of the west to east component of the wind for all days during the study period at 0700, 1100, 1400, 1700 and 2200 MST.

At 0700 MST the mean valley flow was typified by calm to light winds on the valley floor with light to moderate westerly flow on the surrounding ridges (see Figure 6). Nearly all stations, except for those at the highest peaks, had standard deviations of the mean u component greater than the associated mean, indicating valley flow was highly variable. Potential temperatures were lowest within the upper valley and increased towards the lower valley and upwards.

To investigate when a surface station observed flows which were decoupled (not associated with) from the synoptic scale winds, a simple

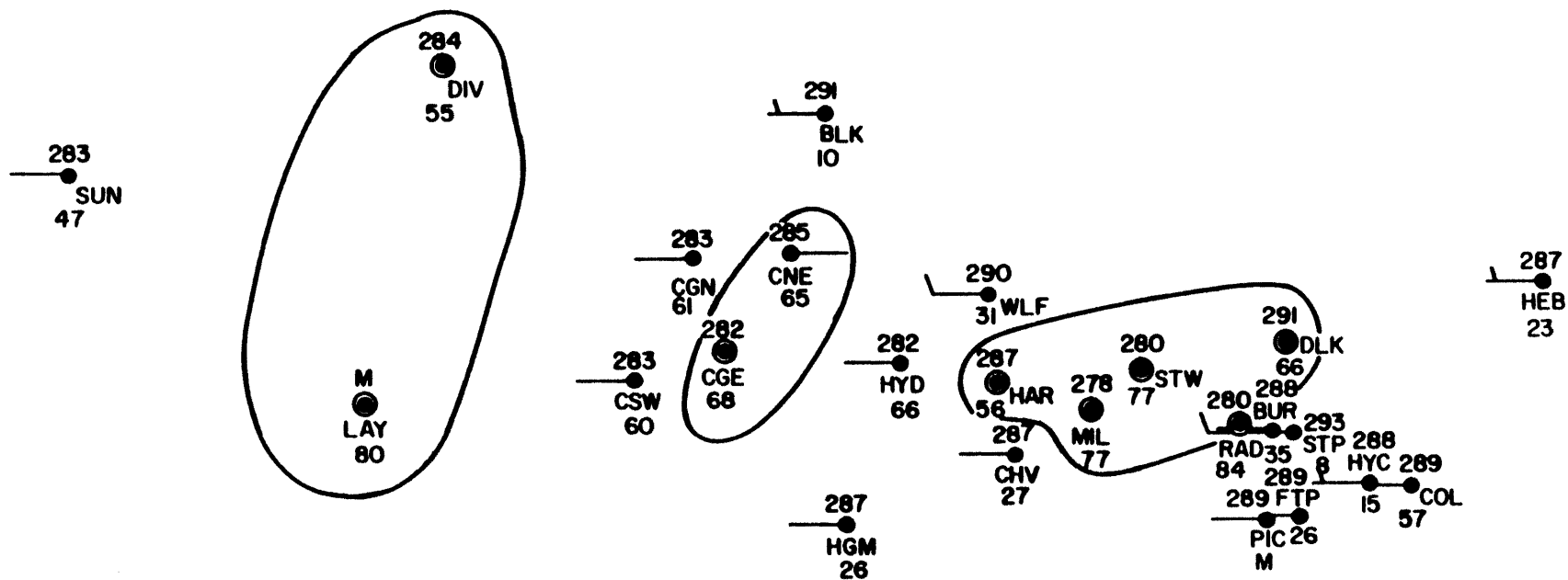


Figure 6. Average west to east component of the wind (knots, shown as wind barbs), average potential temperature (kelvin, shown above the dots), and percent decoupled flow (shown below the dots) at 0700 MST for all days within the study period.

numerical ratio was utilized. Assuming the synoptic airflow has a westerly component, as it typically does at 40.5° N latitude, a surface flow would have a westerly component of the wind in excess of 1.0 knots if the flows were coupled. According to the Glossary of Meteorology (American Meteorological Society, 1959), calm winds are defined as having a wind speed less than 1.0 knots. For the purposes of this study, a westerly flow is characterized by wind speeds greater than 1.0 knots. The ratio of the number of observations in which the u component of the wind was less than 1.0 knots from the west (calm or easterly winds) divided by the total number of observations at each distinct hour is presented. This represents the fraction of time for each hour and for each station that the surface flow was decoupled from the synoptic scale flow. Decoupled flows occurred most commonly (77% to 86%) in the upper valley but occurred only 50% of the time in the middle and lower valley and only 8% of the time on the barrier for the two month study period.

The vertical extent of decoupled flows is typically marked by a temperature discontinuity. To determine the height of a temperature discontinuity, like that of a temperature inversion, a vertical profile of mean (for all days) potential temperature was utilized. Unfortunately, sounding data was only available during storm episodes, not continuously, and not during all types of meteorological conditions. However, by using the PROBE station data plotted as a function of elevation, temperature discontinuities became apparent (see Figure 7). The mean value was computed for all days in the study period, for each PROBE station, at each hour of the day. It must be noted that potential temperatures were observed from surface stations and not the from the free atmosphere.

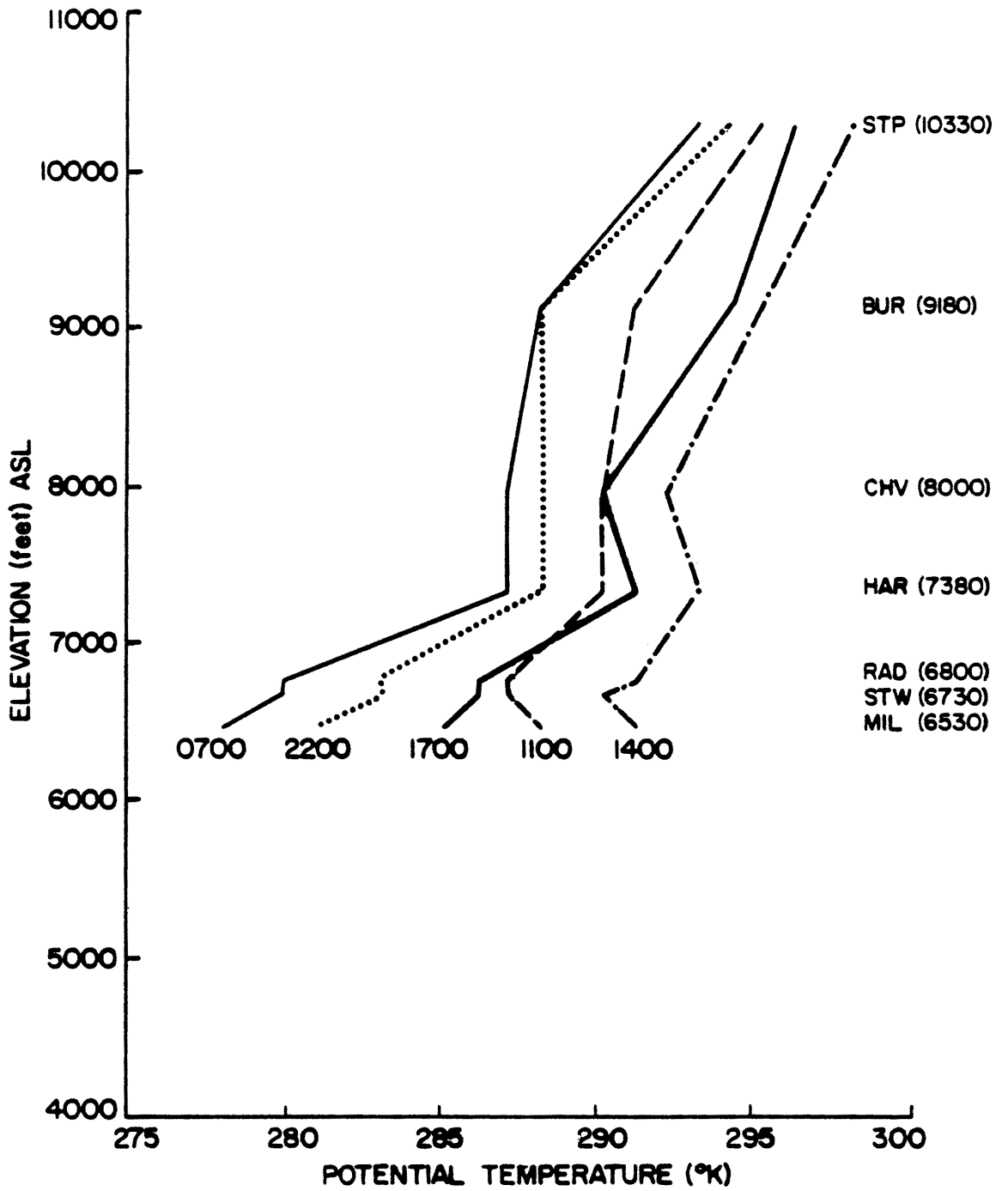


Figure 7. Average vertical profile of potential temperature (kelvin) constructed from selected PROBE station data for all days within the study period.

Therefore, atmospheric stability can not be accurately be determined from Figure 7.

Figure 7 illustrates the average potential temperature as a function of elevation. Only those stations within the upper valley east of the constriction in width between Hayden (HYD) and Milner (MIL) to the crest of the barrier were presented. Because of the large temperature range and the calm winds which were present in the upper valley, it is likely that this portion of the valley contained the strongest temperature inversion.

At 0700 MST, a 7°K temperature discontinuity existed between 6800 ft and 70 ft, approximately 340 ft above the valley floor. The layer of decoupled flow extended to somewhere in between 7380 ft and 8000 ft. The difference in frequency of decoupled flows between these two elevations is illustrated in Figure 6. HAR (7380 ft) experienced decoupled flows 56% of the time while CHV (8000 ft) only experienced decoupled flows 27% of the time during the two month study period. The u component of the wind, as illustrated in Figure 6 also supports this height as the top of the decoupled layer. The mean west to east component of the wind for the two month study period is -0.4 knots at HAR while at CHV the u wind was 4.7 knots. A difference explainable by a discontinuity between the two stations.

b. 1100 Local Time

At 1100 MST, some changes had occurred. The upper valley air had warmed to the same potential temperature as the central and lower valley. In the lower valley decoupled flows decreased up to 30% at LAY (see Figure 8). The entire profile had warmed between 4°K above the discontinuity and 9°K below the discontinuity. However, no change in the height of the top of the decoupled flow layer had occurred by this time.

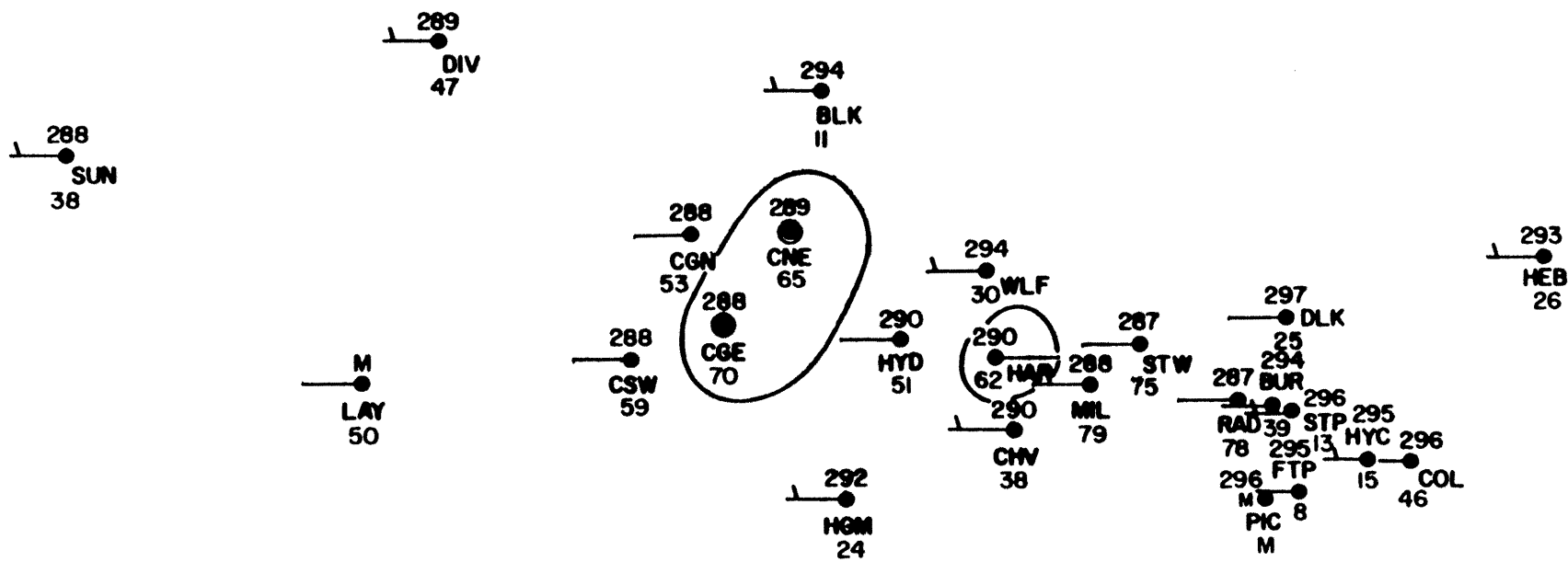


Figure 8. Average west to east component of the wind (knots, shown as wind barbs), average potential temperature (kelvin, shown above the dots), and percent decoupled flow (shown below the dots) at 1100 MST for all days within the study period.

c. 1400 Local Time

By 1400 MST a noticeable change had taken place in the valley (see Figure 9). U component wind speeds increased throughout the study area. As the magnitude of the mean u component wind increased so had the associated standard deviations. Decoupled flows remained relatively frequent (65% to 72%) in the upper valley but the frequency decreased significantly to the west and vertically. No change in the vertical extent of the decoupled flow layer was observed at 1400 MST (see Figure 9).

At 1400 MST there was no thermal gradient observed between the upper and lower valley (see Figure 9). At this time (1400 MST), no up valley flow circulations were driven by thermal gradients in this valley during the two month study period. Because there are no up valley flows, this contrasts with what one would expect during the summer months, when an up valley circulation is the norm.

d. 1700 Local Time

Around the time of sunset, 1700 MST, differential cooling had begun throughout the entire valley; consequently, a thermal gradient was established between the upper and lower valley (see Figure 10). However, no significant changes had occurred in the mean u component winds or the variability of these winds at any stations. The spatial distribution of the decoupled layer remained similar to the 1400 MST observations. Figure 7 illustrates that the vertical extent of the discontinuity had not changed between 1400 MST and 1700 MST.

e. 2200 MST

By 2200 MST the mean west to east airflow had continued to decrease throughout the entire valley (see Figure 11). The valley air continued

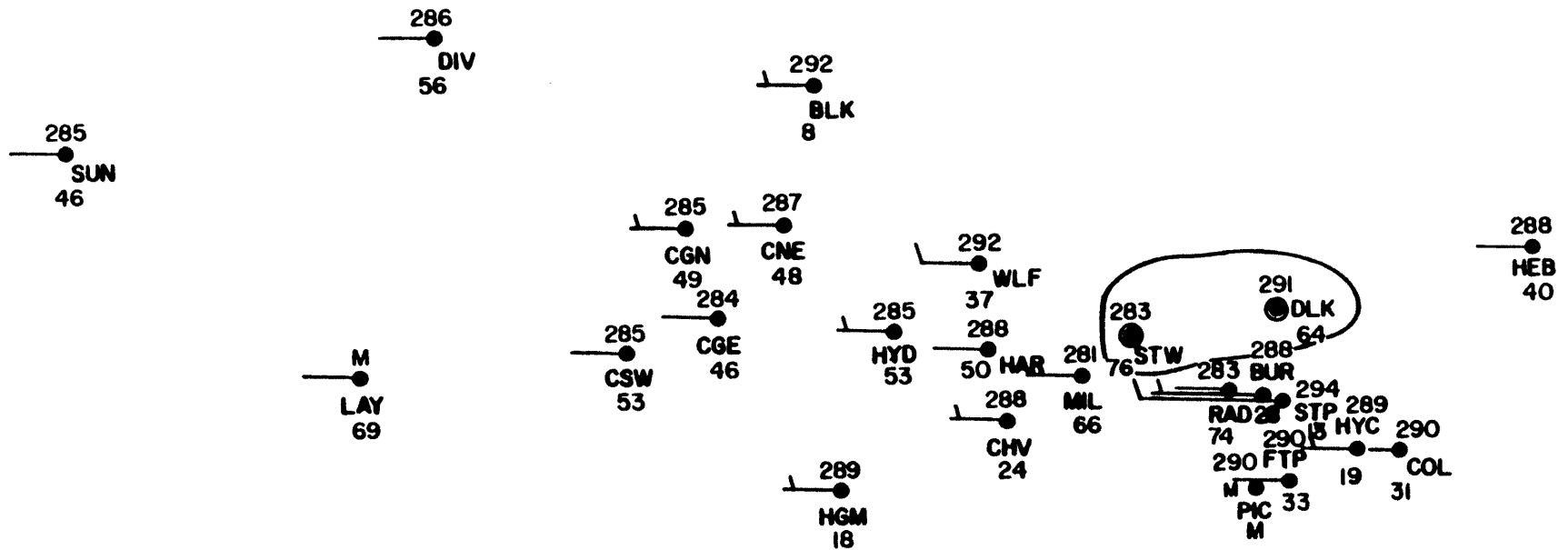


Figure 9. Average west to east component of the wind (knots, shown as wind barbs), average potential temperature (kelvin, shown above the dots), and percent decoupled flow (shown below the dots) at 1400 MST for all days within the study period.

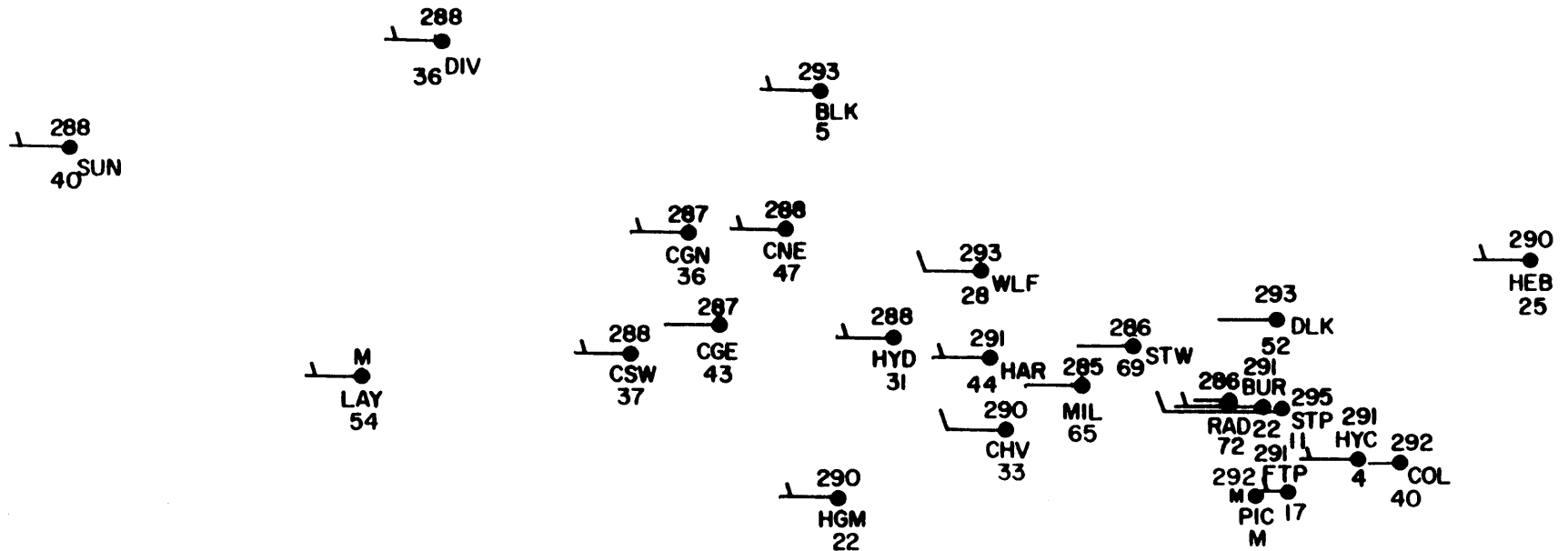


Figure 10. Average west to east component of the wind (knots, shown as wind barbs), average potential temperature (kelvin, shown above the dots), and percent decoupled flow (shown below the dots) at 1700 MST for all days within the study period.

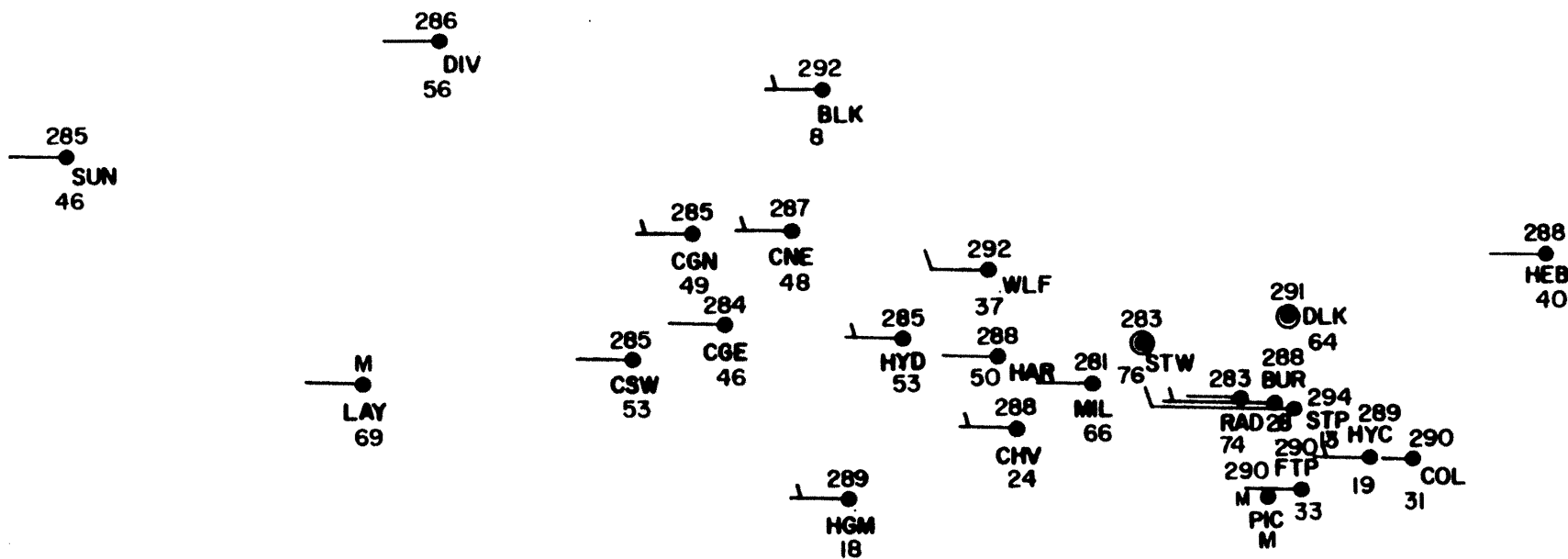


Figure 11. Average west to east component of the wind (knots, shown as wind barbs), average potential temperature (kelvin, shown above the dots), and percent decoupled flow (shown below the dots) at 2200 MST for all days within the study period.

to cool but not as rapidly as that observed around sunset (see Figure 11). The thermal gradient between the upper and lower valley continued to strengthen until morning. The frequency of decoupled flows increased throughout the entire valley with the greatest increases occurring in the middle and lower valleys. The vertical extent of decoupled flows at 2200 MST were similar to those observed at 0700 MST (see Figures 7 and 11).

B. METEOROLOGICAL CONTROLS ON VALLEY BOUNDARY LAYER

1. Meteorological Categories

The synoptic weather patterns are divided into three categories based upon the relative position of the associated extratropical cyclone to the study area (Yu, 1986). From a LaGrangian perspective, each region within the extratropical cyclone has a unique climate associated with it. The appropriate synoptic categories are determined for each twelve hour period for the entire two month data period. This is accomplished by referring to the facsimile surface and 500 mb weather maps and identifying which region of the extratropical cyclone the study area is located in, every twelve hours. Additional local weather information was gained by referring to the COSE III log book (Rauber and Grant, 1982). The regional observations are divided into one of three categories determined by the day and time of the observation.

According to Yu's article, based upon a location's relative position within an extratropical cyclone, several regional atmospheric characteristics are disclosed. Examples of these characteristic parameters include surface winds, vertical motion, temperature inversions, dominant mesoscale systems, ventilation, deposition, and transport. Based upon this association, mountain-valley flows do not usually occur under

all synoptic classes. The percentage of days of each observed synoptic category is presented.

Once the data is stratified, the approach is similar to that used in the two month climatological analysis. The PROBE network is divided into the same groups of stations as defined previously (upper valley, middle valley, etc). Then, using statistical analysis, the mean flow and variability is presented. The objective is to investigate the variability of the mean flow pattern for each synoptic category. A decrease in the variability indicates a more precise relationship between the synoptic and mesoscale atmospheric conditions.

Yu and Pielke (1986) showed that mesoscale phenomenon can be associated with the overlying synoptic conditions. Therefore, their method of synoptic stratification was employed in order to define the synoptic climatology of the Yampa Valley during December 1981 and January 1982.

A subjective classification scheme based on the classical cyclone model was reported by Lindsey (1980). Figure 12 illustrates a typical eastern U.S. wintertime extratropical cyclone; the synoptic flow is divided into five categories as described by Yu and Pielke:

- Category 1: in the warm sector of an extratropical cyclone - prefrontal passage
- Category 2: ahead of the warm front in the region of cyclonic isobaric curvature at the surface
- Category 3: behind the cold front in the region of cyclonic curvature to the surface isobars
- Category 4: under a polar high in a region of anticyclonic curvature to the surface isobars
- Category 5: in the vicinity of a subtropical ridge.

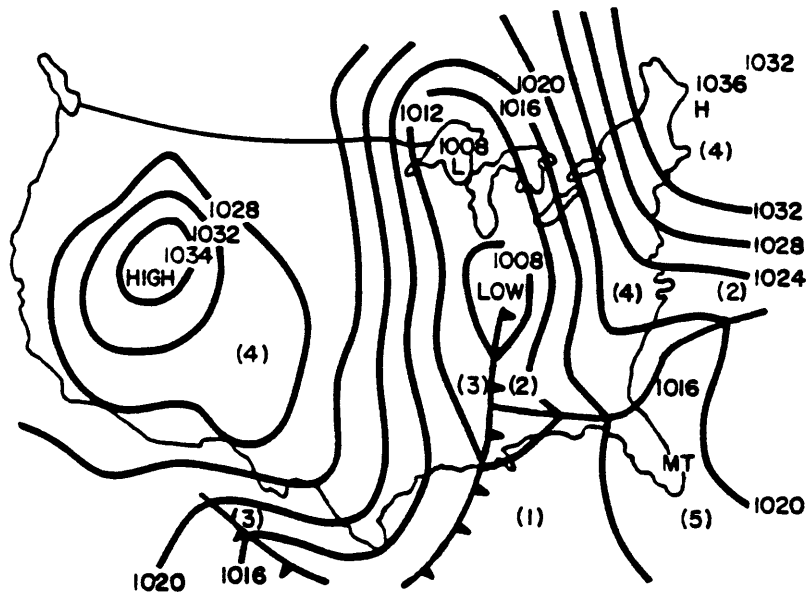


Figure 12. Example of a surface analysis chart (for January 9, 1964) showing the application of the synoptic climatological model for the five synoptic classes listed in Table 2.

Table 2 presents a summary of the meteorological conditions associated with the five synoptic classes related to an extratropical cyclone. Note that only categories four and five mention mountain-valley flows as the dominated mesoscale system. Also, category 3 is associated with forced airflow over rough terrain.

Table 3 lists the results of the synoptic stratification for December 1981 and January 1982. In Table 3, the synoptic pattern that was present, represented by numbers 1,3,4 and undecided, is listed on the right with the time period, to which it applies, listed to the left. Figure 13 illustrates the monthly averaged frequencies for the occurrence of each synoptic climatological categories during the COSE III period. The synoptic summary of the Yampa Valley for the period is characterized as:

- a. High pressure systems dominate the weather occurring 50% in December and 28% in January.
 - b. Subtropical ridges do not occur in the region for the period.
 - c. Warm frontal occurrences do not occur in the region for the period.
 - d. Cold fronts occur 28% during the period.
 - e. Ambiguous situations (undecided) increased from 4% in December to 28% in January.
2. Airflow for Respective Categories
- a. Category 1, in the warm sector of an extratropical cyclone - prefrontal passage
 - (1) Slope Flows

Table 4 presents the mean (for all category 1 days in the study period) component of the wind parallel to the local slope of the terrain for two PROBE stations at five different hours during a twenty-four hour period. Positive values are representative of south to north (V component

Table 2

Overview of air quality aspects of the five synoptic Categories illustrated in Figure 12 (reproduced from Yu and Pielke, 1986).

Category characteristics	Category 1	2	3	4	5
Category class	mT; in the warm sector of an extratropical cyclone	mT/cP, mT/cA, mP/cA; ahead of the warm front in the region of cyclonic curvature at the surface	cP, cA; behind the cold front in the region of cyclonic curvature to the surface isobars	cP, cA; under a polar high in a region of anticyclonic curvature to the surface	mT; in the vicinity and west of a subtropical ridge
Surface winds	Brisk SW surface winds	Light to moderate SE to ENE surface winds	Strong NE to W surface winds	Light and variable winds	Light SE to SW winds
Vertical motion	Weakening synoptic descent as the cold front approaches	Synoptic ascent due to warm advection and positive vorticity advection aloft	Synoptic ascent due to positive vorticity advection aloft (in this region this ascent more than compensates for the descent due to cold advection)	Synoptic descent (due to warm advection and/or negative vorticity advection aloft)	Synoptic subsidence (descending branch of the Hadley cell). Becomes strong as you approach the ridge axis
Inversion	Weak synoptic subsidence inversion caps planetary boundary layer	Boundary layer capped by frontal inversion	Deep planetary boundary layer	Synoptic subsidence inversion and/or warm advection aloft create an inversion which caps the planetary boundary layer	Synoptic subsidence inversion
Dominant mesoscale systems	Squall lines	Embedded lines of convection	Forced airflow over rough terrain systems; lake effect storms	Mountain-valley flows; land-sea breezes; urban circulations (thermally-forced systems)	Mountain-valley flows; land-sea breezes; urban circulations (thermally-forced systems)
Ventilation	Moderate to good ventilation	Poor ventilation of low level (i.e. below frontal inversion) emissions	Excellent ventilation	Night or snow-covered ground: poor ventilation; day: poor to moderate ventilation	Day: moderate to good ventilation; night: moderate to poor ventilation
Deposition	Dry deposition except wet deposition in showers	Dominated by wet deposition	Dry deposition except in showers	Dry deposition	Dry deposition except wet deposition in showers and thunderstorms
Transport	Long range	Long range above inversion	Long range	More local as you approach the center of the polar high	More local as you approach the center of the subtropical high

Table 3

Listing of synoptic stratification results. Dates and times are listed with the assigned synoptic Category for that time period. Asterisk indicates that weather maps were unavailable for this time period.

		(ALL TIMES ARE GMT)	
DATE BEGIN		DATE END	SYNOPTIC CATEGORY
Dec 1, 1981 @ 0000		Dec 1, 1981 @ 2300	4
Dec 2, 1981 @ 0000		Dec 2, 1981 @ 0600	3
Dec 2, 1981 @ 0700		Dec 3, 1981 @ 0300	4
Dec 3, 1981 @ 0400		Dec 3, 1981 @ 0900	1
Dec 3, 1981 @ 1000		Dec 3, 1981 @ 2300	3
Dec 4, 1981 @ 0000		Dec 10, 1981 @ 1100	4
Dec 10, 1981 @ 1200		Dec 11, 1981 @ 0700	1
Dec 11, 1981 @ 0800		Dec 12, 1981 @ 1100	3
Dec 12, 1981 @ 1200		Dec 13, 1981 @ 0300	4
Dec 13, 1981 @ 0400		Dec 13, 1981 @ 1700	1
Dec 13, 1981 @ 1800		Dec 14, 1981 @ 1100	3
Dec 14, 1981 @ 1200		Dec 16, 1981 @ 0600	1
Dec 16, 1981 @ 0700		Dec 17, 1981 @ 0600	3
Dec 17, 1981 @ 0700		Dec 19, 1981 @ 1400	4
Dec 19, 1981 @ 1500		Dec 21, 1981 @ 0700	1
Dec 21, 1981 @ 0800		Dec 22, 1981 @ 2200	3
Dec 22, 1981 @ 2300		Dec 25, 1981 @ 1200	4
Dec 25, 1981 @ 1300		Dec 25, 1981 @ 2100	1
Dec 25, 1981 @ 2200		Dec 26, 1981 @ 0900	3
Dec 26, 1981 @ 1000		Dec 27, 1981 @ 1100	undefined
Dec 27, 1981 @ 1200		Dec 28, 1981 @ 2300	3
Dec 29, 1981 @ 0000		Dec 30, 1981 @ 1100	4
Dec 30, 1981 @ 1200		Dec 30, 1981 @ 2100	1
Dec 30, 1981 @ 2200		Dec 31, 1981 @ 2300	3
Jan 1, 1982 @ 0000		Jan 4, 1982 @ 1100	undefined*
Jan 4, 1982 @ 1200		Jan 5, 1982 @ 2300	1
Jan 6, 1982 @ 0000		Jan 6, 1982 @ 2300	3
Jan 7, 1982 @ 0000		Jan 10, 1982 @ 1100	4
Jan 10, 1982 @ 1200		Jan 13, 1982 @ 1100	undefined
Jan 13, 1982 @ 1200		Jan 13, 1982 @ 2300	3
Jan 14, 1982 @ 0000		Jan 14, 1982 @ 1100	undefined
Jan 14, 1982 @ 1200		Jan 15, 1982 @ 1100	4
Jan 15, 1982 @ 1200		Jan 17, 1982 @ 2300	3
Jan 18, 1982 @ 0000		Jan 18, 1982 @ 1600	1
Jan 18, 1982 @ 1700		Jan 19, 1982 @ 0200	3
Jan 19, 1982 @ 0300		Jan 19, 1982 @ 1100	undefined
Jan 19, 1982 @ 1200		Jan 22, 1982 @ 0600	1
Jan 22, 1982 @ 0700		Jan 24, 1982 @ 2300	3
Jan 25, 1982 @ 0000		Jan 26, 1982 @ 2300	4
Jan 27, 1982 @ 0000		Jan 27, 1982 @ 0500	1
Jan 27, 1982 @ 0600		Jan 27, 1982 @ 1700	3
Jan 27, 1982 @ 1800		Jan 28, 1982 @ 2300	4
Jan 29, 1982 @ 0000		Jan 29, 1982 @ 2300	undefined
Jan 30, 1982 @ 0000		Jan 30, 1982 @ 1100	4
Jan 30, 1982 @ 1200		Jan 30, 1982 @ 2300	3
Jan 31, 1982 @ 0000		Jan 31, 1982 @ 1100	4
Jan 31, 1982 @ 1200		Jan 31, 1982 @ 2300	1

* synoptic weather maps were unavailable for this time period

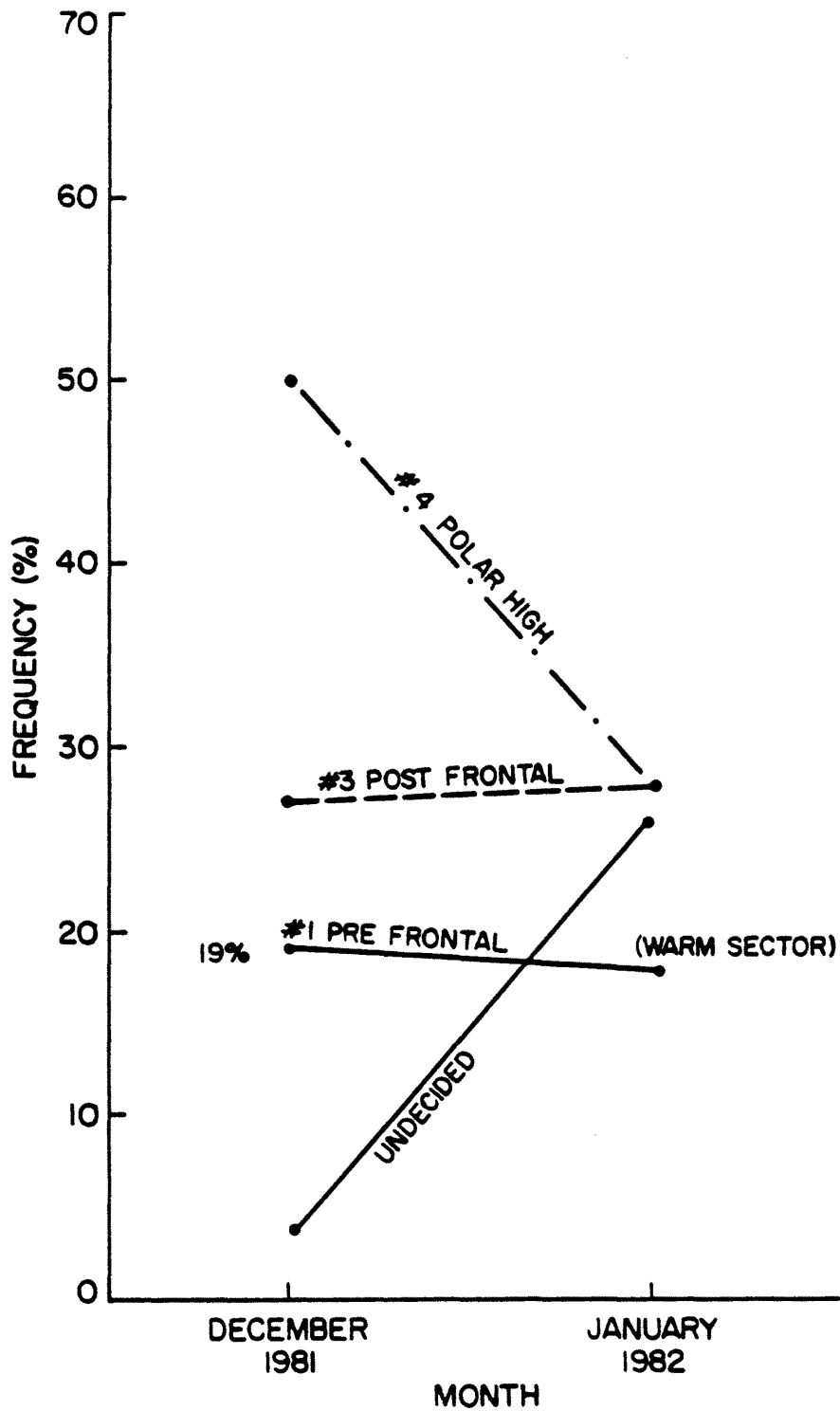


Figure 13. Monthly averaged frequencies of occurrences of each synoptic climatological category during the study period.

Table 4

Summary of the mean (for all days in which synoptic Category #1 was present) diurnal variation of the component of the wind parallel to the slope for selected PROBE stations. Elevations are listed in feet. Wind speed units are knots. Standard deviations are listed in parenthesis. All times are Mountain Standard.

Station (elev.)	0700	1100	1400	1700	2200
LAY (1884)	3.7 (6.2)	6.8 (7.2)	10.1 (8.2)	2.7 (5.1)	4.5 (7.0)
HYD (2003)	-1.2 (2.1)	0.0 (1.7)	3.9 (4.9)	0.8 (5.1)	0.8 (2.9)

of the wind) airflows. Speeds are listed in knots and the standard deviation of the mean is listed in parenthesis.

PROBE station LAY exhibited upslope flows during all five hours listed in Table 4. As diurnal heating progressed, the strength of the flows increased to 10.1 knots at 1400 MST, and decreased by 1700 MST. However, the strength of the V component airflow did not consistently decrease as nocturnal cooling progressed. This was indicated by an increase in speed between 1700 and 2200 MST. Standard deviations of the mean were always larger than the mean V wind, indicating that flows were highly variable and turbulent.

The mean V component airflow at HYD was weaker than at LAY, but followed similar trends. The mean V component airflow reversed from a weak down slope flow at 0700 MST to a 3.9 knot upslope wind at 1400 MST as daytime heating progressed. Mean V component flows decreased with nocturnal cooling, but did not reverse direction by 2200 MST. Large standard deviations indicate these slope flows were also highly variable and turbulent.

When comparing these slope flows to those presented for the entire two month study period, both sites exhibited a larger V component of the wind. This is consistent with Table 2 in which the surface winds are described as being brisk and from the southwest in synoptic category one.

(2) Valley Flows

(a) 0700 MST

Figure 14 illustrates the average u (west to east) component of the surface wind (knots), potential temperature (K), and percent decoupled flow for periods in which the region was characterized by an approaching cold front at 0700 MST. Appendix A (Tables A-6 through A-10) presents the

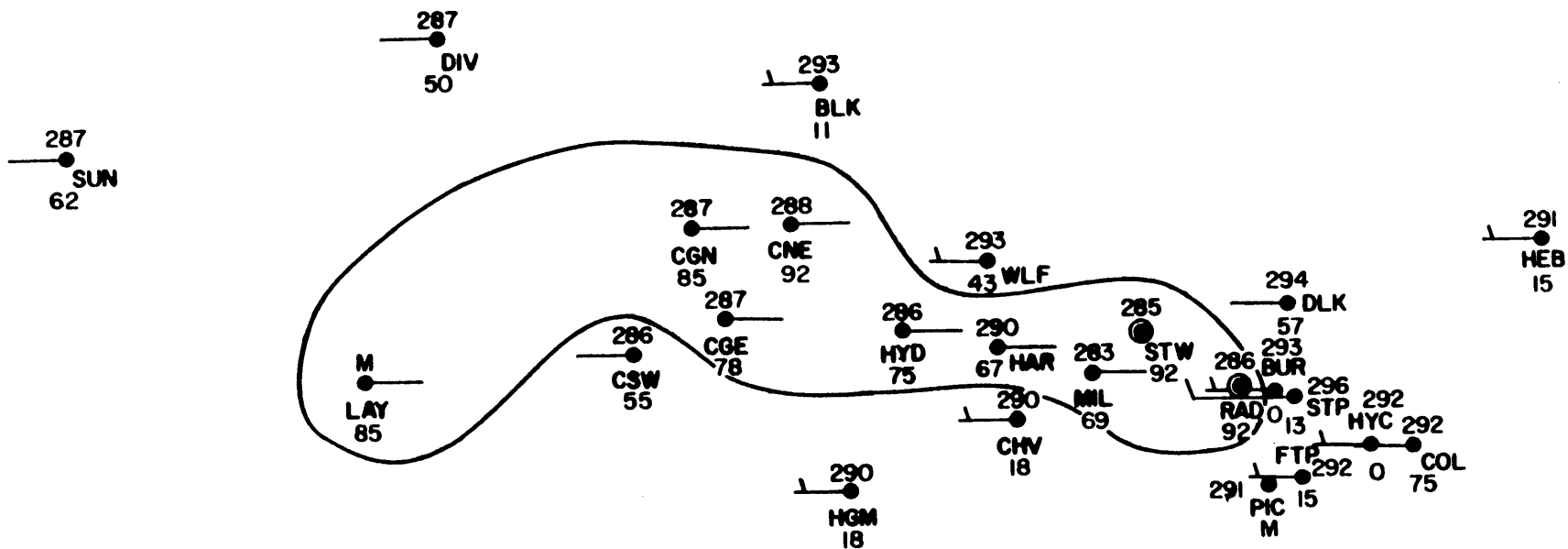


Figure 14. Average west to east component of the wind (knots, shown as wind barbs), average potential temperature (kelvin, shown above the dots), and percent decoupled flow (shown below the dots) at 0700 MST for all days in which synoptic Category #1 was present.

average, standard deviation, minimum, maximum, 75th, 50th, 25th percentiles and the number of observations of the west to east component of the wind for these days during the study period at 0700, 1100, 1400, 1700 and 2200 MST.

At 0700 MST, the valley floor was typified by calm to light downvalley airflows extending from the upper valley to the middle and some parts of the lower valley, while light to moderate up valley winds occurred at the peaks and ridges (see Figure 14 and Table A-6). Downvalley flows began as far east as MIL (6530 ft) in the upper valley and extended to the PROBE station LAY (6180 ft) in the lower valley. These downvalley airflows extended as high as HAR (7380 ft), 830 feet above the valley floor.

For nearly all PROBE stations, the standard deviations were larger than the mean U component wind speed. Nineteen of twenty-three stations had smaller standard deviations (of the mean U wind) than the standard deviations (of the mean U wind) for the entire study period. The standard deviation of the mean U wind was less than the standard deviation of the mean U wind presented in the climatology section.

At 0700 MST a thermal gradient was present on the valley floor in which the upper valley was two to three degrees colder than the middle and lower valleys. Figure 14 illustrate the mean potential temperature distribution at 0700 MST for all periods when the study region was within the warm sector of an extratropical cyclone (synoptic Category 1). The overall distribution of potential temperatures remained very similar to that of Figure 6 (two month mean potential temperature distribution). However, potential temperatures were three to six degrees warmer than the two month mean potential temperature throughout the study period.

At 0700 MST, decoupled flows had a similar spatial distribution as those in the two month climatological study period but frequencies had typically increased by ten percent. Figure 14 illustrates the percent of decoupled flows at 0700 MST for synoptic Category #1 conditions. The upper valley (MIL, STW, and RAD) was characterized by decoupled flow at least 92% of the time. Further west in the middle valley (CGE, CGN, CNE, and HYD) decoupled flow occurred 78% to 92% of the time. Decoupled flow occurred 50% to 62% in the lower valley (CSW, LAY, DIV, and SUN) with the exception of LAY. At HAR (7379 ft), a south facing slope, decoupled flow occurred 67% of the time while directly across the valley at CHV, decoupled flow only occurred 27% of the time. At the higher elevations (WLF, BLK, and STP) decoupled flow occurred less than 43% of the time.

Figure 15 illustrates the mean potential temperature as a function of elevation for selected PROBE stations at 0700 MST, 1100 MST, 1400 MST, 1700 MST, and 2200 MST. At 0700 MST, the vertical distribution of potential temperature remained very similar to that of the two month mean vertical distribution with two important distinctions. First, surface temperature discontinuity was slightly less than that of the two month mean. Second, the entire profile was three degrees warmer than that of the two month study period.

(b) 1100 MST

At 1100 MST, the mean U component airflow in the valley was the same as that observed at 0700 MST, with the exception that downvalley airflows now only extended as far west as CNE (6910 feet), in the middle valley (see Figure 16 and Table A-7). A weak convergence zone was present between the western portions of Craig (CSW and CGN) and the eastern sections of Craig (CNE and CGE). No change in the vertical extent of

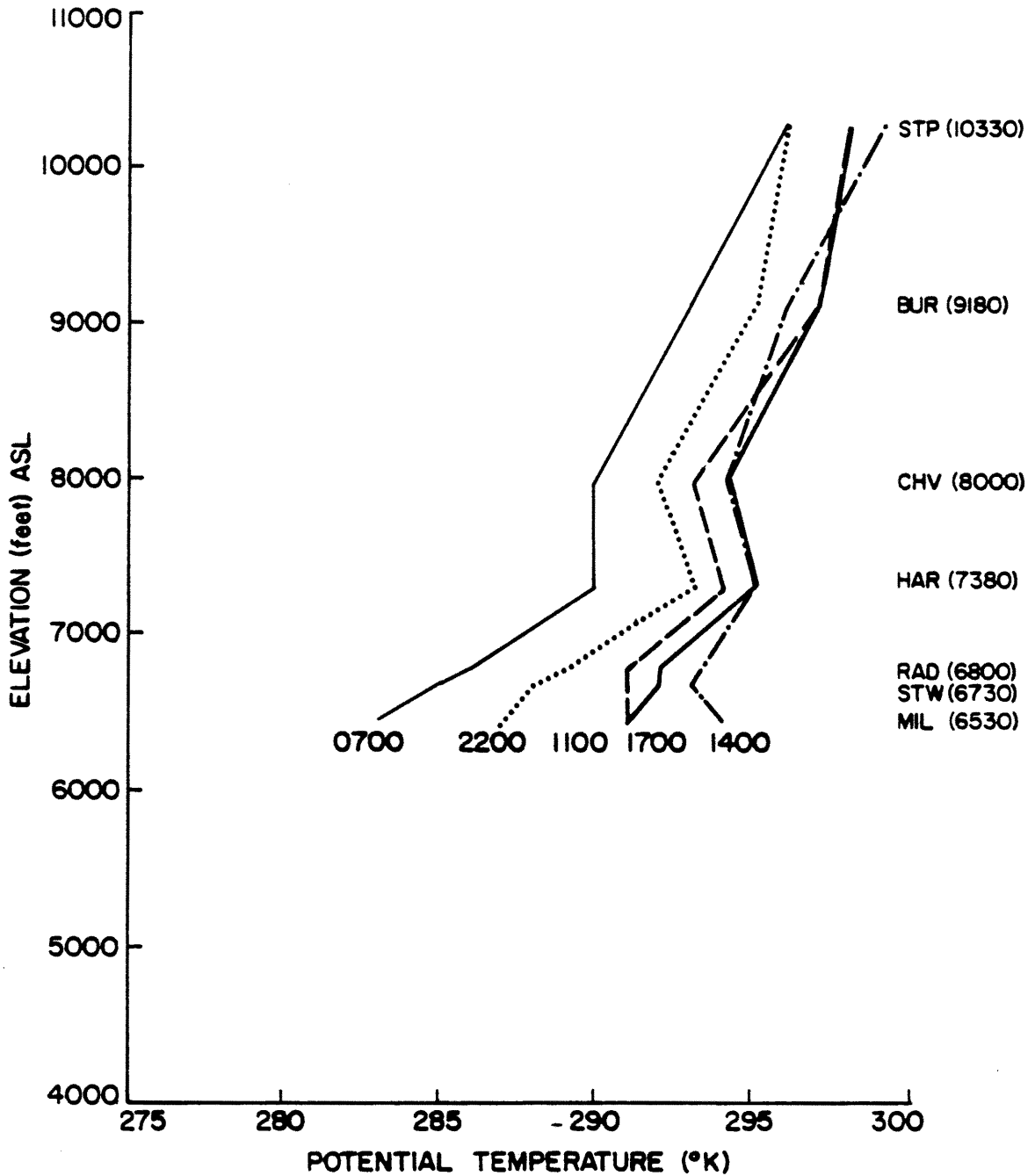


Figure 15. Average vertical profile of potential temperature (kelvin) constructed from selected PROBE station data for all days in which synoptic Category #1 was present.

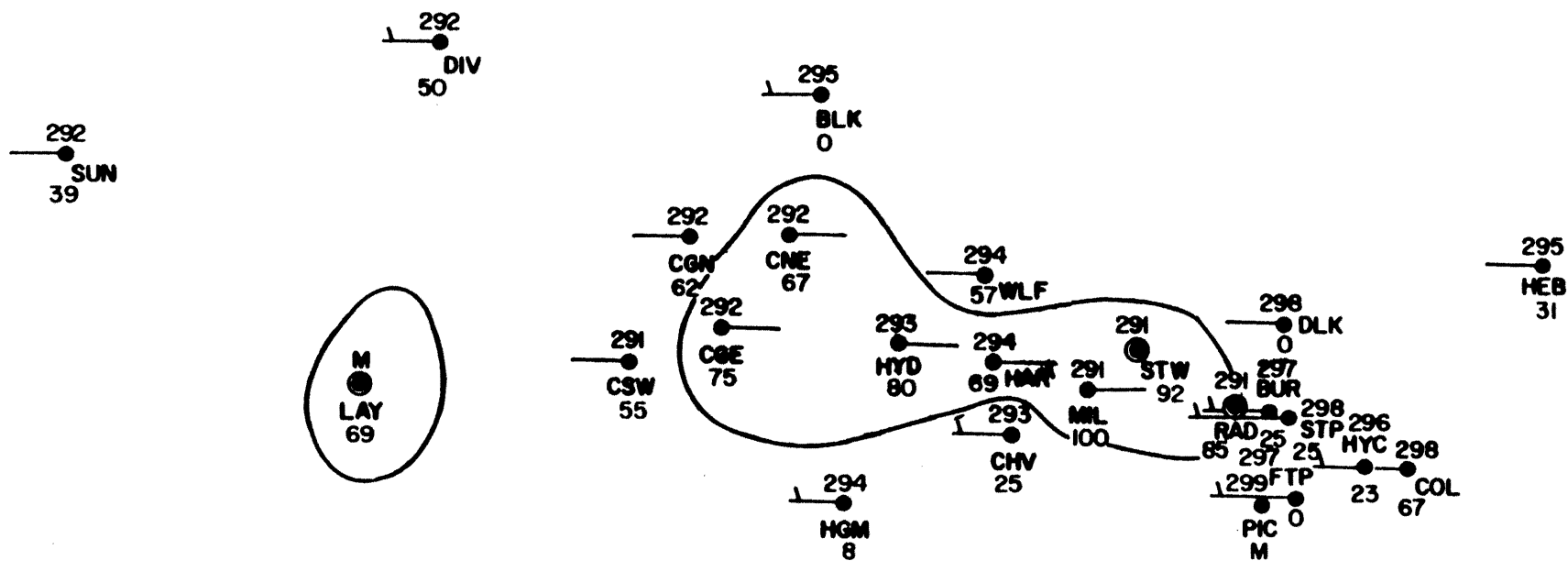


Figure 16. Average west to east component of the wind (knots, shown as wind barbs), average potential temperature (kelvin, shown above the dots), and percent decoupled flow (shown below the dots) at 1100 MST for all days in which synoptic Category #1 was present.

downvalley flows occurred. Fifteen of 23 standard deviations (of the mean U wind) were less than the standard deviations of the two month mean U wind.

At 1100 MST, the thermal gradient between the upper and lower valley had diminished to only a one degree difference (see Figures 15 and 16). Although potential temperatures warmed by three degrees throughout the valley, there still remained a 6 degree kelvin temperature discontinuity in the lowest 830 foot layer within the upper valley.

By 1100 MST, no significant changes in the frequency of decoupled flows were observed within the study area. Figure 16 illustrates the percentage of decoupled flows during this time period.

(c) 1400 MST

By 1400 MST a noticeable change had occurred in the mean U component wind throughout the Yampa Valley. Downvalley flows were no longer present (see Figure 17 and Table A-8). Average U component winds were 2.9 to 11.9 knots and occurred everywhere except the upper valley (MIL, STW, and RAD). Winds in the middle and lower valley were equally as strong as the winds observed at the peaks and ridges above the valley floor.

Variability decreased since the morning hours as noted by mean U component winds exceeding the standard deviation of the mean at most stations within and above the valley (see Table A-8). However, only 12 of 23 stations exhibited a decrease in variability as compared to the two month variability of the mean U wind for the same time. Thus, at 1400 MST this classification scheme does not account for all the observed variability of the mean flow.

The thermal gradient that was present during the morning hours was no longer present at 1400 MST (see Figure 17). The upper valley (MIL,

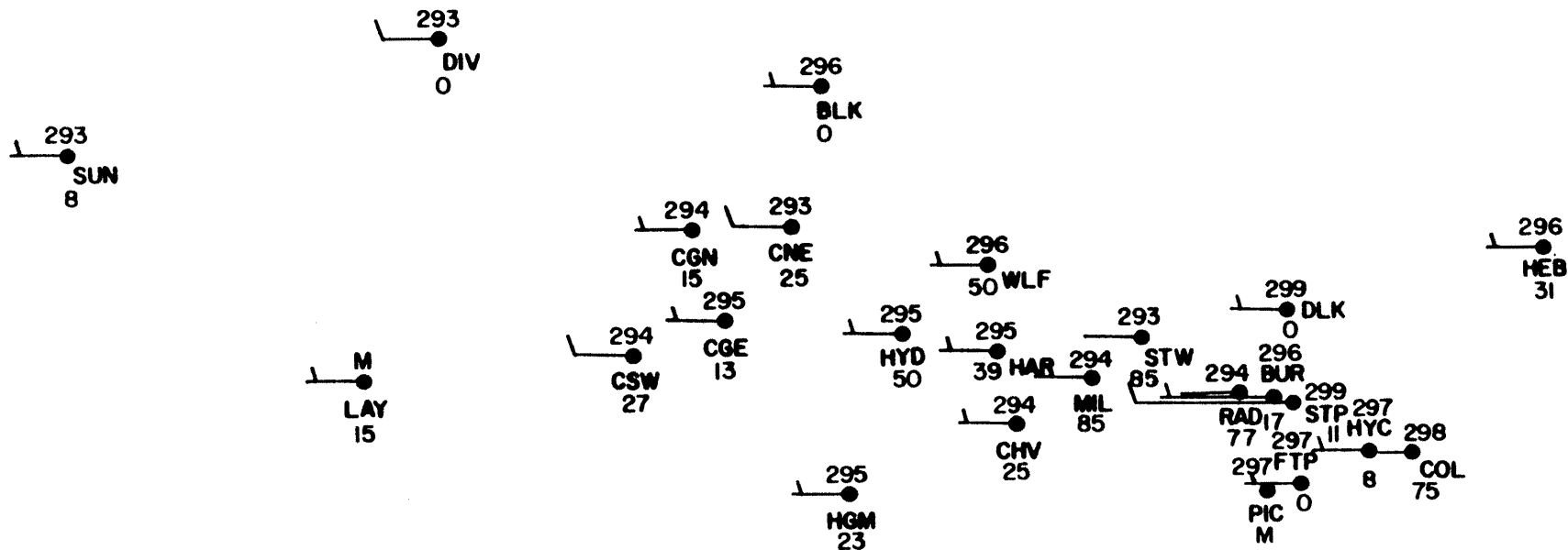


Figure 17. Average west to east component of the wind (knots, shown as wind barbs), average potential temperature (kelvin, shown above the dots), and percent decoupled flow (shown below the dots) at 1400 MST for all days in which synoptic Category #1 was present.

STW, and RAD) had warmed to 294 K, the same temperature observed in the middle and lower valleys.

Figure 15 illustrates that the lower temperature discontinuity that was present during the morning hours had diminished to only a two degree discontinuity between 6730 feet and 7380 feet. No large temperature discontinuities were present above 7380 feet, for the upper valley.

By 1400 MST a noticeable change had occurred in the frequency of occurrence of decoupled flows in the Yampa Valley (see Figure 17). While the occurrence of decoupled flows remained frequent (85%) in the upper valley (MIL, STW, and RAD), the frequency of these events had decreased to 8% - 33% in the lower and middle valley. HYD was the one exception, where decoupled flows were observed 58% of the time period. On the barrier, the frequency of decoupled flows decreased from 25% - 43% at 1100 MST to 11% - 14% at 1400 MST. On the slopes above the constriction in the valley's width between MIL and HYD, the frequency of decoupled flows also decreased as compared to the 1100 MST observations. The frequency of these events ranged from 25% at HAR (7379 ft) to 50% at WLF (8500 ft). Therefore, the region of decoupled flows occurred primarily the in upper valley and had a smaller vertical extent than in the morning hours.

(d) 1700 MST

By 1700 MST, no significant changes had occurred in valley airflow (see Figure 18). Cooling had occurred in the valley, and the upper valley was now one to two degrees cooler than the middle and lower valleys. Although a thermal gradient was present, a down valley circulation had not manifested itself by 1700 MST.

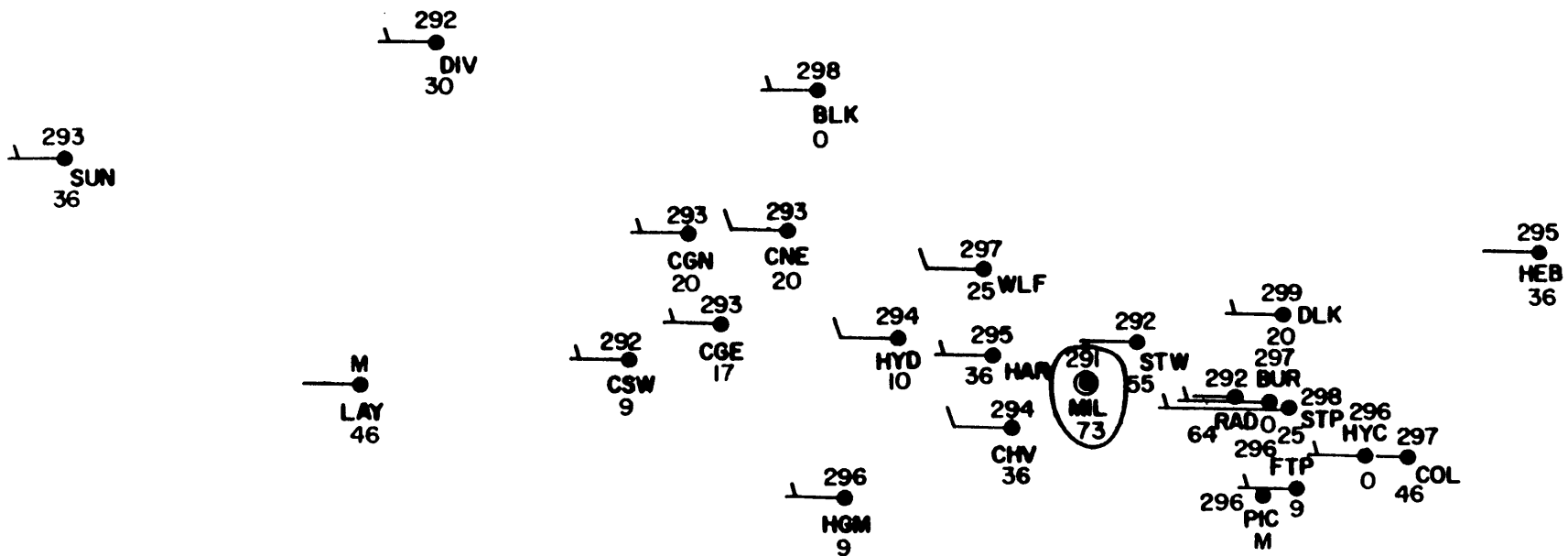


Figure 18. Average west to east component of the wind (knots, shown as wind barbs), average potential temperature (kelvin, shown above the dots), and percent decoupled flow (shown below the dots) at 1700 MST for all days in which synoptic Category #1 was present.

(e) 2200 MST

As the evening progressed, the thermal gradient strengthened, but no downvalley winds were present at 2200 MST (see Figure 19). The mean U component airflow in the valley remained westerly or calm at all stations but decreased in magnitude within the valley (see Figure 19 and Table A-10). The middle valley was three to four degrees warmer than the upper valley at 2200 MST. Farther west, the lower valley was cooler than the middle valley, and two degrees warmer than the upper valley. A six degree kelvin temperature discontinuity was reestablished in the lowest 830 foot layer of the upper valley (see Figure 15). The frequency of decoupled flows remained highest in the upper valley (62 - 75%) and decreased toward the middle and lower valleys (50%). The frequency of decoupled flows also decreased with elevation, decreasing to 54% at 7380 feet and to less than 20% above 8000 feet.

b. Category 3, Post Frontal Flows(1) Slope Flows

Table 5 presents the mean (for all days in which synoptic category #3 was present) component of the wind parallel to the slope for selected PROBE stations at five different hours of the diurnal cycle. At HYD (6570 ft), the airflow was consistently down slope (from the north), and very light. At LAY (6180 ft) the airflow was always blowing upslope and at less than two meters per second. The speed of the slope wind at LAY increased from 0700 MST to 1400 MST and decreased the rest of the period. Therefore, while the V winds at LAY exhibited slope flow characteristics embedded in the net flow, the V winds at HYD did not exhibit any slope flow characteristics.

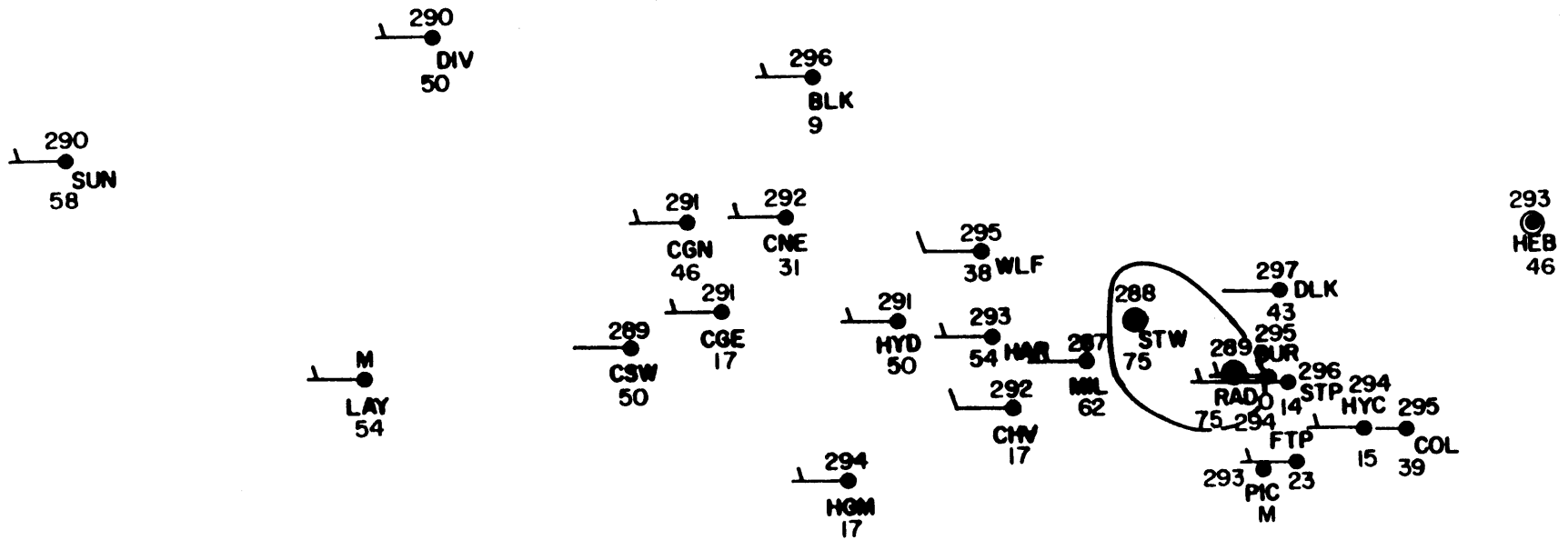


Figure 19. Average west to east component of the wind (knots, shown as wind barbs), average potential temperature (kelvin, shown above the dots), and percent decoupled flow (shown below the dots) at 2200 MST for all days in which synoptic Category #1 was present.

Table 5

Summary of the mean (for all days in which synoptic Category #3 was present) diurnal variation of the component of the wind parallel to the slope for selected PROBE stations. Elevations are listed in feet. Wind speed units are knots. Standard deviations are listed in parenthesis. All times are Mountain Standard.

Station (elev.)	0700	1100	1400	1700	2200
LAY (6180)	0.6 (4.1)	2.7 (4.7)	3.5 (5.8)	1.6 (5.6)	1.2 (3.7)
HYD (6570)	-0.6 (2.9)	-0.2 (3.1)	-1.2 (3.7)	-1.6 (3.1)	-1.2 (2.9)

(1) Valley Flows(a) 0700 MST

Figure 20 illustrates the average u (west to east) component of the surface wind (knots), potential temperature (K), and percent decoupled flow for periods in which the region was characterized by the recent passage of a cold front at 0700 MST. Appendix A (Tables A-11 through A-15) presents the average, standard deviation, minimum, maximum, 75th, 50th, 25th percentiles and the number of observations of the west to east component of the wind for these days during the study period at 0700, 1100, 1400, 1700 and 2200 MST.

At 0700 MST, downvalley flows (referring only to the mean U component airflow at each PROBE station) did not exist (see Figure 20 and Table A-11). Speeds varied from 1.2 knots in the upper valley (RAD and STW) to 11.1 knots on top of Wolf Mountain (WLF). Standard deviations of the mean U component wind were larger than the mean on the valley floor but not on the slopes, ridges, and peaks above the valley floor. U component wind speeds were stronger on the slope (HAR and CHV) above the constriction in valley width than at Black Mountain (BLK, 9900 ft) which may indicate channelling of the flow. As compared to the climatology study at 0700 MST, 10 of 23 stations had decreases in the standard deviation of the mean U component wind.

Figure 20 illustrates the mean potential temperature (K) distribution within the study area for periods in which synoptic Category #3 (post-frontal) were present at 0700 MST. Considering only those stations on the valley floor (MIL, STW, RAD, HYD, CNE, CGE, CGN, CSW, DIV, LAY and SUN) the upper valley was typically 283 K while the middle and lower valley were typically 284 to 285 K. Therefore, a thermal gradient

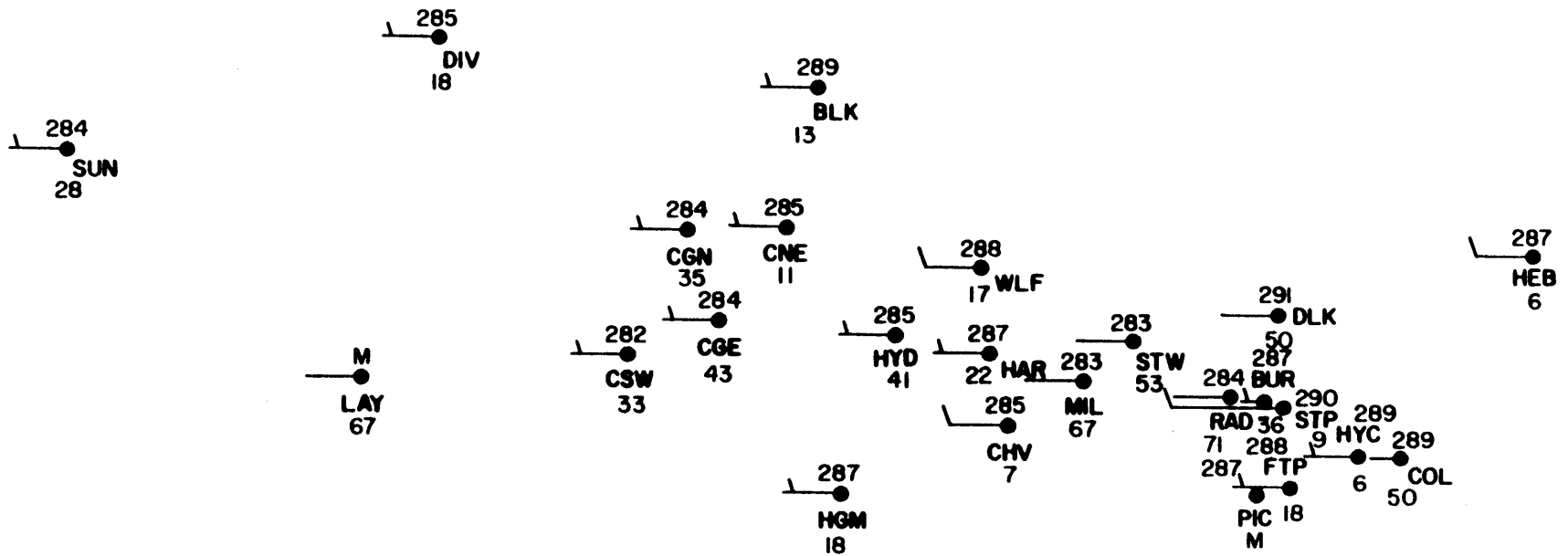


Figure 20. Average west to east component of the wind (knots, shown as wind barbs), average potential temperature (kelvin, shown above the dots), and percent decoupled flow (shown below the dots) at 0700 MST for all days in which synoptic Category #3 was present.

existed at 0700 MST, with potential temperatures increasing toward the lower end of the valley.

Figure 21 illustrates the vertical profile of potential temperature. It was constructed using PROBE data for selected stations in the upper valley. At 0700 MST, a four degree kelvin temperature discontinuity existed between RAD (6800 ft) and HAR (7380 ft). This discontinuity is much weaker than the mean temperature discontinuity observed for all days in which synoptic Category #1 (prefrontal flows) was present. When this profile is compared to that of the climatology, mean potential temperatures were warmer below 7380 feet during post frontal flows. Also, the mean potential temperature at STP was three degrees colder than the mean potential temperature for the climatology. The upper level discontinuity observed at 0700 MST for the climatology was not present during post frontal flows.

As mentioned previously, the frequency of decoupled flow at a PROBE station, as defined in this paper, is the ratio of the number of occurrences in which the west to east component of the wind was less than 1.0 knots to the total number of observations multiplied by 100. In this particular section this ratio is expressed as a percentage and only applies to times in the study period in which post-frontal flows (synoptic Category #3) occurred.

Figure 20 illustrates the percent occurrence of decoupled flows at 0700 MST for all days in which synoptic category #3 was present. The frequency of decoupled flows ranged from 67% at LAY (6180 ft) to 9% at STP (10330 ft). With the exception of LAY, the upper valley (MIL, STW, and RAD) had the highest frequency of decoupled flows in the study area, greater than 53%. The next highest frequency of decoupled flow occurred

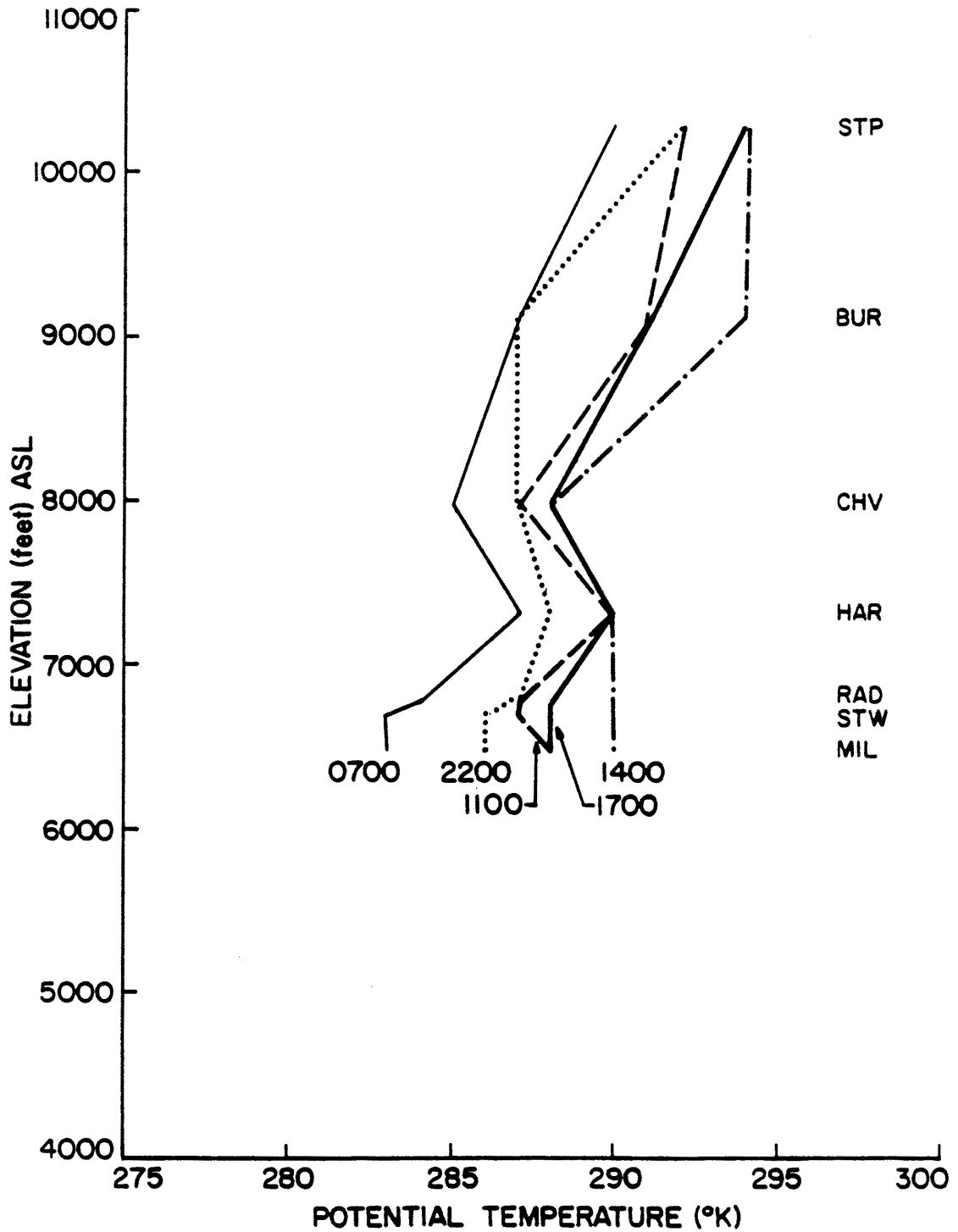


Figure 21. Average vertical profile of potential temperature (kelvin) constructed from selected PROBE station data for all days in which synoptic Category #3 was present.

in the middle and lower valley ranging from 11% at CNE (6910 ft) to 67% at LAY. On the slopes above the constriction in valley width, decoupled flows occurred 22% of the time at HAR (7380 ft), while directly across the valley, decoupled flows occurred only 7% of the time at CHV (8000 ft). On the barrier, the occurrence of decoupled flow varied from 50% at DLK (9180 ft) to 9% at STP (10330 ft). The distribution of decoupled flows remained similar to that observed at 0700 MST during synoptic Category #1. However, the frequencies are substantially lower than those observed during synoptic Category #1.

(b) 1100 MST

At 1100 MST, winds remained up valley, the thermal gradient no longer existed on the valley floor, the temperature discontinuity had strongly diminished and the spatial distribution of the frequency of decoupled flow remained the same as that observed at 0700 MST. Seventeen stations experienced an increase in wind speed, only five reported a decrease, all flows remained up valley (see Figure 22 and Table A-12). Three of the decreases in wind speed occurred near the constriction at HAR, CHV, and WLF. While increases in potential temperature were observed at all stations, the greatest increases occurred in the upper valley. The temperature discontinuity between RAD (6800 ft) and HAR (7380 ft) had now diminished to half of its previous value at 0700 MST. The frequency of decoupled flows decreased slightly from the 0700 MST observations (see Figure 21). Frequencies ranged from 56% at RAD (6800 ft) to 0 % at HYC (9590 ft) on the lee side of barrier. The overall spacial distribution of decoupled flows remained very similar to that of 0700 MST.

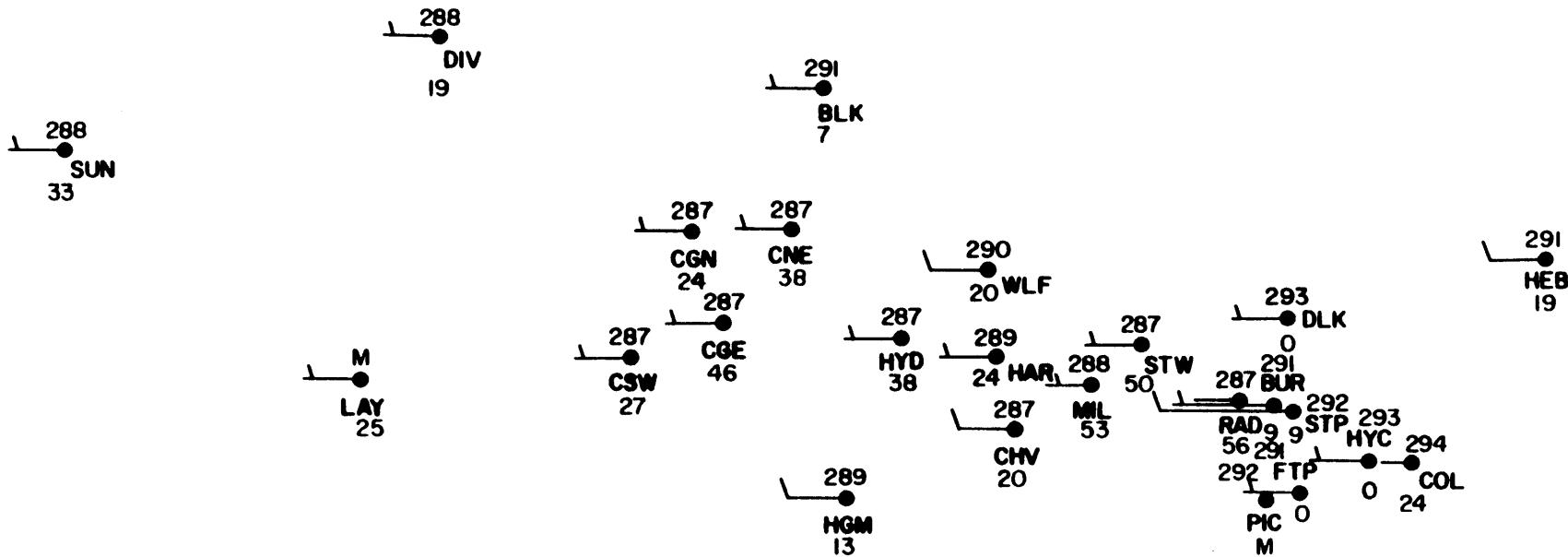


Figure 22. Average west to east component of the wind (knots, shown as wind barbs), average potential temperature (kelvin, shown above the dots), and percent decoupled flow (shown below the dots) at 1100 MST for all days in which synoptic Category #3 was present.

(c) 1400 MST

By 1400 MST a noticeable change had occurred in the valley airflow and thermal structure. Significant increases in the mean U component wind speed had occurred in the lower and middle valley while the rest of the valley experienced increases of lessor magnitude (see Figure 23 and Table A-13). Wind speeds in the lower and middle valley had increased from four to six knots to six to eight knots. By 1400 MST the upper valley (RAD, STW, MIL) had warmed to one degree kelvin greater than the middle valley (CGN, CSW, CNE, CGE, HYD). Although very weak, this thermal gradient would have contributed to up valley flows. The temperature discontinuity previously present at 0700 MST was no longer present at 1400 MST in the lower layer. However, a 6 degree discontinuity was present between CHV (8000 ft) and BUR (9180 ft). The frequency of occurrence of decoupled flows had continued to decrease but the same spatial distribution as observed earlier remained (see Figure 21).

(d) 1700 MST

Although cooling had begun throughout the valley by 1700 MST, no discernable changes had occurred in the valley airflow (see Figure 24). Mean U component wind speeds ranged from 1.6 knots at RAD (6800 ft) to 15.4 knots at STP (10330 ft) (see Table A-14). With the exception of STP, the strongest mean flows occurred at and above the constriction in valley width (HAR, CHV, and WLF). The thermal gradient present along the valley floor at 1400 MST was no longer present. Most areas continued to observe decreases in decoupled flow frequency and the overall occurrence of decoupled flows was at a minimum (see Figure 24). The spatial distribution of decoupled flow remained the same.

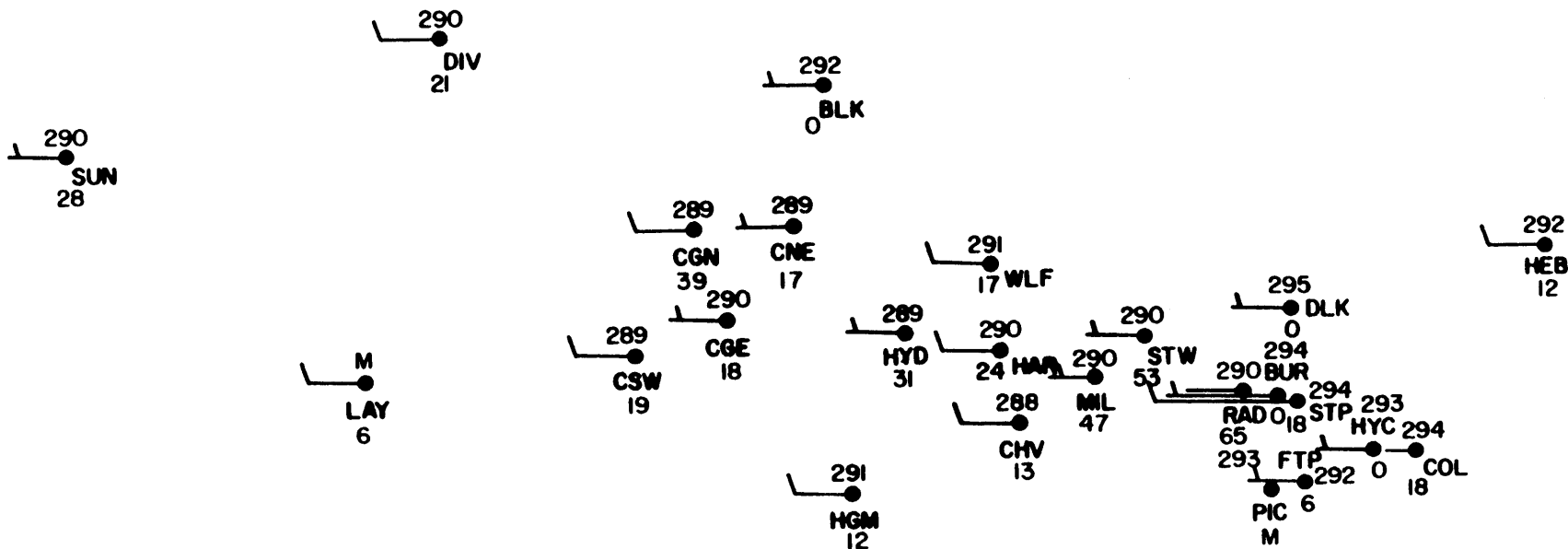


Figure 23. Average west to east component of the wind (knots, shown as wind barbs), average potential temperature (kelvin, shown above the dots), and percent decoupled flow (shown below the dots) at 1400 MST for all days in which synoptic Category #3 was present.

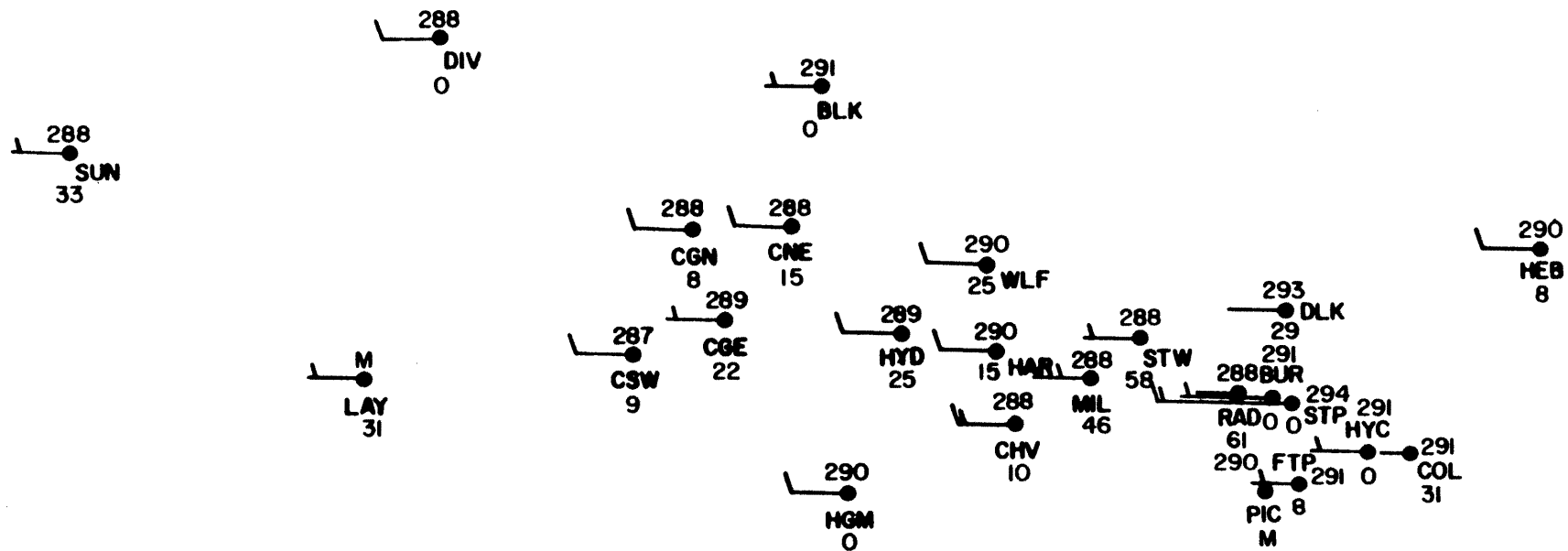


Figure 24. Average west to east component of the wind (knots, shown as wind barbs), average potential temperature (kelvin, shown above the dots), and percent decoupled flow (shown below the dots) at 1700 MST for all days in which synoptic Category #3 was present.

(e) 2200 MST

By 2200 MST, a noticeable decrease in mean U component wind speed had occurred in the study area but up valley flows were still the mean for all stations (see Figure 25 and Table A-15). Thirteen stations experienced decreases in the mean U component wind, while only five stations experienced increases. Mean west to east component wind speeds ranged from 1.2 knots at STW (6730 ft) to 15.4 knots at STP (10330 ft). Fifteen of 23 stations had a decrease in the standard deviation of the mean U component wind as compared to the mean U component wind for all days during the study period.

Cooling continued throughout the study area at 2200 MST (see Figure 25). The horizontal distribution of mean potential temperatures was the same at 2200 MST as at 1700 MST. At 2200 MST, a five degree kelvin temperature discontinuity existed between 9180 feet and 10330 feet. This discontinuity was further supported by a 10 knot wind sheer existing between these two stations (BUR [9180 ft] and STP [10330 ft]).

By 2200 MST the frequency of decoupled flows increased in the lower, middle and upper valley. The slope stations above the valley floor (HGM, CHV, HAR, DLK, BUR, and FTP) and the PROBE stations at the peaks and ridges observed about the same frequency of decoupled flows as at 1700 MST. The frequency of decoupled flow remained the highest in the upper valley (23 - 58%). Toward the middle valley these frequencies decreased to 15 to 31% and 20 to 62% in the lower valley. The occurrence of decoupled flow also decreased with elevation and ranged from 0% to 43%.

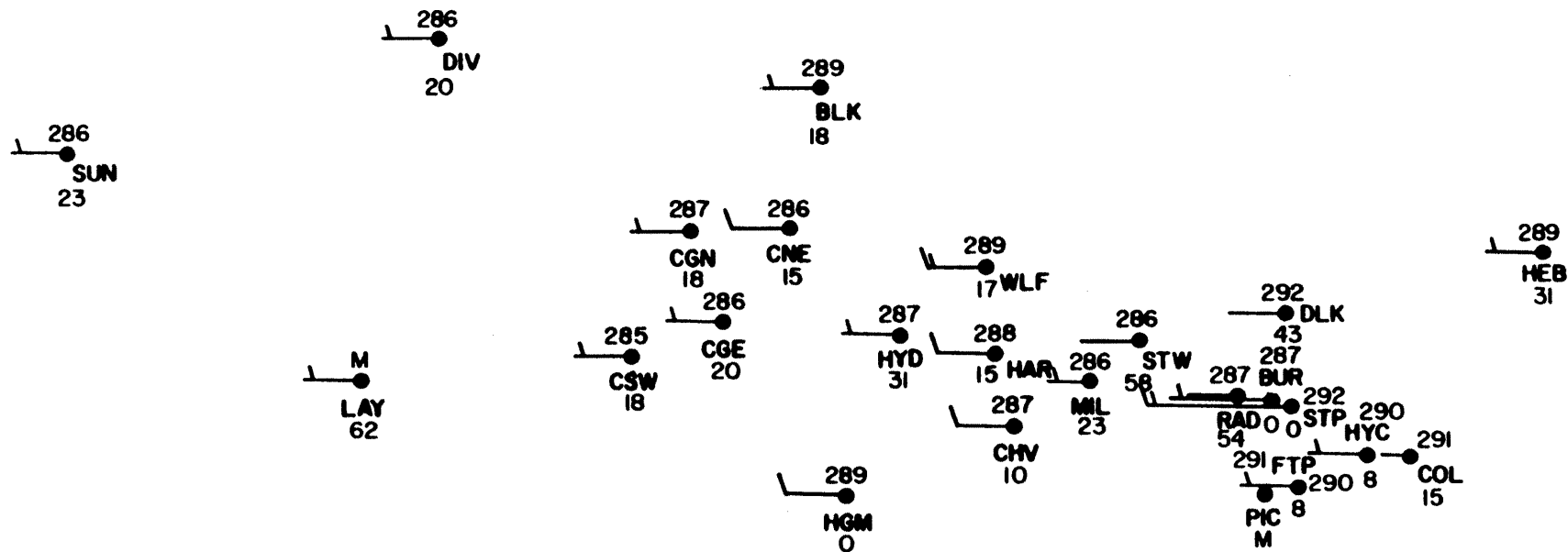


Figure 25. Average west to east component of the wind (knots, shown as wind barbs), average potential temperature (kelvin, shown above the dots), and percent decoupled flow (shown below the dots) at 2200 MST for all days in which synoptic Category #3 was present.

c. Category 4. Under a polar high in a region of anticyclonic curvature to the surface isobars

(1) Slope Flows

Table 6 is a listing of the mean component of the wind parallel to the slope of the local terrain for all days in which a polar high pressure system was the dominant synoptic feature encompassing the Yampa Valley of northwestern Colorado. Units are listed in knots and standard deviations of the mean are listed in parenthesis.

At PROBE station LAY (6180 ft.) a diurnal trend existed in the slope flow. Although no downslope winds were observed at the hours listed here, a diurnal variation was apparent in the strength of the upslope wind. At 0700 MST, the mean slope wind was 1.2 knots and gradually strengthened to 3.3 knots by 1400 MST. By 1700 MST, the strength of the upslope flow had weakened to 1.0 knots and remained less than 2.0 knots throughout the rest of the observation period. The standard deviation was larger than the mean in all cases but 1100 MST, indicating highly variable and turbulent flows, characteristic of slope flows.

At PROBE station HYD (6570 feet) a similar diurnal trend was observed. At 0700 MST, a 0.4 knot downslope flow existed which reversed directions to 1.0 knot upslope flow by 1100 MST. At 1400 MST the mean airflow was 0.2 knots, essentially calm. The direction reversed by 1700 MST to a 1.9 knot downslope flow. By 2200 MST the strength of the downslope flow had decreased to 1.2 knots. In each hour listed, the standard deviation remained larger than the mean slope flow. Embedded in the net flow at HYD, an upslope component was apparent during the morning heating hours and a downslope component was observed during the afternoon cooling hours.

Table 6

Summary of the mean (for all days in which synoptic Category #4 was present) diurnal variation of the component of the wind parallel to the slope for selected PROBE stations. Elevations are listed in feet. Wind speed units are knots. Standard deviations are listed in parenthesis. All times are Mountain Standard.

Station (elev.)	0700	1100	1400	1700	2200
LAY (6180)	1.2 (2.3)	2.3 (1.9)	3.3 (5.1)	1.0 (5.2)	1.6 (6.6)
HYD (6570)	-0.4 (2.1)	1.0 (1.7)	0.2 (2.1)	-1.9 (2.1)	-1.2 (1.9)

(2) Valley Flows(a) 0700 MST

Figure 26 illustrates the average u (west to east) component of the surface wind (knots), potential temperature (K), and percent decoupled flow for periods in which the region was dominated by a high pressure system at 0700 MST. Appendix A (Tables A-16 through A-20) presents the average, standard deviation, minimum, maximum, 75th, 50th, 25th percentiles and the number of observations of the west to east component of the wind for these days during the study period at 0700, 1100, 1400, 1700 and 2200 MST.

At 0700 MST, downvalley flows were present throughout the valley floor and on the adjacent slopes (see Figure 26 and Table A-16). In the upper valley, the airflow was calm. Further west, on the slopes above the constriction in valley width (HAR, and CHV) downvalley flows were stronger ranging from 1.9 knots at CHV (8000 ft) to 6.4 knots at HAR (7380 ft). In the middle valley (HYD, CGE, CNE, and CGN), downvalley flows ranged from calm at HYD (6570 ft) to 6.2 knots at CNE (6910 ft). Further west, in the lower valley (CSW, LAY, DIV, and SUN) downvalley flows were generally not as strong as the middle valley. On the barrier, DLK (9180 ft) was the only station to experience downvalley flows. The vertical extent of downvalley flow was located somewhere between 8000 feet (CHV) and 9135 feet (WLF).

At 0700 MST, mean potential temperatures along the valley floor ranged from 271 to 273 kelvin in the upper valley (MIL, STW, and RAD) to 276 (CGE) to 283 (CNE) in the middle and lower valleys. Thus, a strong thermal gradient existed along the valley floor at 0700 MST.

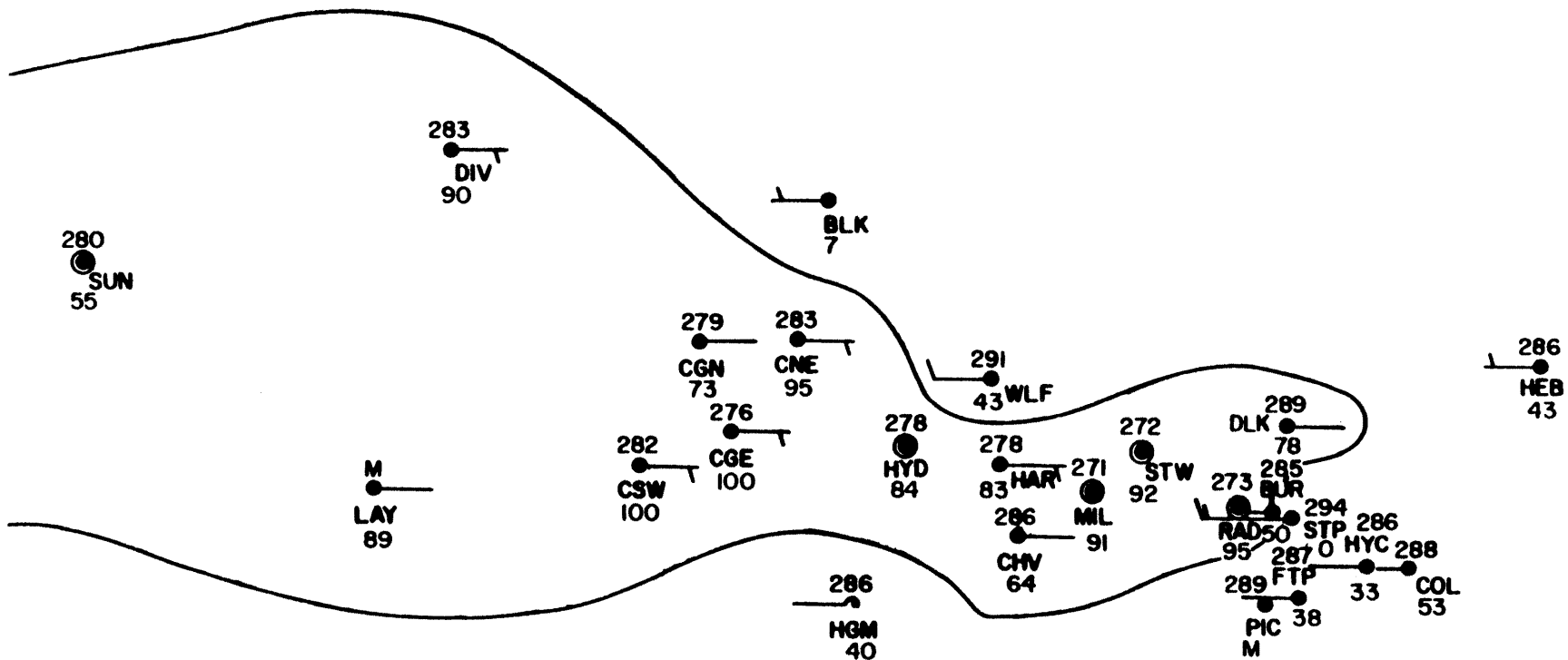


Figure 26. Average west to east component of the wind (knots, shown as wind barbs), average potential temperature (kelvin, shown above the dots), and percent decoupled flow (shown below the dots) at 0700 MST for all days in which synoptic Category #4 was present.

Figure 27 is a plot of the mean potential temperature (K) for selected PROBE stations, against elevation during periods in which high pressure was the dominant synoptic scale feature. The PROBE stations were chosen because they occupied an upper valley location or were within close proximity. Five time periods are shown in Figure 27 and were chosen to represent the change in vertical structure during the diurnal cycle.

The most prominent features in Figure 27 are the large scale temperature discontinuity at the lower levels and the difference in diurnal temperature variation between the lower elevation stations and the higher elevation stations. At 0700 MST, a 14 degree temperature discontinuity existed in 850 feet between MIL (6530 ft.) and HAR (7380 ft.). Above 9000 feet, another temperature discontinuity was apparent between BUR (9180 ft) and STP (10330 ft) in which the temperature increased 9 degrees in 1150 feet. Based on this information, it is likely that a strong temperature inversion was present in the upper valley at 0700 MST.

Figure 26 illustrates the percent of total observations (for synoptic Category #4 only) in which the U component airflow was less than 1.0 knots from the west at 0700 MST, referred to as percent decoupled flow. In the upper valley at 0700 MST, decoupled flow occurred greater than 90% of all days in which high pressure dominated the region. In the middle valley, the frequency of decoupled flow ranged from 73% (CGN) to 100% (CGE). Further west, in the lower valley, the frequency of decoupled flow was slightly less and ranged from 55% at SUN (6340 ft) to 90% at DIV (7130 ft). Within the constriction in valley width, decoupled flow ranged from 64% to 83% at CHV and HAR, respectively. This is in great contrast to the frequency of decoupled flow at the highest stations. Storm Peak

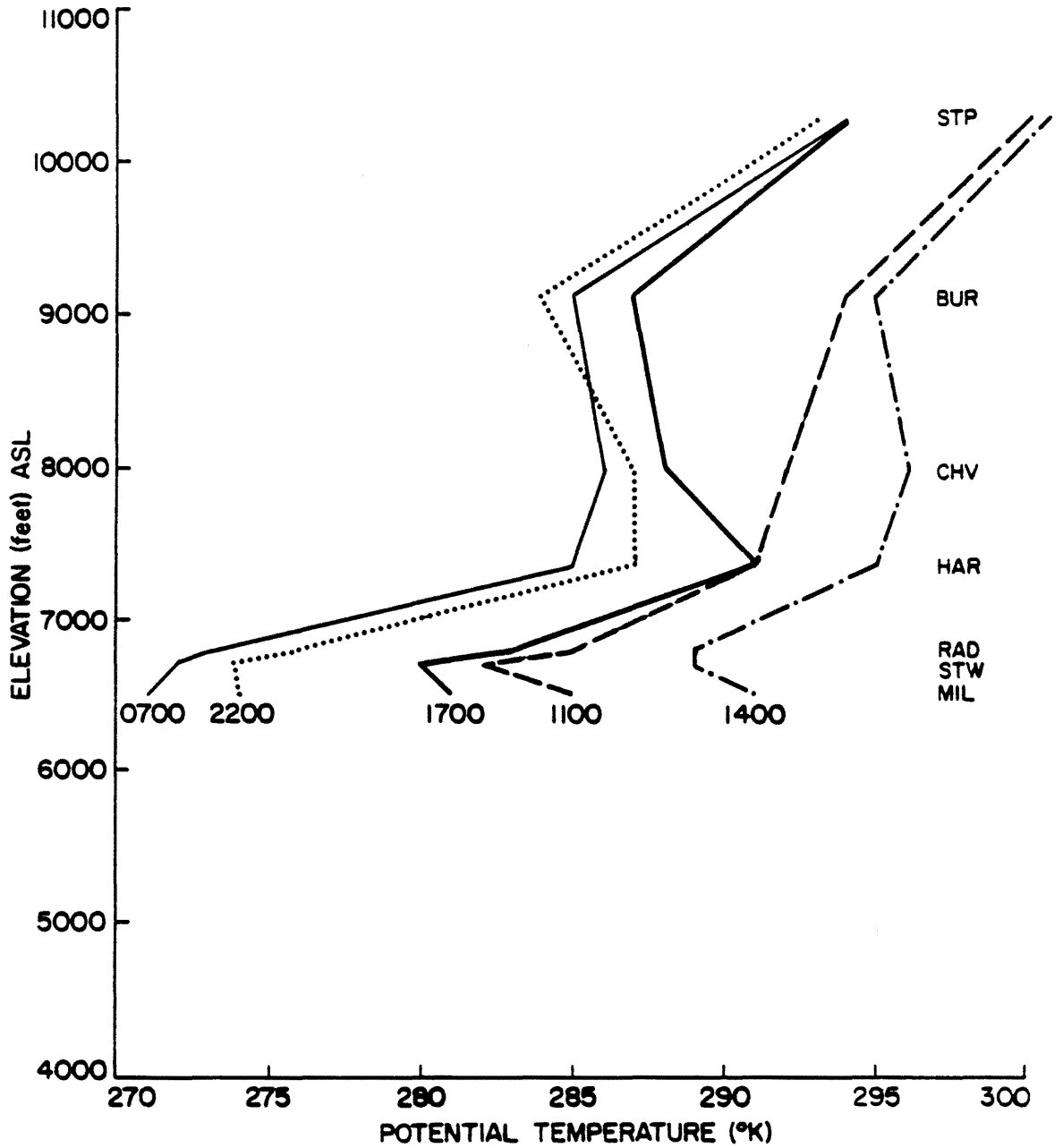


Figure 27. Average vertical profile of potential temperature (kelvin) constructed from selected PROBE station data for all days in which synoptic Category #4 was present.

(STP, 10330 ft) and Black Mountain (BLK, 9900 ft) experienced decoupled flow less than 10% of the time.

(b) 1100 MST

At 1100 MST, no significant changes had occurred in the valley airflow or thermal structure (see Figure 28 and Table A-17). Although the thermal gradient along the valley floor weakened, it still remained. The temperature discontinuity in the lower layer still remained (see Figure 27). The spacial distribution of the decoupled flow remained very similar to that observed at 0700 MST.

(c) 1400 MST

By 1400 MST, downvalley flows only occurred at three stations, CSW (6400 ft), CGE (6570 ft) and HAR (7380 ft) (see Figure 29 and Table A-18).

Mean U component winds in the upper valley (MIL, STW, and RAD) did not exceed 1.0 knots. For all times in the study period, this region continued to have the lightest winds throughout the study area. Up valley flow was present throughout most of the middle and lower valley and did not exceed 4.1 knots. Above the constriction in valley width, the north side of the river (HAR, 7380 ft) observed downvalley flows of 1.6 knots while on the south side and 620 feet higher CHV (8000 ft) up valley flows of 2.7 knots occurred. On the barrier, up valley flows occurred at all stations and varied from 2.1 knots at DLK (9180 ft) to 11.1 knots at STP (10330 ft).

By 1400 MST, the middle and lower valleys still remained warmer than the upper valley, although the thermal gradient had continued to diminish (see Figure 29). This thermal structure was not conducive to up valley circulation, but did support down valley circulations. As expected, the

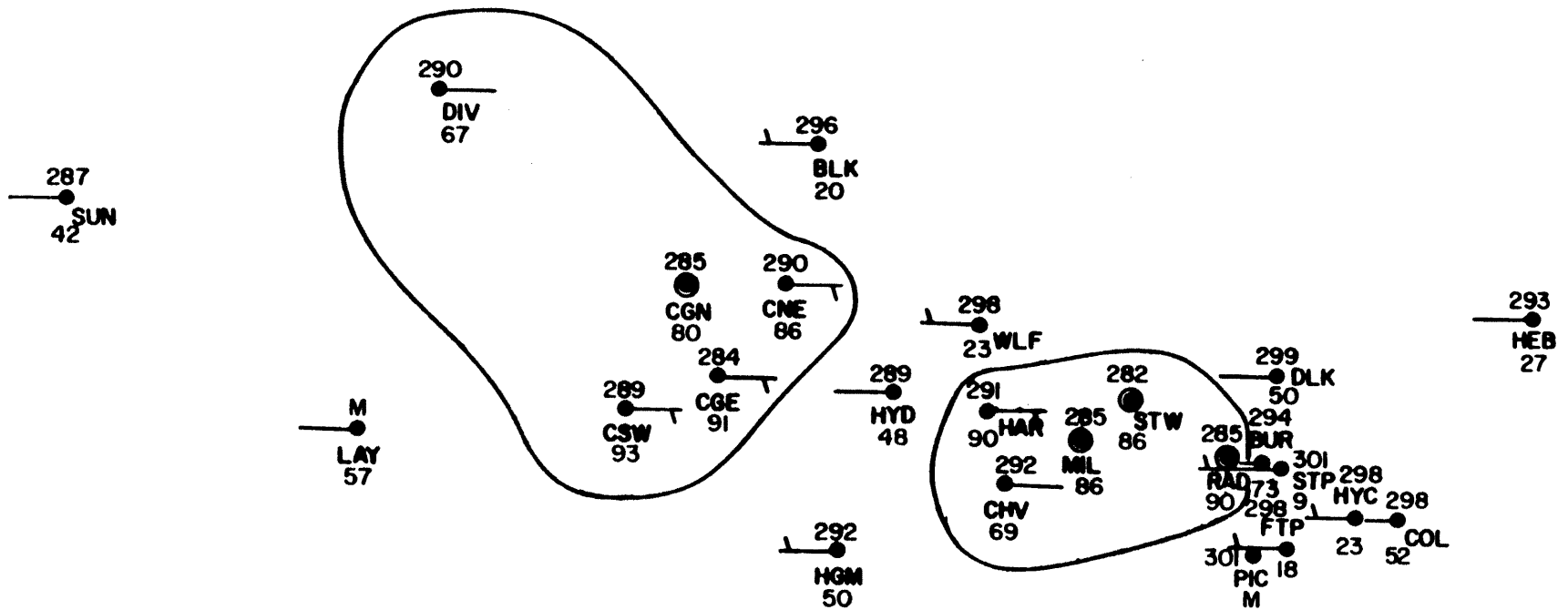


Figure 28. Average west to east component of the wind (knots, shown as wind barbs), average potential temperature (kelvin, shown above the dots), and percent decoupled flow (shown below the dots) at 1100 MST for all days in which synoptic Category #4 was present.

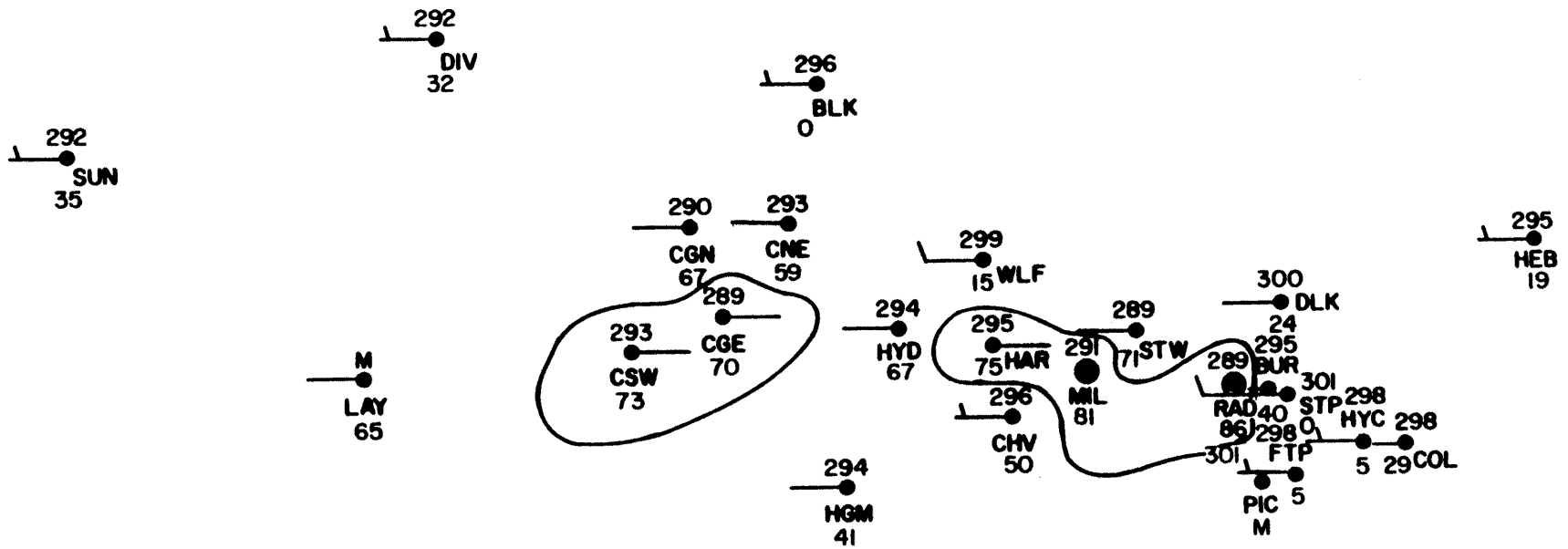


Figure 29. Average west to east component of the wind (knots, shown as wind barbs), average potential temperature (kelvin, shown above the dots), and percent decoupled flow (shown below the dots) at 1400 MST for all days in which synoptic Category #4 was present. M= missing data

valley had reached the warmest mean potential temperatures of the diurnal period.

By 1400 MST, the lower elevation stations (MIL, STW, and RAD) had warmed by 18 degrees since 0700 MST, while the higher elevation stations had only warmed by 10 degrees since 0700 MST (see Figure 27). Thus, the temperature discontinuity apparent at 0700 MST had diminished to 6 degrees in 650 feet between STW and HAR. The temperature discontinuity between 9180 feet and 10330 feet was still present at 1400 MST, although it too had diminished to only a 6 degree discontinuity.

From the temperature discontinuity information and the difference in wind direction between HAR (7380 ft) and CHV (8000 ft) the top of the decoupled layer appeared to be between 7380 feet and 8000 feet in the upper valley. Below this discontinuity, the frequency of decoupled flow continued to be above 50% but less than the 90% seen earlier at 0700 MST. The horizontal extent of this decoupled layer extended to the middle valley and even to the lower valley but only along the river as seen by LAY (6180 ft).

(d) 1700 MST

By 1700 MST, differential cooling had begun throughout the valley and westerly flows had weakened at most valley locations but did not reverse to downvalley flows (see Figure 30 and Table A-19). The middle valley had cooled up to nine degrees colder than the upper valley while the lower valley had cooled up to seven degrees colder than the upper valley. Therefore, the thermal gradient along the valley floor was strengthening. Figure 27 illustrates the increase in the temperature discontinuity between 6730 feet (STW) and 7380 feet (HAR).

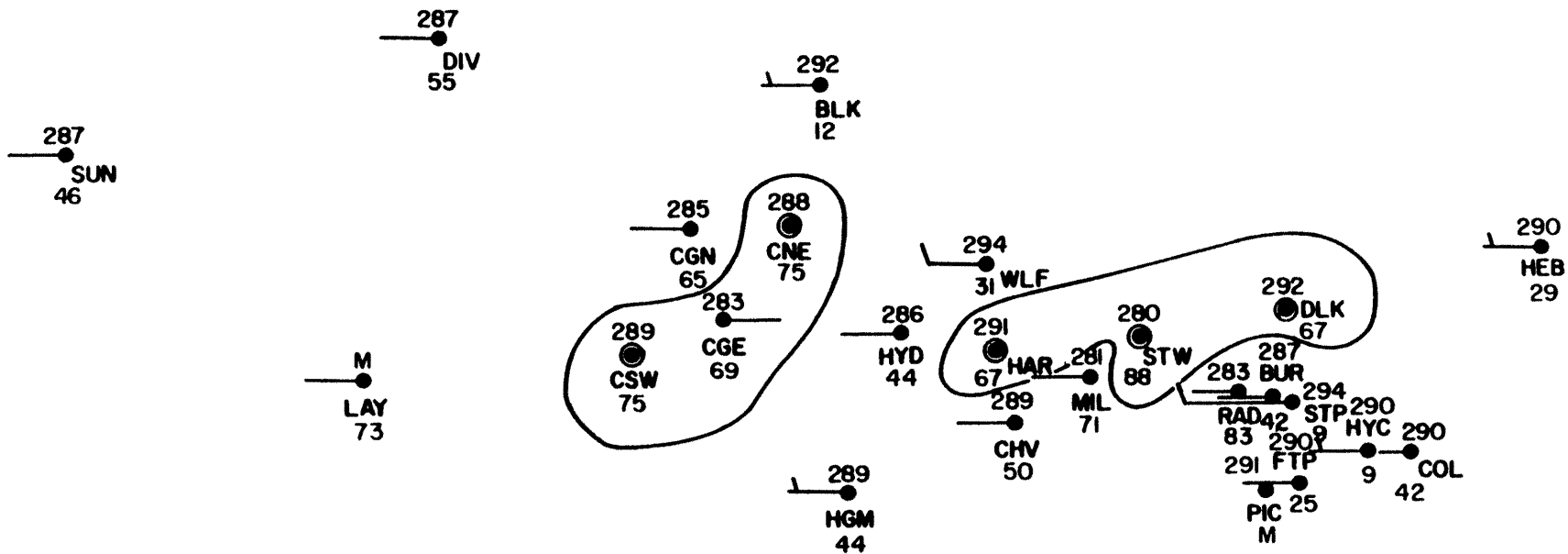


Figure 30. Average west to east component of the wind (knots, shown as wind barbs), average potential temperature (kelvin, shown above the dots), and percent decoupled flow (shown below the dots) at 1700 MST for all days in which synoptic Category #4 was present.

The extent of the decoupled flow layer was increasing since 1400 MST. Figure 30 illustrates the difference between the wind at HAR (7380 ft) and CHV (8000 ft). The top of the decoupled layer was somewhere between these two stations. The horizontal extent of the decoupled layer was increasing in width in the lower valley as indicated by the increase in frequency of decoupled flow at SUN (6340 ft) and DIV (7130 ft).

(e) 2200 MST

By 2200 MST downvalley flows were more prevalent (see Figure 31 and Table A-20). The upper valley (MIL, STW, and RAD) still remained relatively calm, while downvalley flows in the middle and lower valleys were accelerating. Mean U component winds in this region ranged from 1.9 knots up valley at HYD (6570 ft) to 2.5 knots down valley at CGE (6570 ft). Above the constriction in valley width HAR experienced a mean downvalley flow of 3.7 knots while across the valley at CHV (8000 ft), a mean up valley flow of 1.7 knots occurred. As expected, westerly flows continued at the higher elevations of WLF (9135 ft), BLK (9900 ft), and STP (10330 ft).

By 2200 MST, the valley had continued to cool and the mean potential temperature distribution was very similar to that of 0700 MST (see Figure 31). Mean potential temperatures along the valley floor ranged from 274°K at MIL and STW in the upper valley, to 284°K at CSW in the middle valley. Thus, the thermal gradient along the valley floor continued to strengthen in support of a down valley circulation.

By 2200 MST, differential cooling had continued to occur along the valley floor and with elevation. The large temperature discontinuities that were present at 0700 MST, were reestablished by 2200 MST at both levels (see Figure 27).

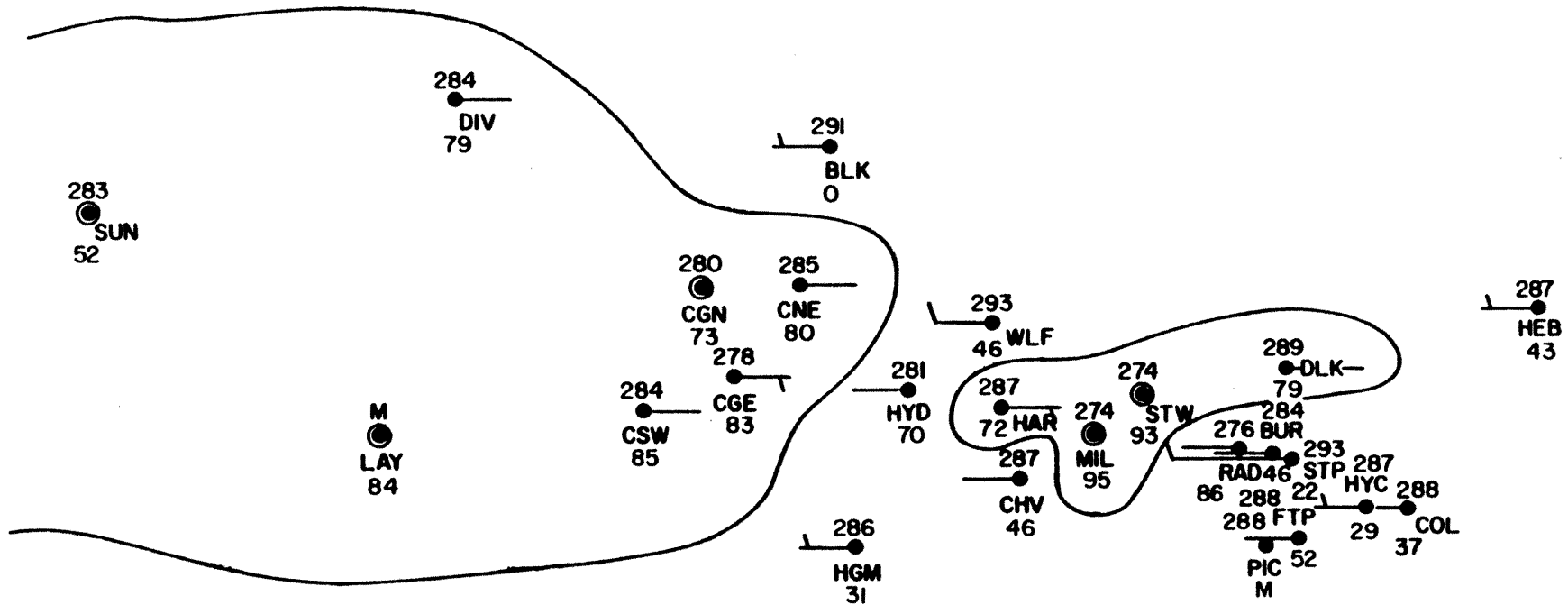


Figure 31. Average west to east component of the wind (knots, shown as wind barbs), average potential temperature (kelvin, shown above the dots), and percent decoupled flow (shown below the dots) at 2200 MST for all days in which synoptic Category #4 was present.

As evening cooling progressed, the frequency of decoupled flows increased throughout the study area (see Figure 31). By 2200 MST, the frequency of these decoupled flows ranged from 95% at MIL (6530 ft), in the upper valley, to 0% at BLK (9900 ft) at the higher elevations. On the valley floor, decoupled flow occurred more than half the time. It extended all the way out to the lower valley and vertically to between 7380 feet and 8000 feet.

C. CASE STUDIES

1. 8 December 1981

a. Synoptic Pattern

Figure 32 illustrates the 500 mb (32a), 700 mb (32b), and surface (32c) synoptic weather maps for 8 December 1981 at 0500 MST. The surface map illustrates that the region of interest is influenced by high pressure in the region of anticyclonic curvature to the surface isobars, a category 4 classification. Above the valley, at 500 mb, winds were from the northwest at 40 knots; the potential temperature was 315°K. Below this level, at 700 mb, winds were from the west-northwest at 15 knots and the potential temperature was 305°K. Snowpack was considered unusually heavy. Conditions did not change significantly throughout this case study.

b. Summary of PROBE Observations

Free atmospheric synoptic flows were observed at stations located only at the highest elevations over 10000 feet, 3350 feet above the valley floor and only during periods of maximum temperature (1100-1700 MST). Storm Peak (STP, 10330 ft) experienced synoptic flow characteristics during the afternoon. Figure 33 illustrates at 1400 MST the winds at STP were from the west-northwest at 15 knots. Figure 34 illustrates that the

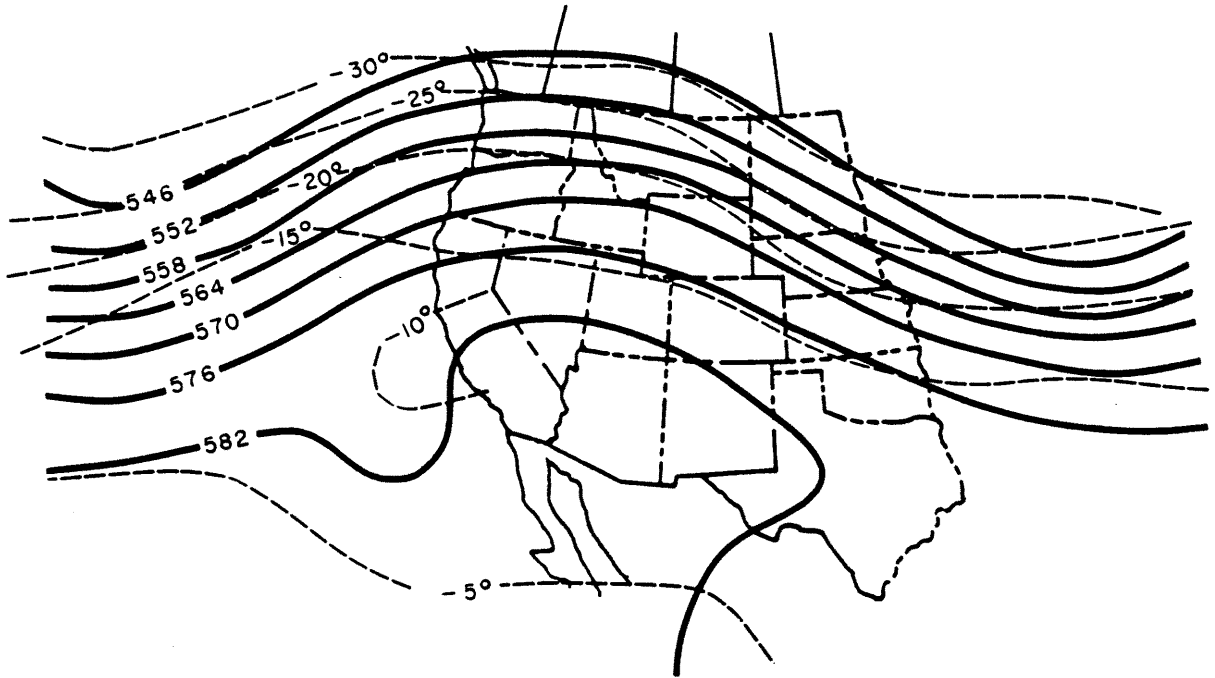


Figure 32a. 500 mb upper level map depicting synoptic conditions of December 8, 1981 at 0500 MST.

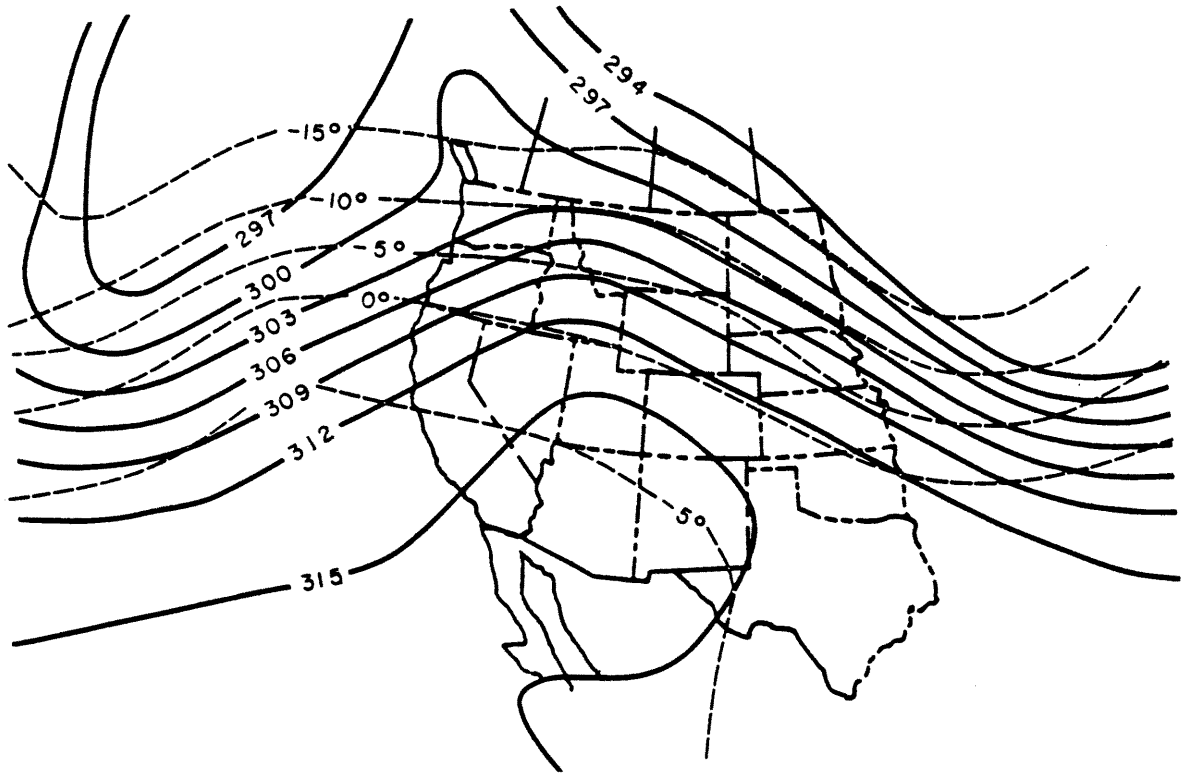


Figure 32b. 700 mb upper level map depicting synoptic conditions of December 8, 1981 at 0500 MST.

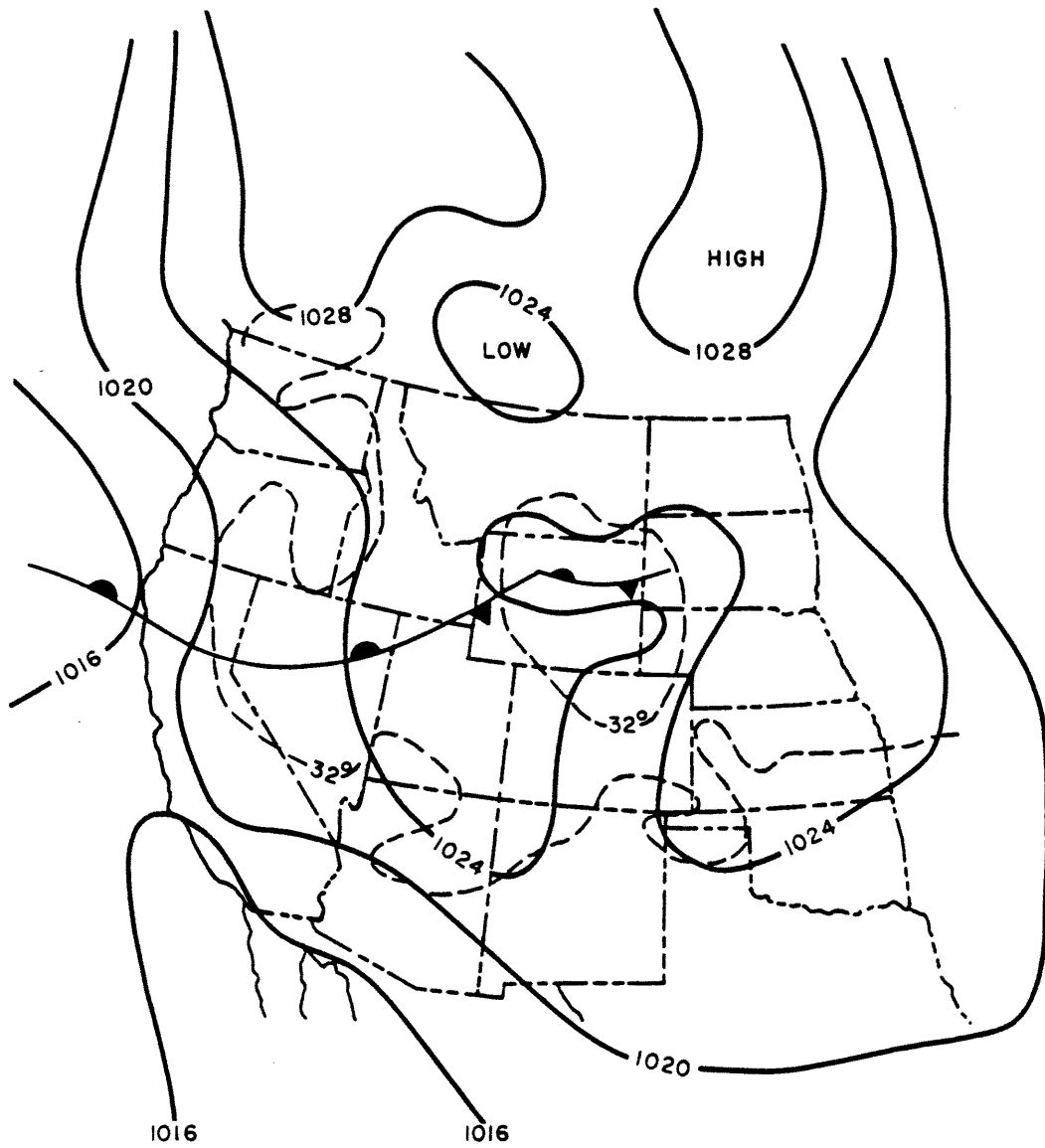


Figure 32c. Surface map depicting synoptic conditions of December 8, 1981 at 0500 MST.

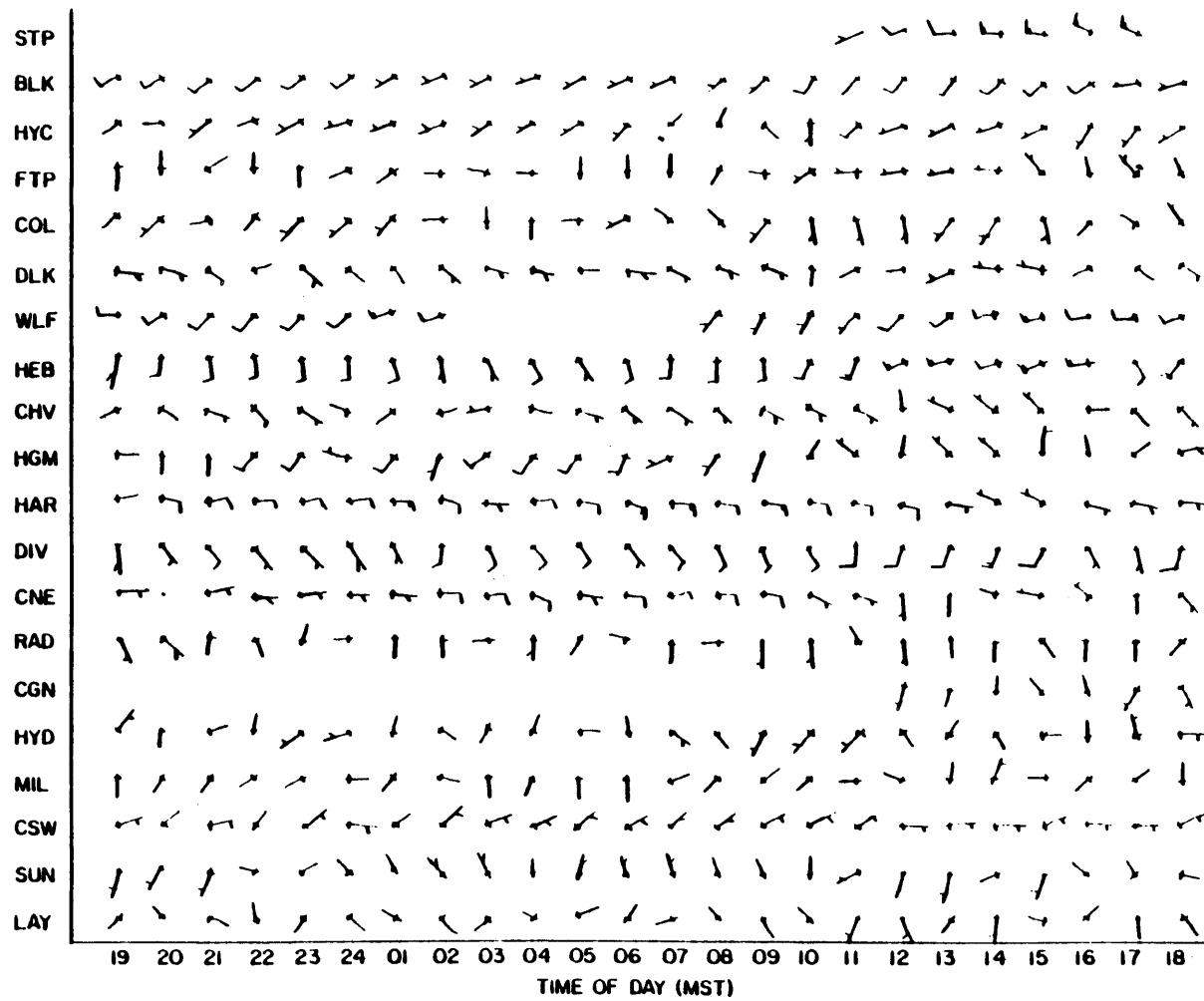


Figure 33. PROBE wind histories for 7 December 1981 at 1900 MST through 8 December 1981 at 1800 MST.

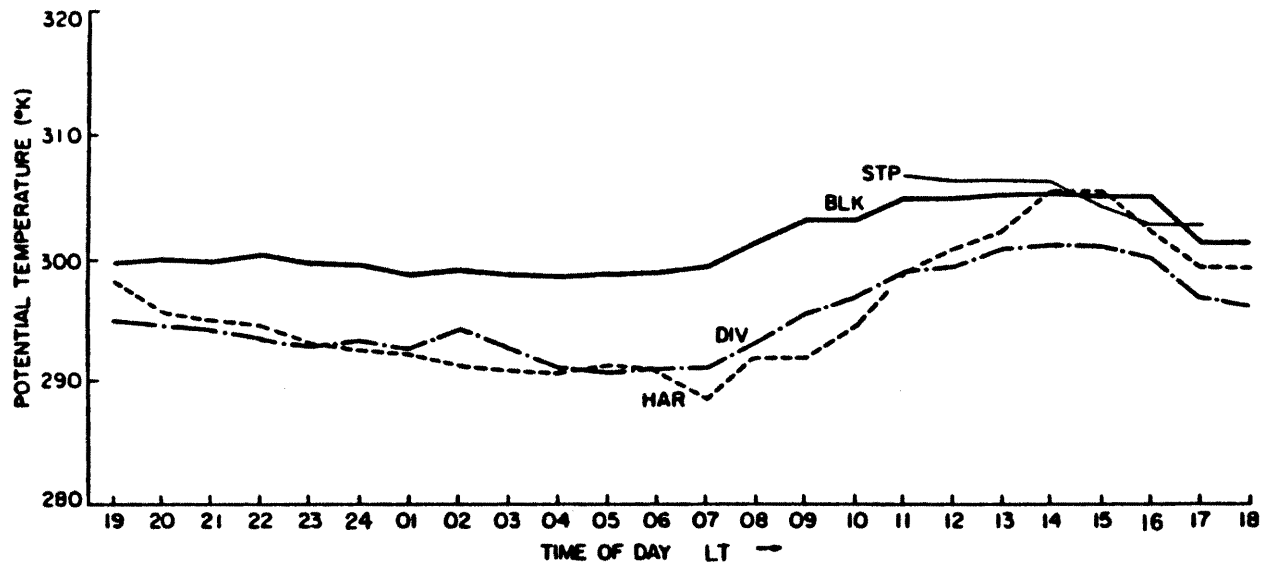


Figure 34. Potential temperature (kelvin) for selected PROBE stations (STP (10330 feet), BLK (9900 feet), HAR (7380 feet) and DIV (7130 feet)) from 7 December 1981 at 1900 MST to 8 December 1981 at 1800 MST.

potential temperature was 306°K , indicating the same airmass as the 700 mb synoptic wind.

Regional flow extended below the ridge tops down to BLK (9900 ft) and WLF (9135 ft) during the night and down to the valley floor at MIL (6530 ft) during the day. BLK (9900 ft) experienced regional flow throughout the 24 hour period. Figure 33 illustrates the winds at BLK were southwesterly at 5 knots through the night and southwesterly at 10 knots during the day. The wind speed was greater than that below at MIL (6530 ft) but less than the gradient winds aloft. Large scale pressure gradients caused the westerly direction. Figure 34 illustrates the potential temperature for BLK (9900 ft) was 300 K during the nocturnal period and increased to 307°K during the day, very close to that of the 700 mb synoptic airmass. During the cooler period of the day (1800-1000 MST) these regional flows extended down to WLF (9135 ft) as illustrated in Figure 33 by the south-southwesterly, 5 knot winds between 0800-1000 MST. During daytime heating these flows can extend down to MIL (6530 ft) on the valley floor, as illustrated in Figure 33 by light, west-southwesterly wind between 1500 and 1600 MST.

Figure 35 illustrates that the large temperature discontinuity between RAD (6800 ft, on the valley floor) and HAR (7380 ft, 835 feet above the valley floor), that was present during the evening and early morning hours (1700, 2200 and 0700 MST) was no longer present by late morning and afternoon (1100 and 1400 MST). This allowed mixing to occur all the way down to the valley floor.

Valley airflow was observed to vary diurnally and was typically directed down valley. During the nocturnal cooling period these flows extended as high as DLK (9180 ft), in the upper valley, roughly 2380 feet

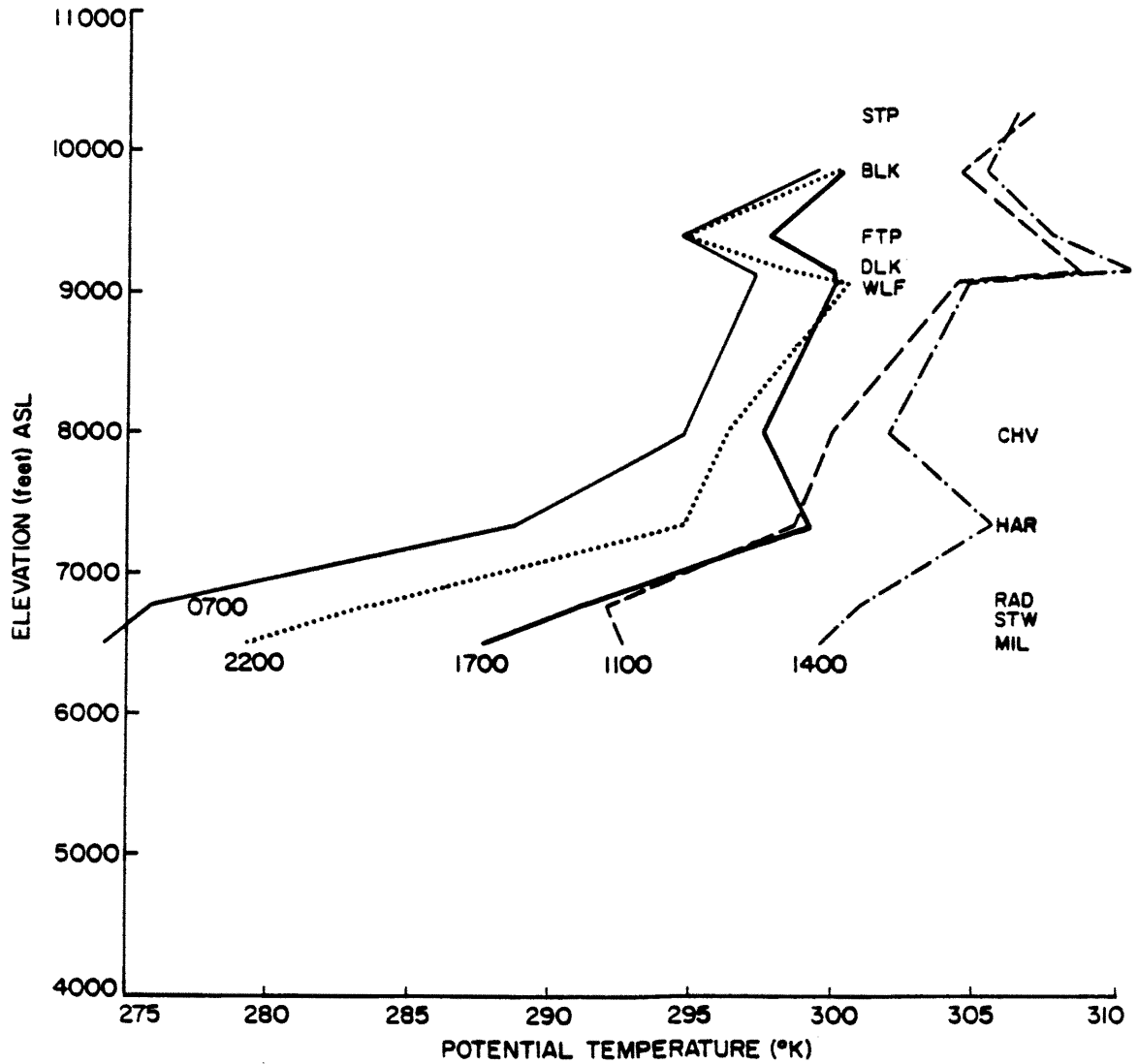


Figure 35. Vertical profile of potential temperature (kelvin) constructed from selected PROBE station data for 7 December 1981 at 1700 MST and 2200 MST to 8 December 1981 at 0700 MST, 1100 MST and 1400 MST. This time period is representative of synoptic Category #4.

above the valley floor as illustrated by the 5 knot easterlies between 1700 and 0900 MST in Figure 33. These valley flows were not observed on the upper valley floor during this period as shown by the calm winds at RAD (6800 ft) and MIL (6530 ft) in Figure 33. However, on the other side of the constriction between Hayden and Milner, downvalley winds were observed on the valley floor at CSW (6400 ft) during the nocturnal cooling period. Figure 36 illustrates the thermal gradient along the valley floor during the evening and early morning hours (1700, 2200 and 0700 MST). The upper valley always remained colder than the middle and lower valleys during these hours. It is this thermal gradient which forces the downvalley flow.

In contrast, during maximum daytime heating (1500 MST), valley flows were only observed at CSW (6400 ft). Figure 36 illustrates the thermal gradient at 1400 MST along the valley floor. The airmass in the upper valley (MIL, STW and RAD) never warmed greater than the middle and lower valleys enough to force an up valley flow. However, the airmass at Hayden (HYD) in the far eastern portion of the middle valley was warmer than the airmass in the western valley. Therefore, up valley flows could have been thermally forced in the middle and lower valleys.

The diurnal variation of the Valley flow was exemplified by the airflow at Mt. Harris (HAR, 7380 ft). Figure 33 illustrates HAR (7380 ft) experienced easterly, 5-10 knot winds between 1900 and 1300 MST. Figure 34 illustrates HAR's potential temperature during this period was colder than the regional airmass observed by BLK (9900 ft). However, at 1400 MST winds reversed to northwesterly at 5 knot (see Figure 33). At the same time, the potential temperature had increased to the same temperature as BLK (9900 ft) (see Figure 34). By 1600 MST the winds reversed back to

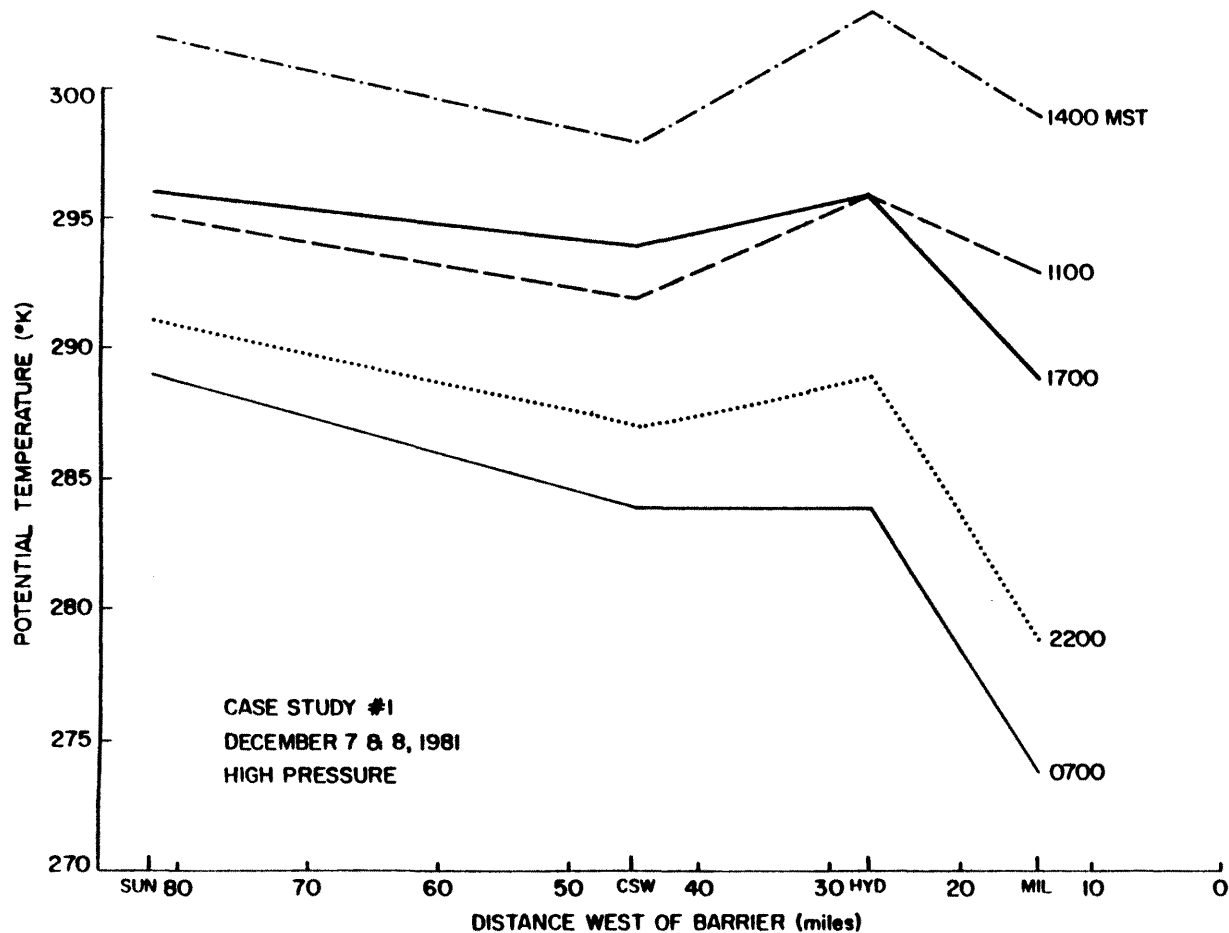


Figure 36. Time series of potential temperature (kelvin) for selected PROBE stations along the valley floor. Elevations are listed on the ordinate in feet (ASL). Distances west of the Barrier are listed along the abscissa in miles; the Barrier is located on the far right. Five hourly values are shown from 1700 MST on 7 December 1981 to 1400 MST on 8 December 1981.

easterly flow and the potential temperature began to decrease to colder temperatures than experienced by BLK (9900 ft).

Slope flow characteristics were observed in a variety of locations from high ridges [e.g., HYC (9590 ft)] to the valley floor [e.g., SUN (6340 ft)]. Figure 33 illustrates a downslope flow for DIV (7130 ft) between 2000 and 1000 MST. Winds were southeasterly at 5-10 kt, blowing in a downslope direction. The potential temperatures for this station was approximately 294°K, colder than the regional airmass experienced by BLK (9900 ft) (see Figure 34). However, at 1100 MST winds were blowing from the southwest at 10-15 knots. The potential temperature at this time indicated this station was still in a colder airmass than at BLK (9900 ft). Due to the late morning reversal and increased wind speeds, it is likely that DIV (7130 ft) was experiencing regional flow during 1100 MST on this day.

2. 15 December 1981

a. Synoptic Pattern

Figure 37 illustrates the 500 mb (37a), 700 mb (37b), and surface (37c) synoptic weather maps for 16 December 1981 at 0000 MST. The study area is characterized by an approaching cold front associated with a transient wave in the westerlies. At 500 mb, the coldest air (-35°C) was located over Canada, on the Manitoba-Ontario border. Over the northwestern United States a wave of cold air was moving towards northwestern Colorado with temperatures of -27 C. Above the study area at 500 mb, winds were from the west-northwest at 50 knots; the potential temperature was 309 K. Below this level, at 700 mb, winds were from the west-northwest at 27 knots and the potential temperature was 301 K. Figure 37a and 37b both illustrate falling geopotential heights at a rate

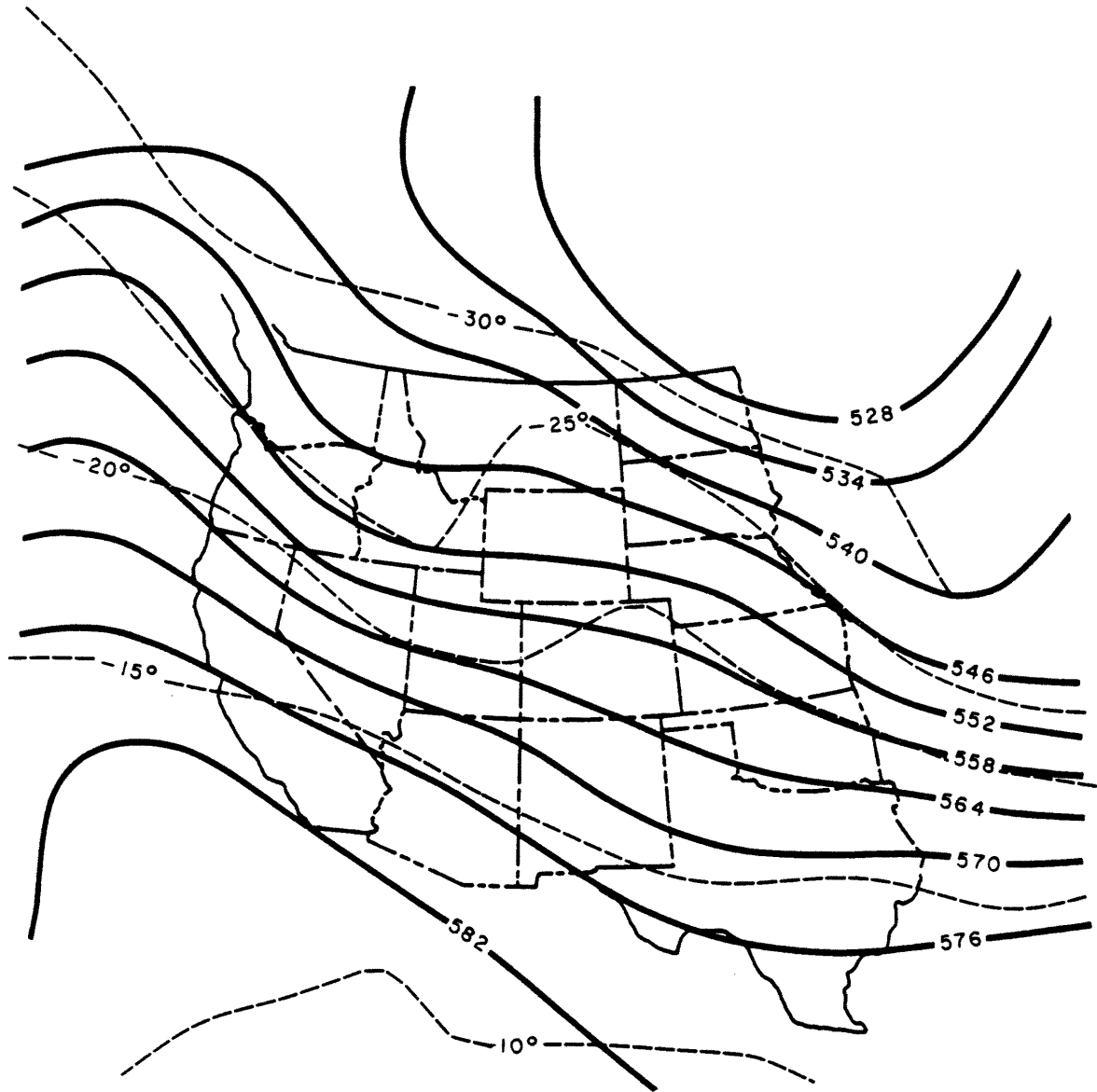


Figure 37a. 500 mb upper level map depicting synoptic conditions of 15 December 1981 at 1700 MST.

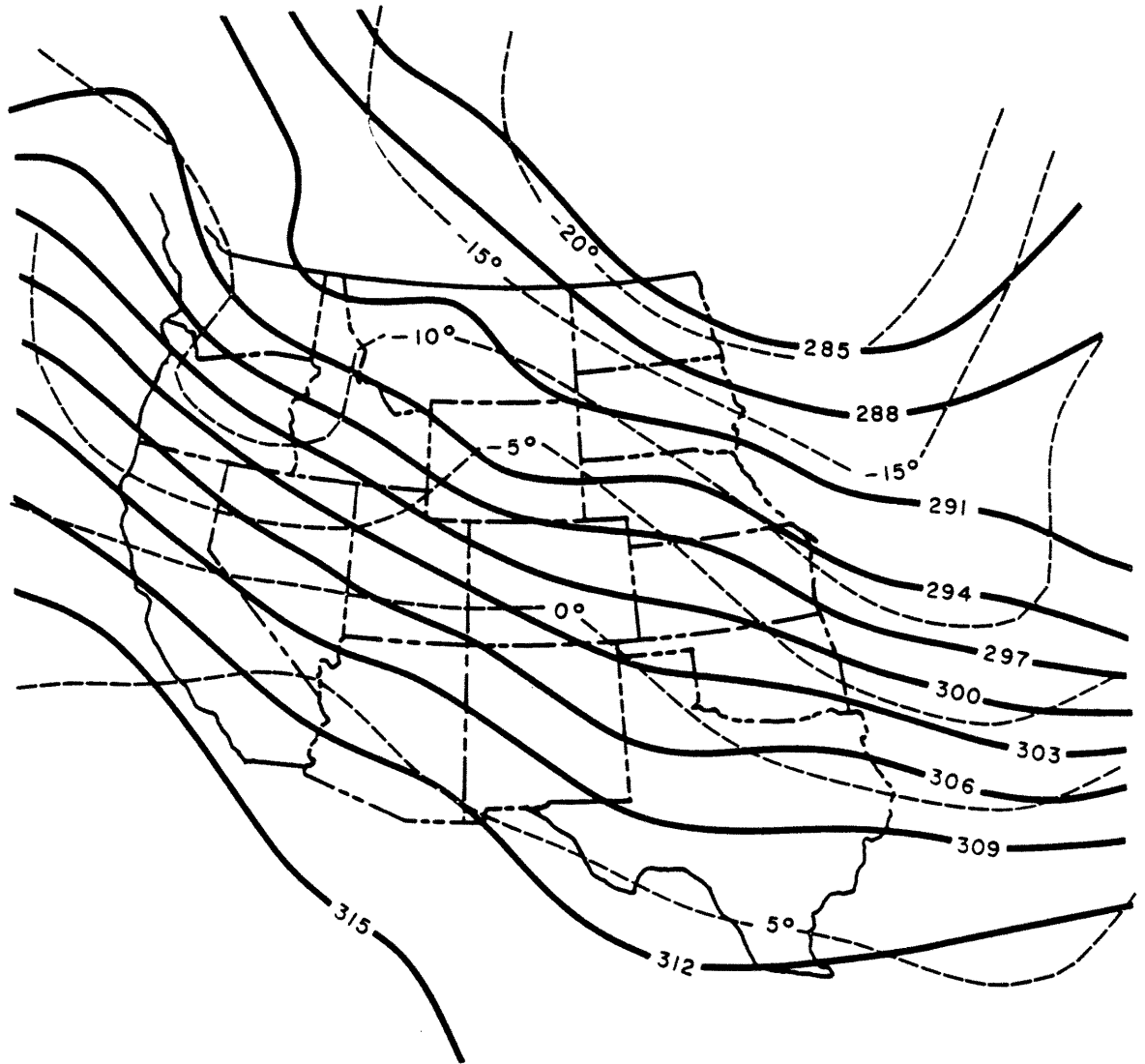


Figure 37b. 700 mb upper level map depicting synoptic conditions of 15 December 1981 at 1700 MST.

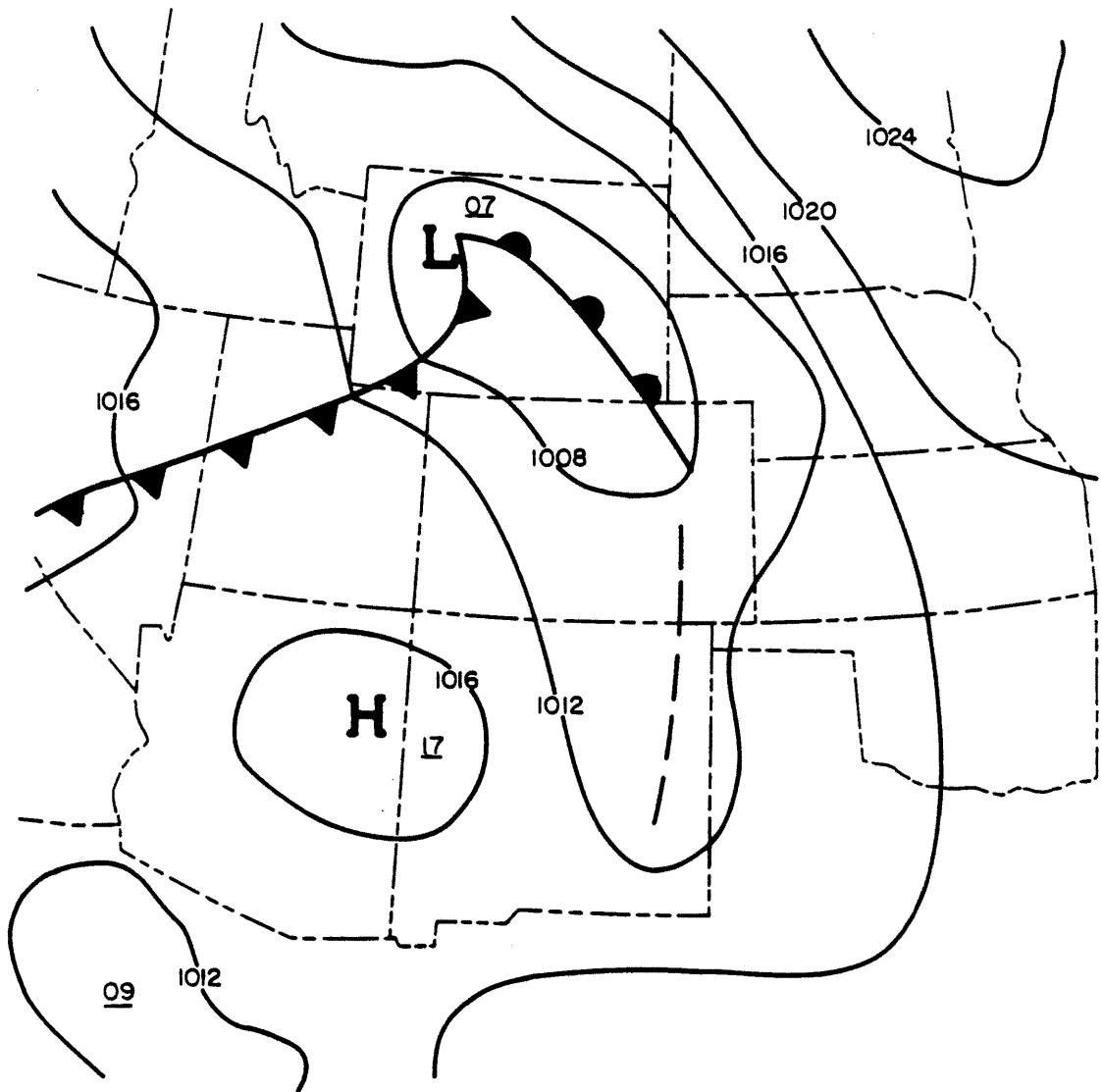


Figure 37c. Surface map depicting synoptic conditions of 15 December 1981 at 1700 MST.

of 5 decameters over the last 12 hours. The surface map illustrates the study area was located in the warm sector of the extratropical cyclone. Craig, Colorado was reporting precipitation in sight, but none falling at the station. Snowpack was considered unusually heavy for this time of the year.

b. Summary of PROBE Observations

Synoptic flows were not observed during this case study, with the noted distinction that no observations were available for the highest elevation PROBE station, STP (10330 ft). Synoptic flows were determined by the 700 mb map (Figure 37b). These flows were characterized by winds from the northwest at 25-30 knots and potential temperatures of 301 K. No stations reported winds and potential temperatures matching this description throughout the entire case study (see Figure 38 and 39).

Regional flows were observed all the way down to the valley floor during the afternoon and earlier evening hours but were only observed at the higher elevations during the early morning, before sunrise (see Figure 38 and 39). These regional flows were characterized by wind directions with westerly components, light to moderate speeds. Large discontinuities in the vertical profile of potential temperature would have limited the downward mixing of these regional airflow. Thus, regional airflows occurred above large temperature discontinuities.

Black Mountain (BLK, 9900 ft) was characterized by southwesterly winds between 5 and 10 knots throughout the entire case study period (see Figure 38). The potential temperature was 295 K at 1700 MST on 14 December 1981, only 3 degrees less than the 700 mb free atmospheric airmass over the study area. The potential temperature continued to cool slightly at BLK until 0300 MST 15 December 1981, at which time it began

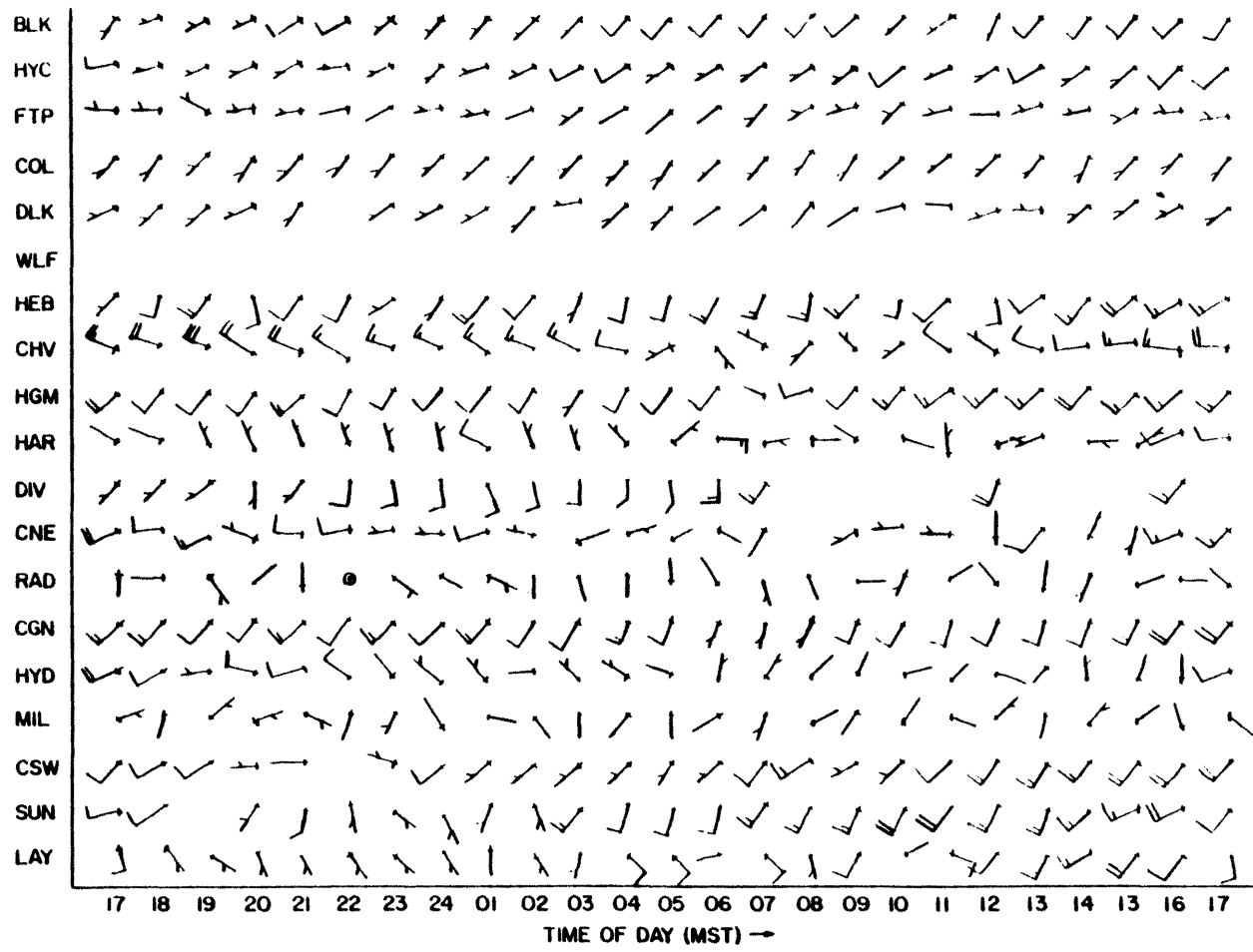


Figure 38. PROBE wind histories for 14 December 1981 at 1700 MST through 15 December 1981 at 1700 MST.

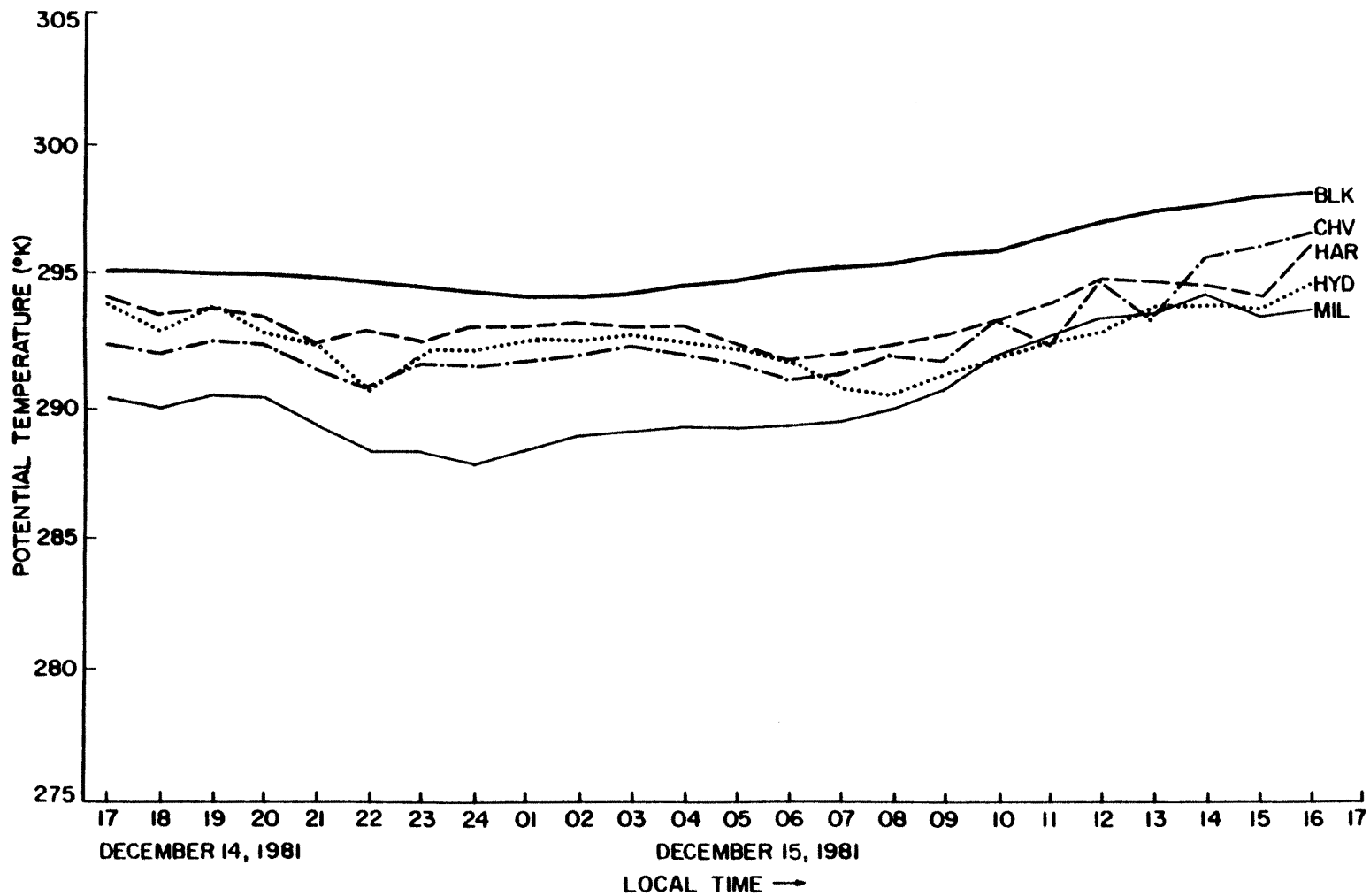


Figure 39. Potential temperature (kelvin) for selected PROBE stations (STP (10330 feet), BLK (9900 feet), HAR (7380 feet) and DIV (7130 feet)) from 14 December 1981 at 1700 MST to 15 December 1981 at 1700 MST.

to rise, indicating warm air advection. Figure 40 illustrates any temperature discontinuity during this case study occurred below the level of BLK (9900 feet). At 0700 MST BLK had a Froude number of 2.76.

Mt. Harris (HAR, 7380 ft), Mt. Chavez (CHV, 8000 ft) and Hayden (HYD, 6570 ft), all situated near the constriction in valley width, were all characterized by regional flows from 1700 MST (14 December, 1981) to 0400 MST (15 December, 1981), at which time a transition occurred (see Figure 38). Between 0400 and 0500 MST the wind direction at HAR (7380 ft) reversed to a down valley direction. The wind speed at HYD (6570 ft) was now calm. By 0600 MST the wind direction at CHV (8000 ft) reversed to downvalley flow. Figure 40 illustrates the decrease in the potential temperature at HAR (7380 feet) between the hours of 2200 MST and 0700 MST associated with an increase in the vertical extent of the lower temperature discontinuity. This corresponds to the same time period in which regional flows ended in this region. As the height of the temperature discontinuity increases, the vertical extent of valley flows increase and the downward extent of regional flows decreases. At 0700 MST, HAR had a Froude number of 0.86.

Valley flow features extended as high as 1450 feet above the valley floor (referring to CHV (8000 ft) at 0600 MST) and horizontally out to Craig but developed much later than in the first case study. The best evidence of valley flow was the flow reversal that occurred at 0300 MST at CNE (6910 ft) and at 0600 MST at HAR (7380 ft) and CHV (8000 ft) (see Fig 38). As compared to Case Study #1, valley flow features did not develop as quickly or as extensively in this case study. Figure 41 illustrates at 1700 MST the lower (SUN), middle (CSW) and upper valley (MIL) floor all had the same potential temperature. This lack of strong

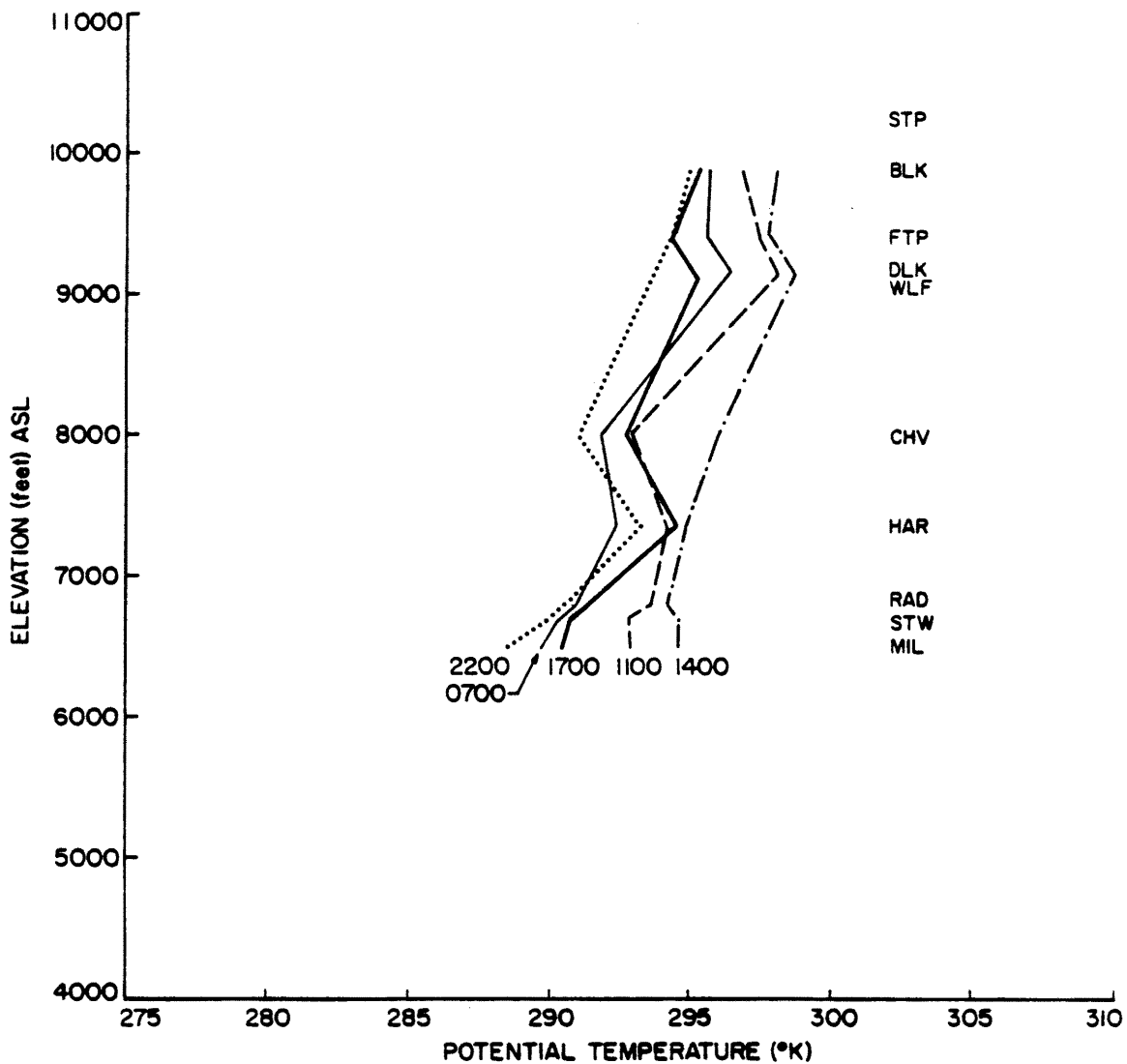


Figure 40. Vertical profile of potential temperature (kelvin) constructed from selected PROBE station data for 14 December 1981 at 1700 MST and 2200 MST to 15 December 1981 at 0700 MST, 1100 MST and 1400 MST. This time period is representative of synoptic Category #1.

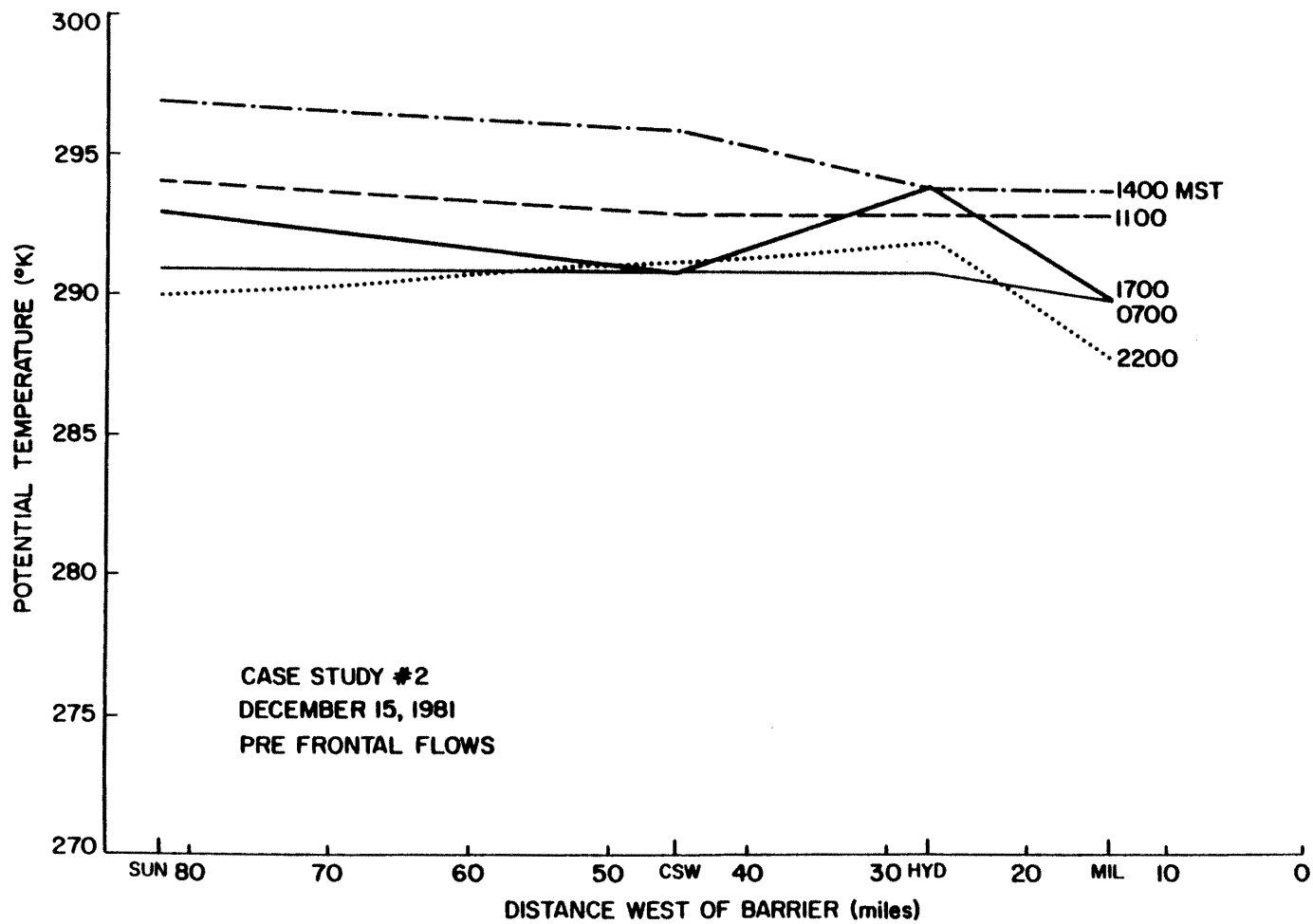


Figure 41. Time series of potential temperature (kelvin) for selected PROBE stations along the valley floor. Elevations are listed on the ordinate in feet (ASL). Distances west of the Barrier are listed along the abscissa in miles; the Barrier is located on the far right. Five hourly values are shown from 1700 MST on 14 December 1981 to 1400 MST on 15 December 1981.

thermal gradient continued throughout the night. Figure 40 illustrates the constructed temperature profile in the upper valley at 0700 MST. It is apparent that a large temperature discontinuity did not exist as at the same time in Case Study #1. Figure 41 also illustrates the lack of a thermal gradient favorable for up valley flows during the late morning and afternoon, thus up valley flows were not identified. Froude numbers at 0700 MST for some valley stations were 0.79 at RAD (6800 feet),), 0.76 at HYD (6570 feet) and 0.74 at SUN (6340 feet). Slope flows were not apparent during the case study.

3. 16 December 1981

a. Synoptic

A fast moving, pacific cold front passed through the study area between 1700 and 2000 MST on the 15 December 1981. Associated with this cold front was a strong low pressure system centered over the plains of northeast Colorado at 0200 MST (0900 GMT) 16 December 1981 (see Figure 42a). The 700 mb flow at 1700 MST 16 December 1981 (0000 GMT 17 December) is illustrated in Figure 42b which shows north-northwesterly flow of 10 knots was bringing down cold Canadian air; the potential temperature over the study area was 292 Kelvin. Figure 42c illustrates the 500 mb flow at 0500 MST (1200 GMT) 16 December 1981. Winds over the Yampa Valley were northwesterly at 50 knots and the potential temperature was 294 kelvin.

b. Summary of PROBE Observations

Synoptic winds were determined by linear interpolation of the 700 mb synoptic maps of 0000 GMT 16 December 1981 (1700 MST 15 December 1981, Figure 37b) and 0000 GMT 17 December 1981 (1700 MST 16 December 1981, Figure 42b). At 1700 MST 15 December 1981, synoptic level flows were characterized by north-northwesterly winds of 27 knots and a potential

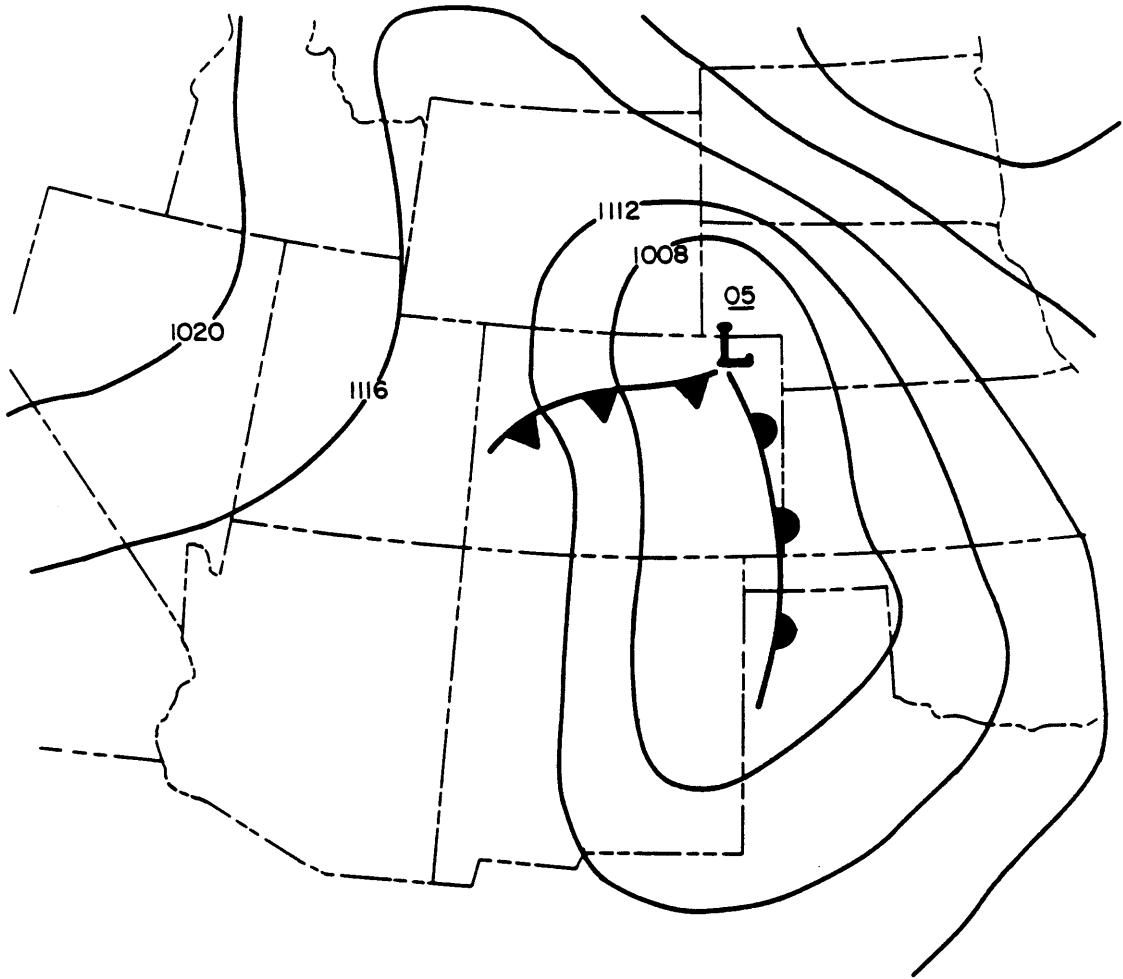


Figure 42a. Surface map depicting synoptic conditions of 16 December 1981 at 0200 MST.

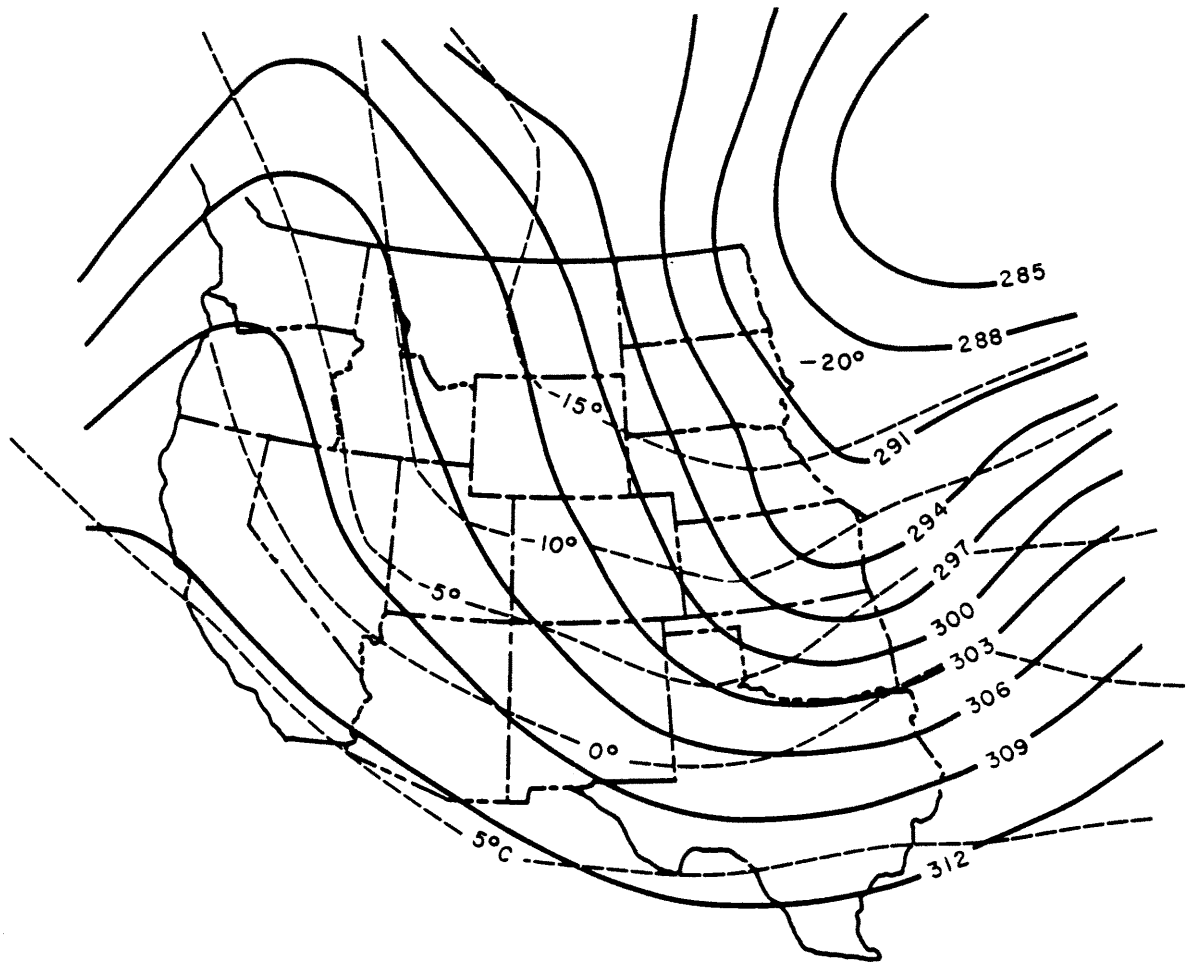


Figure 42b. 700 mb upper level map depicting synoptic conditions of 16 December 1981 at 0200 MST.

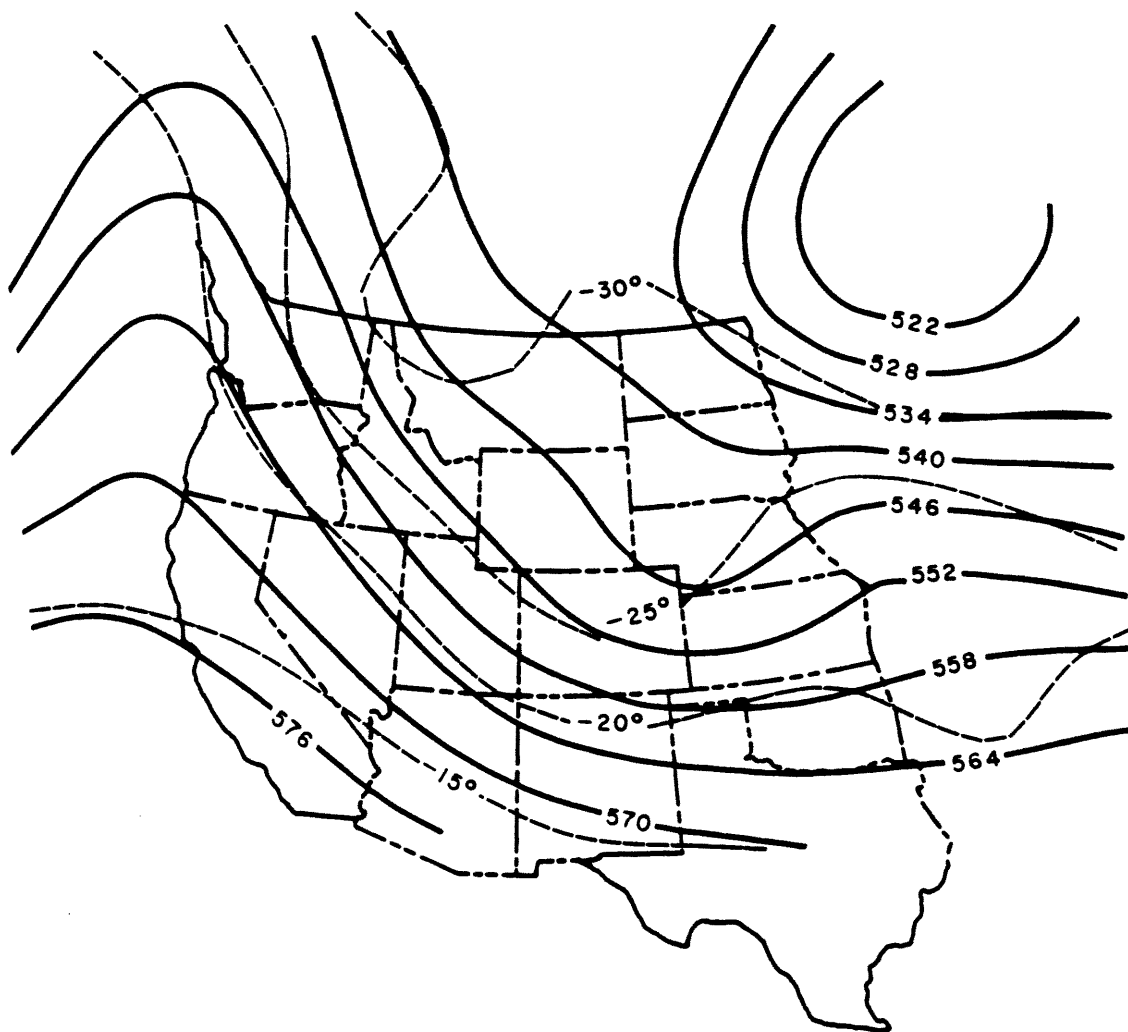


Figure 42c. 500 mb upper level map depicting synoptic conditions of 16 December 1981 at 0200 MST.

temperature of 301 kelvin. Twenty-four hours later, synoptic flows were characterized by north-northwesterly winds of 10 knots and a potential temperature of 292 kelvin. These characteristics were not observed for any PROBE station (see Figures 43 and 44).

Regional flows were characterized by winds responding to synoptic scale pressure gradients and modified by the terrain. Potential temperatures were colder than the synoptic scale airmass. Thus regional flows were westerly in direction with a wide range of wind speeds. They were most easily identified during nocturnal periods when valley flows were typically observed.

Regional flows occurred at most every station from the peaks of Black Mountain (BLK, 9900 ft) to the valley floor (SUN, 6340 ft). Westerly winds occurred at nearly every station prior to and after frontal passage (see Figure 43). Wind speeds varied from near calm (MIL 6530 ft) to 55 knots at CHV (8000 ft). Curiously, the highest wind speeds did not occur at the highest elevations but rather at the constriction in valley width at Mt. Chavez (CHV). Figure 45 illustrates the lack of any temperature discontinuities after frontal passage. The only significant change was a five to seven degree decrease in the entire temperature profile. Froude numbers for selected stations at 0700 MST on 16 December 1981 were 1.80 at BLK (9900 feet), 0.55 at HAR (7380 feet), 0.50 at RAD (6800 feet), 0.48 at HYD (6570 feet) and 0.47 at SUN (6340 feet).

Valley and slope flows were not observed during this case study. Figure 46 illustrates the potential temperature along the lower (SUN), middle (HYD) and upper (MIL) valley floor at five different time periods. The valley floor was lacking in any thermal gradients to force valley flows. Figure 45 illustrates the lack of any large vertical temperature

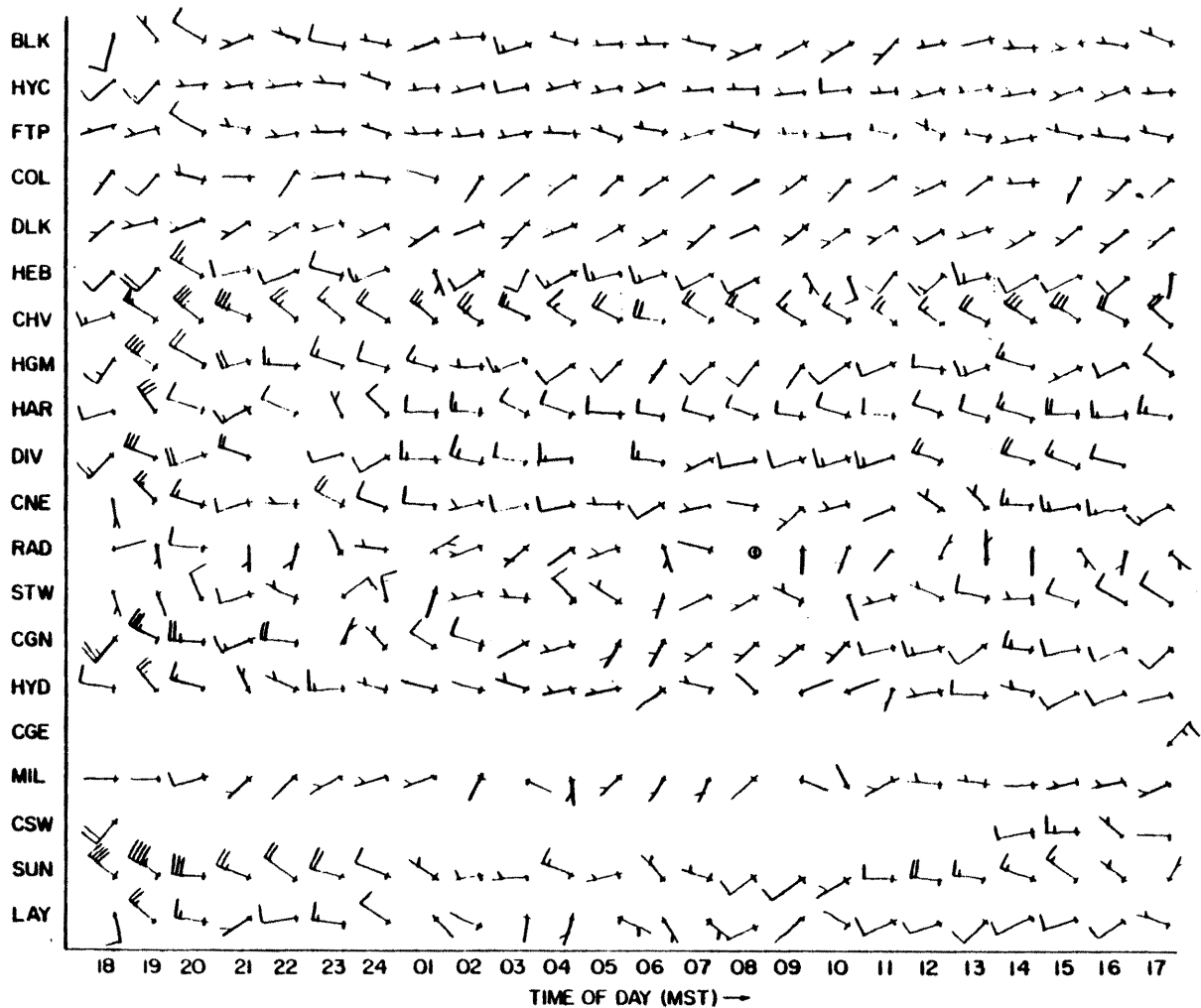


Figure 43. PROBE wind histories for 15 December 1981 at 1800 MST through 16 December 1981 at 1700 MST.

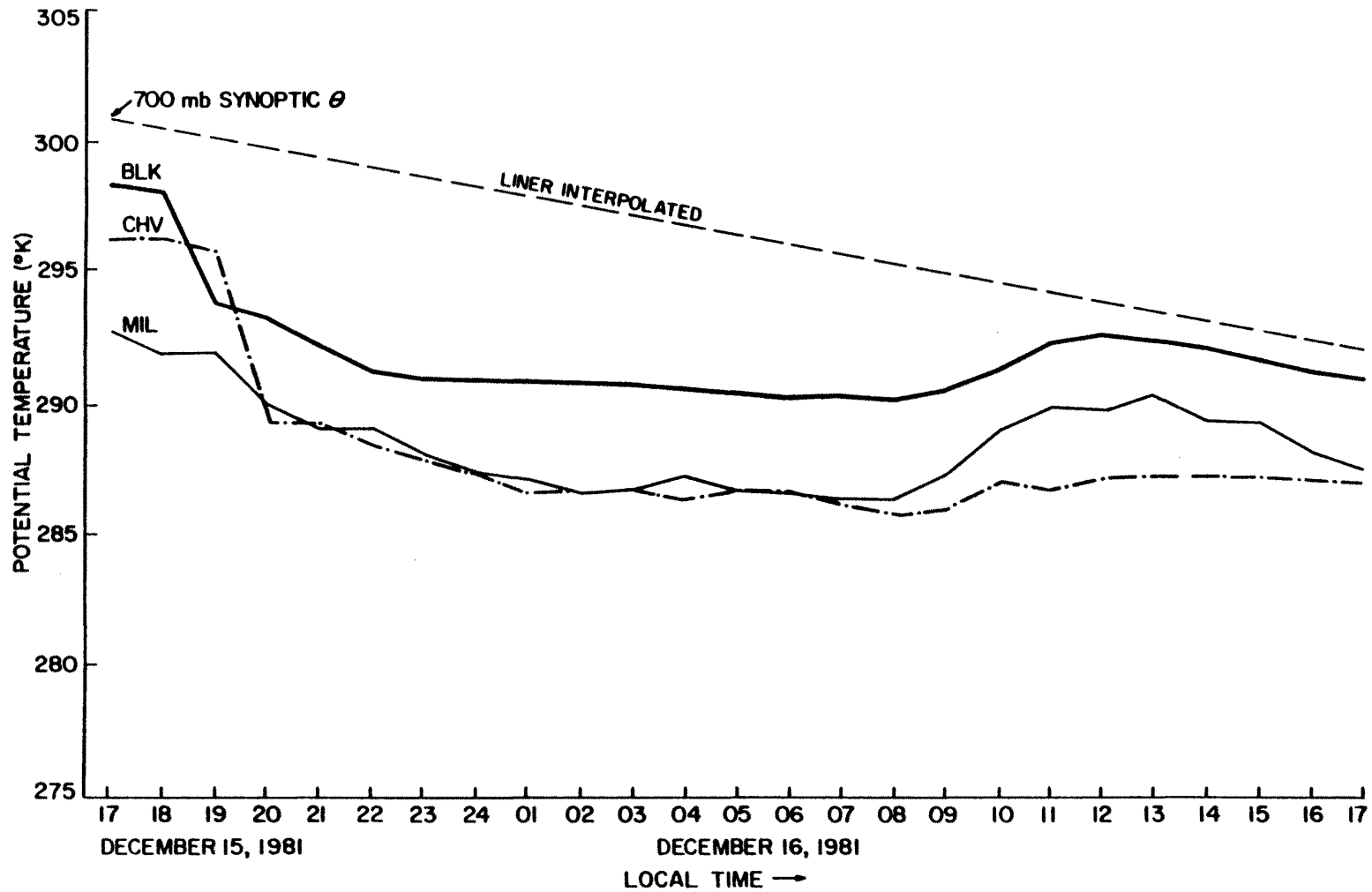


Figure 44. Potential temperature (kelvin) for selected PROBE stations (STP (10330 feet), BLK (9900 feet), HAR (7380 feet) and DIV (7130 feet)) from 15 December 1981 at 1700 MST to 16 December 1981 at 1700 MST.

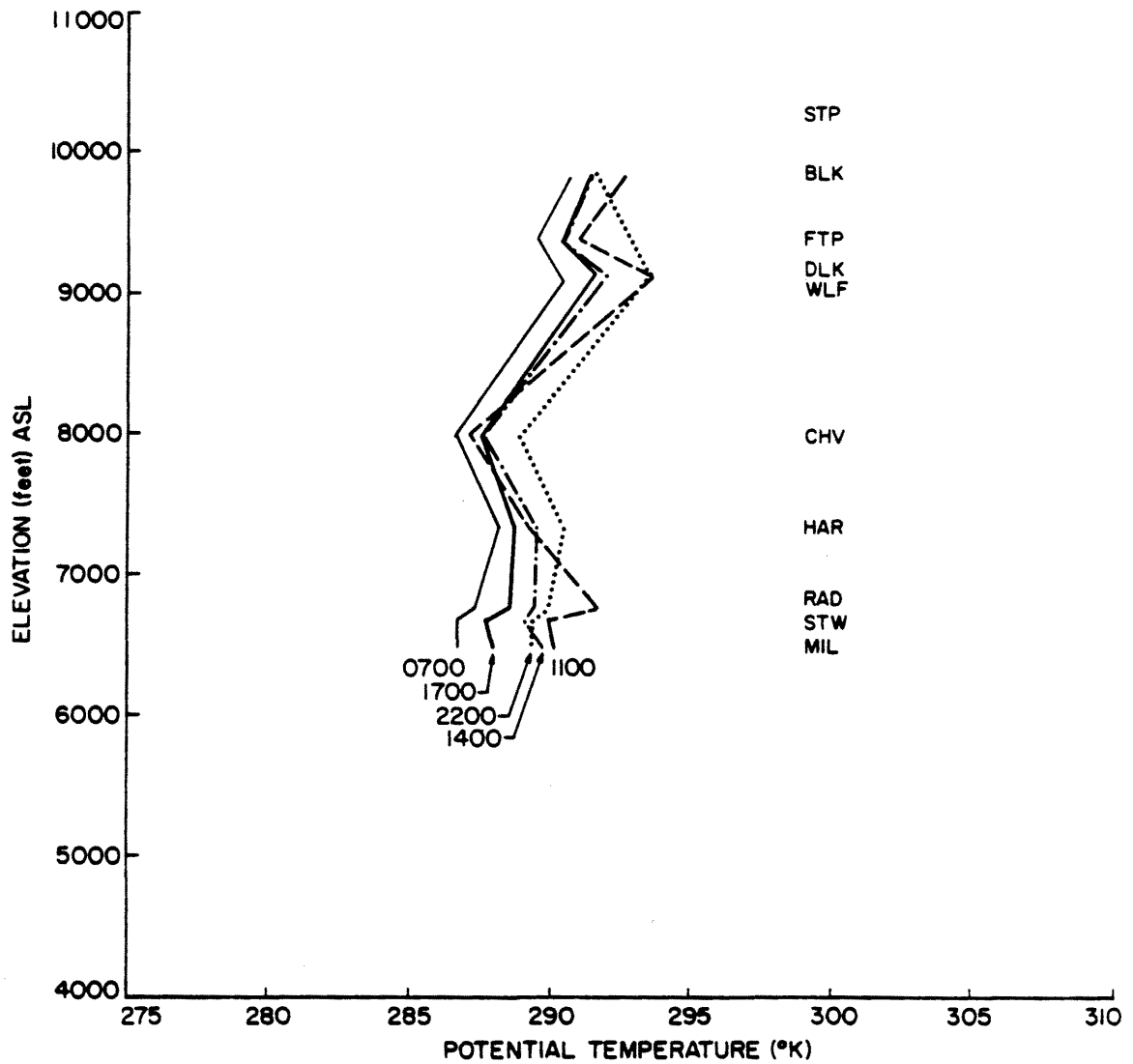


Figure 45. Vertical profile of potential temperature (kelvin) constructed from selected PROBE station data for 15 December 1981 at 2200 MST to 15 December 1981 at 0700 MST, 1100 MST, 1400 MST and 2200 MST. This time period is representative of synoptic Category #3.

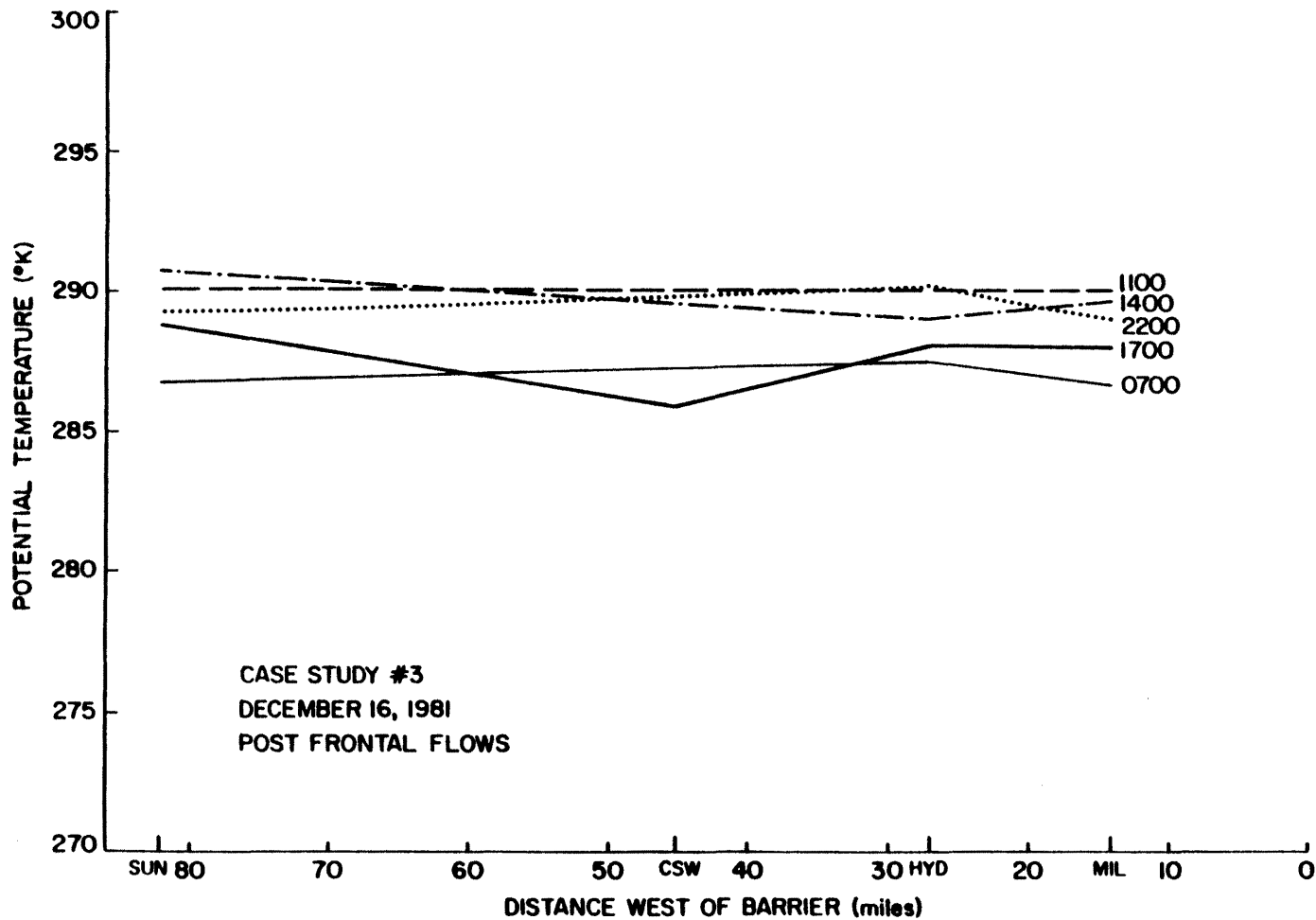


Figure 46. Time series of potential temperature (kelvin) for selected PROBE stations along the valley floor. Elevations are listed on the ordinate in feet (ASL). Distances west of the Barrier are listed along the abscissa in miles; the Barrier is located on the far right. Five hourly values are shown from 2200 MST on 15 December 1981 to 1700 MST on 16 December 1981.

gradients, thus supporting a well mixed valley atmosphere. Therefore, valley and slope flows were not observed during this case study.

VII. DISCUSSION AND CONCLUSIONS

The following picture of airflow evolves for the winter in the Yampa Valley under clear, stable conditions. A complexity of downvalley and downslope flows converge on the Valley from the upper valley blocking ridge and from the ridges on either side of the Valley. They start in the mid to late afternoon as the respective mountain slopes with different orientations become shaded from direct incoming solar radiation. This process accelerates after sunset. Slope flows from various parts of the Valley override or/and are overridden by other slope flows that have originated from other slopes or have started at different times due to variations in the times at which the respective slopes become shaded during the later afternoon.

The respective layers of slope flows converge into a broad, downvalley flow toward the west. Horizontal differences occur along the Valley's axis. The cold, stable, decoupled airmass in the Upper Valley remains essentially intact as can be noted from the observations at all of the Upper Valley floor stations (MIL, STW, and RAD). In the middle valley, downvalley flows are strongest with speeds up to seven knots. Broadening of the width in the western Valley decelerates and decreases the depth of the downvalley airflow.

Above the stable core within the valley, regional westward flows occur all the way up to the highest ridges during the evening and below this level during the day. During the afternoon from about 1400 to 1800

MST the free atmospheric synoptic flows penetrated to the highest peaks overlying the regional airflow. As the afternoon and evening progress, the stable valley core deepens, thus raising the effective height of the overlying layers of airflow. Hence, during the evening hours, regional westward flows extend up to and including the highest elevations.

Beginning at 1100 MST, the downvalley winds diminish in the broader western Valley and regional flows extend down to the Valley floor. During years with heavy snow accumulation, the cold, stable airmass in the upper Valley does not warm enough to thermally force up valley flows. A convergence zone is formed approximately 50 miles west of the barrier, between the westerly regional flows in the western portion of the Valley and the relatively calm winds in the upper portion of the Valley. By 1900 MST, downvalley flows are reestablished on the Valley floor and free atmospheric flows no longer extend down to this level.

The most significant difference in valley airflow between periods of clear weather with weak gradient winds and periods marked by an approaching cold front is the time at which the onset of downvalley flows occur. The 700 mb winds are stronger during periods characterized by an approaching cold front; therefore, more kinetic energy is available for vertical mixing. In addition, the upper valley floor remains much warmer than periods of clear weather with weak gradient winds. Only, until late at night does enough cooling occurred in the Upper Valley to establish an along valley temperature gradient strong enough to force a downvalley airflow. Once a decoupled valley atmosphere is established, downvalley flows develop, typically between 2200 and 0700 MST. These downvalley winds were light, less than 3.0 knots.

During the late morning, solar heating allows the convective boundary layer (CBL) to grow and eventually couple with the stronger (as compared to gradient winds during periods dominated by a polar high pressure system) westerlies aloft. Therefore, late morning and afternoon winds are stronger, 4 to 12 knots everywhere except the narrow upper Valley, where winds remain relatively calm. Within the upper Valley, excessive snowcover during the study period may account for the calm conditions observed during the afternoon hours. Solar energy is used to melt the snow cover; therefore, less energy is available for the sensible heating of the Upper Valley atmosphere. Conditions remain this way until radiational cooling develops a thermal gradient strong enough to force a downvalley airflow, around 2200 MST.

With the passage of a cold front in the Yampa Valley a dramatic difference in airflow occurs in the study area. Slope or valley flows are not observed after the passage of a cold front. Regional flows are observed everywhere. Westerly winds range from 1.0 to 13 knots, with the strongest winds occurring at the constriction in valley width. A well mixed CBL exists with no temperature discontinuities, thus allowing stronger winds aloft to mix down to the valley floor. Only slight decreases in wind speed occur during the nocturnal cooling period, but downslope and downvalley winds are not observed.

Comparing this study to the work of others, under clear and synoptically undisturbed periods the diurnal variations of airflow at the respective stations are only partially consistent with Whiteman's conceptual model (Whiteman, 1981). Whiteman states, "the diurnal forcing is realized as the nocturnal boundary layer builds in height due to a mass influx into the valley from downslope flows (Whiteman, 1981). This raises

the height of each successive layer of airflow. During the daylight hours, a mass divergence out of the valley occurs due to upslope flows, essentially lowering the top of the stable layer. This phenomenon allows for the apparent lowering of the entire wind structure profile".

Because upslope winds were not consistently observed and thermally forced upvalley winds were not observed at all, Whiteman's conceptual model does not fully explain the observed local circulations. Turbulent mixing, as presented by Banta (1982) offers a credible explanation of the observed boundary layer circulation. As sensible heating increases during the morning the surface layer warms greater than the atmosphere immediately above. This heating diminishes the surface stable layer allowing coupling of the surface layer with the CBL above. Because the CBL is deeper than the surface layer, it has more mass and its properties dominate those of the surface layer. Mixing of regional flows occurs down to the valley floor. This was typical of the western and middle portions of the Valley floor.

The formation of a well-mixed boundary layer depends on local heating. Vergeiner (1987) explains this as a function of geometry. As the topography varies so will the surface area to volume ratio. The greater the surface area, the greater the heating (or cooling) of the volume of the overlying airmass. This helps to account for the horizontal differences in observed flows between the upper and lower valley. Excessive snowcover in the Upper Valley prevents the development of thermally forced upvalley airflows.

The development, height, and destruction of the temperature inversion above the valley floor depends on the unique surface energy budget for that particular day. That energy budget varies with amount of

incoming solar radiation and moisture available for evaporation. So throughout the winter or in different years, the local circulations may differ but the general stratification should be similar. For example, during a year with an unusually low snowpack, more energy is available for the development of the convective boundary layer. This in turn may result in recoupling of the valley atmosphere with the free atmosphere and consequent daily "cleaning" of pollutants out of the upper valley. However, during years with an unusually heavy snowpack, the opposite may occur. With a greater amount of energy being contributed to evaporation, less energy is available for the development of the convective boundary layer. Consequently, there is not a daily destruction of the inversion layer and local pollutants would be trapped within the valley's calm and decoupled atmosphere.

The stratification of the entire data set into synoptically defined categories to reduce the variability of the observed valley airflows was only partially successful. While variability was decreased in some instances, standard deviations of the observed airflow still remained high. The use of Lindsey's extratropical cyclone model was only partially applicable. Only three out of five possible synoptic categories occurred in the study region and many remained undefined by this methodology. Of the three synoptic categories that did occur, there was good agreement between the synoptically stratified summaries and the case studies.

This study also described the change in valley airflow with the onset and passage of a cold front. The same principles applied as in the case of clear and synoptically undisturbed valley airflow but the strength of the individual parameters varied and accounted for differing local

circulations. This is promising for numerical modeling of these mesoscale mountainous circulations.

VIII. APPLICATIONS AND SUGGESTIONS FOR FUTURE RESEARCH

A. AIR POLLUTION

The largest population center of the Yampa Valley, Steamboat Springs is currently considering an ordinance which prohibits the burning of wood stoves and fireplaces, in a effort to improve air quality. Based upon the limited results of this study, such an ordinance would be very practical. If the lowest layer of the valley atmosphere does not warm enough to couple with the CBL then the local pollution of Steamboat Springs would reside in a stagnant airmass over the town. This situation occurred approximately 75%-80% of the period of study. However, during periods with little or no snow cover a wood burning ordinance may not be necessary. During these periods, the Upper Valley may couple with the overlying CBL allowing better ventilation within the valley.

The results of this study also illustrate how monitoring the meteorological conditions with just one weather station is limited and not fully representative of the meteorology of the entire location. Such practices are commonly used to gather data for use in atmospheric dispersion models. The single station data set can unjustly bias the dispersion characteristics of the model output. Therefore, site selection is critical in properly representing the local meteorology in high mountain valleys.

B. WEATHER MODIFICATION

According to Rauber (1985, Ph.D. dissertation on cloud systems of Northwestern Colorado), "shallow orographic cloud systems with cloud top temperatures greater than -20°C have been identified as the system with the largest potential for precipitation augmentation." He further described three zones to have persistent and significant amounts of liquid water including the region between cloud base and the -12°C level, and the region of strong orographic ascent, near the barrier. Because cloud bases often extend below the minimum flight level in this region, ground based seeding generators would have been most likely to effectively deliver artificial nuclei to this portion of the cloud if precipitation augmentation was desired.

The proper placement of these ground based seeding generators is critical to ensure proper delivery of artificial nuclei to the cloud. Rauber (1985) described the 16 December 1981 (Case study #3 in this thesis) as an orographic cloud system suitable for seeding with conditions as described above. Westerly winds occurred throughout the depth of the entire valley. In this case, placement of ground based seeding generators at any location upstream of the cloud would have been suitable, the higher the location the better assurance of delivery to cloud base. The upstream placement should allow enough time for ice nucleation, crystal growth and fall trajectory to occur within the desired watershed. Another possibility, as suggested by Rogers (personal communication), would be to release the artificial nuclei within a buoyant plume from elevated smoke stacks owned by the power plants located in Craig or Hayden.

C. SUGGESTIONS FOR FUTURE RESEARCH

Several areas associated with local circulations in mountainous terrain require further investigation to enhance knowledge of this field. Quantitative information on each parameter of the surface energy budget, including snowpack, would compliment the wind and temperature data for use in numerical simulation studies. To add to this, the use of sondings in all conditions, in the upper and lower valley is advised to more accurately depict stability and inversion heights. As a final investigation, atmospheric tracer studies under each of the synoptic categories would not only add to the understanding of transport but also provide useful information on dispersion within mountainous terrain.

To add to the understanding of boundary layer interaction with overlying clouds, corresponding aircraft data should be investigated. Microphysical data observed above the surface convergence zones should be inspected for indications of continental CCN introduction into what is typically a marine CCN distribution within these clouds. These areas above the surface convergence zones may also be inspected for regions of increased supercooled liquid water production within the cloud.

This study showed the valley floor to be decoupled from the free atmosphere at least 50% of the time. National Weather Service observations from mountain valleys often report data from a decoupled atmosphere which are used in synoptic analysis. This increases the possibility of misleading current weather analysis and forecasts. If the stations were placed high enough on the surface but above the temperature inversion, for example on top of ski areas, a more accurate depiction of synoptic weather would be attained.

From the large number of synoptic weather patterns that were not categorized into one of the five synoptic climatologies as proposed by Lindsey, another synoptic category is suggested. Often, a trough in the westerlies resides over the state of Colorado for periods of days. These conditions are characterized by high pressure on the west side of the continental divide and low pressure to the east side of the divide. This synoptic pattern is favorable to the formation of orographic clouds over the Park Range. Additional analysis is suggested to investigate the local circulations within the Yampa Valley during these conditions.

IX. SUMMARY

Using two months of wintertime meteorological data, surface flows within the Yampa Valley of Northwestern Colorado were investigated. The primary goals of this study were: 1) describe the climatology of these local circulations, 2) associate synoptic scale weather patterns with regional airflow patterns and 3) present case studies of observed airflow patterns.

Three different procedure were chosen to meet each of the three objectives. A climatological analysis of the two month data set was performed in which statistical methods were used to help define the mean flow and the associated variability. The data set was then stratified into synoptically defined subsets. A climatological analysis was conducted on each subset in which the mean flow and variability were defined. Finally, case studies were presented in which detailed descriptions of the regional flow were presented. One case study was presented for each synoptically defined subset.

Several interesting findings resulted from this research. First, different synoptic conditions were associated with distinct local circulations within the Valley environment. Under synoptically clear and undisturbed periods the Yampa Valley surface flows were found not to be horizontally homogeneous. Due to differing widths along the valley's axis, the surface area to volume of air ratio within each valley cross section forced its own unique temperature structure in that portion of the

valley. Hence, differing stability regimes contributed to heterogenous flows along the valley floor. Four levels of flow were resolved vertically ranging from synoptic flows at ridge level to valley or blocked flows at the valley floor.

The most significant difference in valley airflow between periods of clear, weather with weak gradient winds and periods marked by an approaching cold front was the time at which the onset of downvalley flows occurred. The 700 mb winds were stronger during periods characterized by an approaching cold front; therefore, more kinetic energy was available for vertical mixing. In addition, the upper valley floor remained much warmer than periods of clear weather with weak gradient winds. Only, until late at night did enough cooling occur in the Upper Valley to establish an along valley temperature gradient strong enough to force a downvalley airflow. Once a decoupled valley atmosphere was established, downvalley flows developed, typically between 2200 and 0700 MST. These downvalley winds were less than 3.0 knots.

During the late morning, solar heating allowed the convective boundary layer (CBL) to grow and eventually couple with the stronger (as compared to gradient winds during periods dominated by a polar high pressure system) westerlies aloft. Therefore, late morning and afternoon winds were stronger, 4 to 12 knots everywhere except the narrow upper Valley, where winds remain relatively calm. Within the upper Valley, excessive snowcover during the study period may have accounted for the calm conditions observed during the afternoon hours. Solar energy was used to melt the snow cover; therefore, less energy was available for the sensible heating of the Upper Valley atmosphere. Conditions remained this

way until radiational cooling produced a thermal gradient strong enough to force a downvalley airflow, around 2200 MST.

With the passage of a cold front in the Yampa Valley a dramatic difference in airflow occurred in the study area. No slope or valley flows occurred after the passage of a cold front. Regional flows were observed everywhere. Westerly winds ranged from 1.0 to 13.0 knots, with the strongest winds having occurred at the constriction in valley width. A well-mixed CBL existed with no temperature discontinuities, thus allowing stronger winds aloft to mix down to the valley floor. Only slight decreases in wind speed occurred during the nocturnal cooling period, but downslope and downvalley winds were not observed.

REFERENCES

- Atkinson, B.W., 1981: *Meso-scale Atmospheric Circulations*, Academic Press, New York, New York.
- Bader, D.C., 1985: Mesoscale boundary layer development over mountainous terrain. *Atmospheric Science*, Paper No. 396, Dept. of Atmos. Sci., Colorado State University, Fort Collins, CO, 251 pp.
- Banta, R.M., 1982: An Observational and Numerical Study of Mountain Boundary - Layer Flow, Paper No. 350, Dept. of Atmos. Sci., Colorado State University, Fort Collins, CO, 203 pp.
- Banta, R.M. and Cotton, W.R., 1981: An Analysis of the Structure of Local Wind Systems in a Broad Mountain Basin. *J. Appl. Meteor.*, 20, 1255-1266.
- Banta, R.M., 1984: Late-Morning Jump in TKE in the Mixed Layer over a Mountain Basin. *J. Atmos. Sci.*, 42, 407-411.
- Banta, R.M., 1984: Daytime Boundary-Layer Evolution over Mountainous Terrain. Part I: Observations of the Dry Circulations. *Mon. Wea. Rev.*, 112, 340-356.
- Banta, R.M., 1984: Daytime Boundary Layer Evolution over Mountainous Terrain. Part II: Numerical Studies of Upslope Flow Duration. *Mon. Wea. Rev.*, 114, 1112-1130.
- Burger, A., und Ekhardt, E., 1937: Uber die tagliche zirkulation dir atmosphere im bereiche der alpen. *Beitr. Geophys.*, 49, 341-367.
- Defant, F., 1951: Local winds. *Compendium of Meteorology*, T.M. Malone, Ed., Boston, American Meteorological Society, 655-672.
- Ekhardt, E., 1940: Zum klima der freien atmosphere uber USA. I,II, und III. *Beitr. Phys. Frei. Atmos.*, 26, 50-56, 77-106, 210-242.
- Lindsey III, C.G., 1980: Analysis of coastal wind energy regimes. M.S. thesis, Department of Enviromental Science, University of Virginia, Charlottesville, Virginia.
- Marwitz, J.D., 1980: Winter storms over the San Juan Mountains. Part I: Dynamical Processes. *J. Appl. Meteor.*, 19, 913-926.
- McNider, R.T., and Pielke, R.A., 1984: Numerical simulation of slope and mountain flows. *J. Clim. Appl. Meteor.*, 23, 1441-1453.

- Pielke, R.A., 1984: Mesoscale Meteorological Modelling, Academic Press, New York, New York.
- Prandtl, L., 1942: Fuhrer durch die stromungslehre. Braunschweig, F. Vieweg & Sohn, 373-375.
- Steinacker, R., 1984: Area height distribution of a valley and its relation to the valley wind. Beitr. Phys. Atm., 57, 64-71.
- Wagner, A., 1938: Theorie und beobachtung der periodischen gebirg swinde. Gerlands Beitr. Geophys. (Leipzig), 52, 408-449.
- Whiteman, C.D., 1980: Breakup of temperature inversions in Colorado mountain valleys. Atmospheric Science Paper No. 328, Dept. of Atmos. Sci., Colorado State University, Fort Collins, CO, 250 pp.
- Whiteman, C.D., 1981: Temperature inversion buildup in valleys of the Rocky Mountains. Proc. Second Conf. on Mountain Meteorology, AMS, Steamboat Springs, Colorado, Nov 9-12.
- Vergeiner, I., and Dreiseitl, E., 1987: Valley winds and slope winds-observations and elementary thoughts. Meteor. and Atmos. Phys., 264-286.
- Yu, C-H, and Pielke, R.A., 1986: Mesoscale air quality under stagnant synoptic cold season conditions in the Lake Powell area. Atmos. Envr., 20, 1751-1762.

APPENDIX A

APPENDIX

LIST OF TABLES

Table A-1. Statistical summary of west to east component winds for all days during the study period at 0700 MST.

Table A-2. Statistical summary of west to east component winds for all days during the study period at 1100 MST.

Table A-3. Statistical summary of west to east component winds for all days during the study period at 1400 MST.

Table A-4. Statistical summary of west to east component winds for all days during the study period at 1700 MST.

Table A-5. Statistical summary of west to east component winds for all days during the study period at 2200 MST.

Table A-6. Statistical summary of west to east component winds for all days in which synoptic Category #1 was present at 0700 MST.

Table A-7. Statistical summary of west to east component winds for all days in which synoptic Category #1 was present at 1100 MST.

Table A-8. Statistical summary of west to east component winds for all days in which synoptic Category #1 was present at 1400 MST.

Table A-9. Statistical summary of west to east component winds for all days in which synoptic Category #1 was present at 1700 MST.

Table A-10. Statistical summary of west to east component winds for all days in which synoptic Category #1 was present at 2200 MST.

Table A-11. Statistical summary of west to east component winds for all days in which synoptic Category #3 was present at 0700 MST.

Table A-12. Statistical summary of west to east component winds for all days in which synoptic Category #3 was present at 1100 MST.

Table A-13. Statistical summary of west to east component winds for all days in which synoptic Category #3 was present at 1400 MST.

Table A-14. Statistical summary of west to east component winds for all days in which synoptic Category #3 was present at 1700 MST.

Table A-15. Statistical summary of west to east component winds for all days in which synoptic Category #3 was present at 2200 MST.

Table A-16. Statistical summary of west to east component winds for all days in which synoptic Category #4 was present at 0700 MST.

Table A-17. Statistical summary of west to east component winds for all days in which synoptic Category #4 was present at 1100 MST.

Table A-18. Statistical summary of west to east component winds for all days in which synoptic Category #4 was present at 1400 MST.

Table A-19. Statistical summary of west to east component winds for all days in which synoptic Category #4 was present at 1700 MST.

Table A-20. Statistical summary of west to east component winds for all days in which synoptic Category #4 was present at 2200 MST.

Table A-1. Statistical summary of west to east component winds for all days during the study period at 0700 MST. Units are knots. For each PROBE station the average (AVG), standard deviation (STD), minimum value (MIN), maximum value (MAX), 75th percentile value (75%), median value (50%), 25th percentile value (25%) and number of observations (# OBS) are listed.

STN	AVG	STD	MIN	MAX	75%	50%	25%	# OBS
SUN	1.4	4.5	-8.7	13.6	2.9	.8	-1.2	59
DIV	.6	5.6	-8.6	16.9	4.5	-.2	-3.9	57
LAY	-.2	4.3	-8.9	19.2	.6	-.4	-2.1	57
CSW	1.4	5.8	-8.9	15.4	5.4	-.2	-3.3	42
CGN	1.9	6.2	-6.2	28.6	4.1	.0	-1.9	49
CGE	.4	7.4	-8.4	20.6	6.8	-2.7	-5.6	38
CNE	-1.0	7.2	-12.6	16.5	2.7	-2.7	-6.6	59
BLK	4.5	2.9	-.8	13.4	5.8	4.3	2.5	45
HYD	1.2	3.5	-6.0	13.2	2.1	.4	-1.4	52
HGM	4.3	4.5	-3.3	15.4	6.6	3.1	.4	51
CHV	4.7	8.4	-12.8	26.2	9.5	5.2	-1.9	45
HAR	-.4	8.2	-13.8	18.7	5.1	-2.7	-8.2	56
WLF	8.7	6.2	-7.2	20.4	11.7	9.1	3.9	22
MIL	.4	2.3	-7.8	9.5	1.0	.2	-.8	60
STW	.2	3.5	-8.4	11.1	.6	-.4	-2.1	51
RAD	.2	1.9	-2.9	8.2	.6	-.2	-1.0	58
BUR	2.1	2.3	-2.1	7.0	3.3	1.7	.4	26
STP	9.7	7.6	-14.4	24.5	14.4	10.5	6.0	32
DLK	.0	2.3	-3.9	4.5	1.4	.2	-2.7	39
FTP	2.1	2.3	-6.4	6.8	3.3	1.9	.8	59
HYC	3.1	2.3	-4.9	7.4	4.9	3.5	1.9	60
COL	1.0	1.2	-1.7	2.9	1.7	1.0	.0	56
HEB	5.1	7.4	-13.4	27.0	9.1	3.9	.8	60

Table A-2. Statistical summary of west to east component winds for all days during the study period at 1100 MST. Units are knots. For each PROBE station the average (AVG), standard deviation (STD), minimum value (MIN), maximum value (MAX), 75th percentile value (75%), median value (50%), 25th percentile value (25%) and number of observations (# OBS) are listed.

STN	AVG	STD	MIN	MAX	75%	50%	25%	# OBS
SUN	2.7	4.7	-9.1	17.9	4.9	1.7	.0	58
DIV	2.7	7.4	-10.1	17.7	7.6	1.4	-3.5	56
LAY	1.9	4.1	-8.6	15.6	3.1	1.0	-.2	56
CSW	.8	7.2	-11.7	15.2	6.6	-1.2	-5.2	47
CGN	2.3	5.8	-4.5	22.4	3.9	.6	-2.1	53
CGE	-.4	7.8	-9.3	16.9	6.2	-3.1	-7.2	36
CNE	.4	7.0	-10.1	17.1	3.7	-1.7	-4.5	57
BLK	4.9	3.3	-3.3	11.5	7.2	4.7	2.1	43
HYD	2.3	4.5	-8.6	14.8	2.1	1.0	-.4	54
HGM	4.9	5.2	-6.0	17.1	8.6	4.3	.6	53
CHV	3.7	9.1	-12.2	27.2	11.9	2.7	-4.5	48
HAR	-.6	8.9	-17.1	19.8	5.4	-3.5	-7.4	58
WLF	6.4	6.8	-13.6	17.3	10.9	6.4	2.7	26
MIL	.6	2.9	-5.1	8.9	1.0	.0	-1.2	60
STW	1.2	4.1	-7.8	17.1	.8	.0	-1.0	51
RAD	.8	2.3	-2.3	11.9	.8	.0	-.4	57
BUR	2.5	3.1	-5.8	11.7	3.7	1.9	.8	30
STP	7.4	8.0	-15.6	24.7	12.1	5.6	2.5	35
DLK	1.9	1.7	-3.1	5.1	3.1	1.9	.6	40
FTP	3.1	2.1	-6.6	6.4	4.5	3.1	1.9	59
HYC	4.3	3.3	-6.2	11.9	6.0	5.2	3.3	60
CUL	1.0	1.7	-3.5	4.5	2.1	1.2	-.2	58
HEB	4.5	8.7	-16.1	23.1	10.3	6.0	-1.2	59

Table A-3. Statistical summary of west to east component winds for all days during the study period at 1400 MST. Units are knots. For each PROBE station the average (AVG), standard deviation (STD), minimum value (MIN), maximum value (MAX), 75th percentile value (75%), median value (50%), 25th percentile value (25%) and number of observations (# OBS) are listed.

STN	AVG	STD	MIN	MAX	75%	50%	25%	# OBS
SUN	5.2	6.0	-6.8	22.7	8.2	4.1	.6	58
DIV	7.0	6.8	-5.2	20.8	10.9	7.6	1.7	51
LAY	5.2	5.6	-1.7	22.4	8.7	3.1	.6	59
CSW	4.7	8.0	-12.1	20.8	11.3	3.9	-2.7	48
CGN	5.4	6.8	-9.1	27.8	9.5	5.1	.0	53
CGE	4.5	9.1	-10.7	23.5	10.1	5.6	-5.1	38
CNE	5.2	8.4	-8.2	25.3	10.3	3.9	-2.3	60
BLK	6.0	2.9	-6.2	11.7	7.8	6.2	5.1	47
HYD	3.5	5.8	-4.5	18.9	7.8	.4	-.8	57
HGM	5.6	5.6	-1.9	19.2	9.9	2.9	.6	55
CHV	7.4	8.7	-8.6	29.2	12.4	6.4	.0	47
HAR	3.5	8.4	-9.7	21.2	9.1	2.3	-4.5	58
WLF	9.7	4.5	-4.9	19.1	10.7	8.9	7.6	29
MIL	1.2	3.7	-3.1	12.1	1.9	.0	-1.6	59
STW	2.1	5.2	-5.8	18.9	2.5	.4	-.6	52
RAD	.4	2.5	-4.3	8.9	.8	.0	-1.0	59
BUR	3.9	2.9	-.2	10.5	5.6	2.9	1.7	28
STP	10.1	6.8	-6.8	28.2	14.4	10.3	5.4	38
DLK	2.7	1.2	-.8	4.7	3.3	2.7	1.7	39
FTP	3.9	1.7	-4.3	8.7	4.9	3.7	3.1	58
HYC	5.4	2.5	-1.9	13.6	6.4	5.6	4.5	59
COL	1.6	1.6	-1.7	6.8	2.7	1.6	.4	58
HER	6.4	11.3	-18.1	35.2	13.6	8.7	1.7	59

Table A-4. Statistical summary of west to east component winds for all days during the study period at 1700 MST. Units are knots. For each PROBE station the average (AVG), standard deviation (STD), minimum value (MIN), maximum value (MAX), 75th percentile value (75%), median value (50%), 25th percentile value (25%) and number of observations (# OBS) are listed.

STN	AVG	STD	MIN	MAX	75%	50%	25%	# OBS
SUN	2.9	5.1	-6.6	18.1	5.1	1.6	.0	57
DIV	3.5	6.2	-5.6	19.8	6.6	1.7	-1.4	52
LAY	2.5	5.8	-6.8	16.1	5.4	.4	-1.6	56
CSW	3.7	7.4	-9.3	16.7	9.1	2.1	-2.9	45
CGN	4.7	7.2	-7.6	19.6	8.9	3.5	-1.9	49
CGE	2.1	8.2	-9.1	19.6	8.7	-1.9	-5.4	35
CNE	3.9	8.4	-9.3	21.6	10.9	1.9	-4.1	57
BLK	5.8	3.5	-1.9	14.2	8.2	5.4	2.9	45
HYD	4.9	6.0	-3.9	16.5	8.7	1.7	.0	55
HGM	6.0	5.6	-4.1	16.5	10.7	5.8	.6	51
CHV	7.8	8.9	-8.0	22.4	15.9	6.6	-1.4	43
HAR	4.1	8.6	-9.1	21.2	11.5	2.1	-4.5	55
WLF	10.9	4.7	1.6	20.4	14.0	10.7	7.2	27
MIL	1.0	2.9	-2.9	10.1	1.4	.2	-1.0	58
STW	1.0	4.1	-6.0	9.9	1.0	.0	-1.9	49
RAD	1.2	3.3	-3.7	14.4	1.4	.0	-.2	57
BUR	3.5	3.1	-1.6	11.5	4.9	2.1	1.2	26
STP	10.7	8.2	-5.8	27.0	17.5	8.9	3.9	34
DLK	.8	2.3	-3.7	5.6	2.3	.4	-1.2	38
FTP	2.5	1.9	-1.4	8.2	3.5	2.5	1.2	57
HYC	3.9	2.1	-.8	9.7	4.9	3.3	2.3	57
COL	1.6	1.2	-1.2	4.7	2.5	1.6	.8	58
HEB	5.2	9.5	-19.4	42.2	10.1	4.9	.6	58

Table A-5. Statistical summary of west to east component winds for all days during the study period at 2200 MST. Units are knots. For each PROBE station the average (AVG), standard deviation (STD), minimum value (MIN), maximum value (MAX), 75th percentile value (75%), median value (50%), 25th percentile value (25%) and number of observations (# OBS) are listed.

STN	AVG	STD	MIN	MAX	75%	50%	25%	# OBS
SUN	2.3	5.4	-7.8	18.7	3.9	1.2	-.8	57
DIV	1.6	5.1	-5.2	11.7	5.8	-.2	-3.3	51
LAY	1.6	5.2	-6.0	15.2	2.5	-.4	-1.9	56
CSW	1.4	7.2	-13.0	19.6	8.2	-1.2	-4.5	42
CGN	3.5	7.0	-6.8	19.8	7.2	.8	-2.1	48
CGE	1.9	8.0	-12.2	16.9	8.4	.2	-5.2	36
CNE	2.5	9.1	-12.2	23.9	11.1	1.0	-4.9	57
BLK	5.8	3.1	-.4	12.1	8.0	6.0	3.5	44
HYD	3.7	5.4	-2.3	17.5	7.2	1.0	-.4	56
HGM	6.4	5.6	-2.9	20.2	8.9	5.6	1.6	51
CHV	6.6	8.4	-9.5	23.9	12.6	6.8	1.0	44
HAR	2.1	8.9	-11.1	18.9	10.1	1.6	-7.4	54
WLF	9.1	7.0	-6.8	19.8	14.8	8.9	4.3	25
MIL	1.0	2.7	-3.7	11.5	1.6	.4	-.8	58
STW	.2	2.7	-5.6	7.2	.8	.0	-1.2	49
RAD	1.0	3.1	-2.5	15.4	.8	.0	-.6	57
BUR	2.7	2.9	-2.1	8.0	4.1	1.6	.2	23
STP	10.7	7.4	-4.1	29.2	15.4	9.1	5.4	31
DLK	.0	2.9	-4.3	5.8	1.4	-.2	-3.1	38
FTP	2.3	2.1	-1.0	8.0	3.3	1.9	.6	57
HYC	3.5	2.7	-1.9	13.0	5.1	3.7	1.9	58
COL	1.6	1.0	-.8	3.9	1.9	1.4	1.0	56
HEB	2.3	7.8	-14.8	20.6	8.6	1.9	-2.9	58

Table A-6. Statistical summary of west to east component winds for all days in which synoptic Category #1 was present at 0700 MST. Units are knots. For each PROBE station the average (AVG), standard deviation (STD), minimum value (MIN), maximum value (MAX), 75th percentile value (75%), median value (50%), 25th percentile value (25%) and number of observations (# OBS) are listed.

STN	AVG	STD	MIN	MAX	75%	50%	25%	# OBS
SUN	.8	4.7	-8.7	7.8	2.9	-1.2	-2.7	13
DIV	.8	4.1	-4.9	5.6	4.3	.6	-3.9	12
LAY	-1.4	3.3	-8.9	4.7	.4	-1.2	-3.7	13
CSW	1.6	4.9	-6.6	8.0	5.4	-.6	-4.1	11
CGN	-1.0	4.3	-6.2	10.5	.4	-2.7	-4.7	13
CGE	-.8	6.6	-6.0	12.2	-3.3	-4.7	-5.6	9
CNE	-2.1	3.7	-6.6	7.4	-.2	-2.9	-5.1	12
BLK	4.1	1.9	.0	5.8	5.4	3.9	1.7	9
HYD	-.6	2.5	-6.0	2.3	1.0	.0	-2.3	8
HGM	3.5	2.9	-.8	9.3	4.3	2.1	.0	11
CHV	5.2	7.2	-12.8	16.3	8.6	5.4	.6	11
HAR	-1.7	5.6	-11.9	8.6	2.1	-3.7	-6.2	12
WLF	4.9	6.4	-7.2	10.9	8.2	3.9	-7.2	5
MIL	-.6	2.3	-7.8	1.6	.8	-.6	-1.4	13
STW	.0	1.9	-3.3	5.2	.4	-.6	-1.2	13
RAD	.0	1.0	-1.4	2.3	.0	.0	-1.0	13
BUR	4.3	1.0	3.3	5.4	5.1	3.3	3.3	4
STP	8.2	7.8	-4.7	21.0	11.3	6.0	3.1	8
DLK	1.2	1.0	.0	3.3	1.4	1.0	.0	7
PIC	M	M	M	M	M	M	M	M
FTP	2.7	1.6	.8	5.8	3.5	2.3	1.2	13
HYC	4.3	1.4	1.6	6.4	5.1	4.3	3.1	13
COL	.8	1.0	-1.4	1.9	1.0	1.0	.0	12
HEB	4.3	8.2	-13.4	16.9	6.6	3.1	1.4	13

Table A-7. Statistical summary of west to east component winds for all days in which synoptic Category #1 was present at 1100 MST. Units are knots. For each PROBE station the average (AVG), standard deviation (STD), minimum value (MIN), maximum value (MAX), 75th percentile value (75%), median value (50%), 25th percentile value (25%) and number of observations (# OBS) are listed.

STN	AVG	STD	MIN	MAX	75%	50%	25%	# OBS
SUN	1.6	4.7	-9.1	10.9	2.3	1.4	-1.6	13
DIV	4.1	7.2	-5.2	17.7	8.7	.4	-3.5	10
LAY	.4	4.9	-8.6	9.7	.6	-.4	-1.9	13
CSW	1.2	7.2	-9.9	14.2	6.8	-2.9	-5.2	11
CGN	.8	3.7	-3.7	8.4	1.6	-.8	-2.7	13
CGE	-.8	5.1	-5.1	11.1	-1.7	-3.1	-3.9	8
CNE	-.8	4.1	-8.4	7.0	1.7	-2.1	-2.9	12
BLK	5.4	1.9	2.9	9.3	5.1	4.3	4.1	9
HYD	-.8	2.9	-8.6	1.4	.8	-.4	-2.3	10
HGM	5.6	4.5	-4.1	13.2	8.4	3.5	2.1	13
CHV	2.5	7.0	-12.1	16.3	6.4	3.3	-4.5	12
HAR	-2.5	8.0	-17.1	12.6	1.0	-2.7	-7.4	13
WLF	1.4	8.7	-13.6	8.4	6.2	4.5	-13.6	4
MIL	-.8	1.6	-5.1	1.0	.0	-.8	-1.2	13
STW	.0	5.2	-7.8	17.1	-.6	-.8	-1.0	13
RAD	.4	1.9	-1.6	6.6	.6	.0	-.6	13
BUR	3.1	1.9	.6	5.8	4.3	1.9	.6	4
STP	7.0	8.7	-6.6	24.7	11.3	4.5	.6	8
DLK	2.1	.8	1.7	3.9	1.9	1.7	1.7	7
PIC	M	M	M	M	M	M	M	M
FTP	3.7	1.4	1.9	5.6	4.5	3.1	2.3	13
HYC	4.3	2.9	-1.7	10.5	5.4	4.3	1.0	13
COL	.6	2.1	-2.9	4.5	2.1	.0	-1.9	12
HEB	2.3	9.7	-13.2	19.8	7.2	4.3	-10.1	13

Table A-8. Statistical summary of west to east component winds for all days in which synoptic Category #1 was present at 1400 MST. Units are knots. For each PROBE station the average (AVG), standard deviation (STD), minimum value (MIN), maximum value (MAX), 75th percentile value (75%), median value (50%), 25th percentile value (25%) and number of observations (# OBS) are listed.

STN	AVG	STD	MIN	MAX	75%	50%	25%	# OBS
SUN	6.8	4.3	-1.6	12.4	9.7	5.8	3.9	12
DIV	11.9	5.1	1.7	19.1	14.6	13.4	4.9	10
LAY	7.4	5.2	-1.7	14.8	9.1	7.8	2.1	13
CSW	7.6	8.0	-7.4	17.7	11.9	8.0	-3.7	11
CGN	6.8	5.2	-2.5	14.0	9.5	5.4	1.2	13
CGE	7.2	4.5	-1.2	13.6	10.1	6.4	2.7	8
CNE	8.6	8.9	-7.0	19.8	14.8	7.4	-1.4	12
BLK	6.0	1.2	4.3	7.8	6.8	6.0	4.9	10
HYD	3.9	7.2	-4.5	15.7	10.7	.0	-2.7	12
HGM	7.4	6.0	.4	19.2	11.9	3.9	.6	13
CHV	6.2	8.6	-8.6	23.1	11.3	6.0	-2.9	12
HAR	3.9	7.2	-7.2	19.4	8.4	1.9	-3.1	13
WLF	5.1	5.6	-4.9	12.2	6.4	4.3	-4.9	5
MIL	.6	4.1	-3.1	11.3	.0	-1.4	-1.7	13
STW	1.6	7.0	-5.8	18.9	.4	.0	-3.5	13
RAD	.8	2.3	-1.9	6.2	.4	.0	-1.0	13
BUR	5.4	3.1	.8	10.5	6.8	4.5	.8	6
STP	10.1	8.6	-3.9	28.2	9.3	8.2	4.7	9
DLK	2.9	.6	1.7	4.1	3.1	2.5	1.7	7
PIC	M	M	M	M	M	M	M	M
FTP	3.9	1.0	2.3	5.6	4.5	3.7	3.1	13
HYC	5.6	2.5	.4	9.5	6.0	5.2	2.9	13
COL	.8	1.0	-1.0	2.7	.8	.8	.0	12
HEB	3.7	13.6	-18.1	21.4	11.5	7.8	-14.6	13

Table A-9. Statistical summary of west to east component winds for all days in which synoptic Category #1 was present at 1700 MST. Units are knots. For each PROBE station the average (AVG), standard deviation (STD), minimum value (MIN), maximum value (MAX), 75th percentile value (75%), median value (50%), 25th percentile value (25%) and number of observations (# OBS) are listed.

STN	AVG	STD	MIN	MAX	75%	50%	25%	# OBS
SUN	3.1	5.2	-5.8	11.9	6.8	1.4	-3.7	11
DIV	5.4	6.6	-5.4	15.2	6.2	3.9	-1.4	10
LAY	2.1	4.5	-4.7	9.7	3.9	.2	-2.5	11
CSW	7.2	6.2	-7.6	15.9	10.7	6.4	1.9	11
CGN	6.0	6.8	-5.4	15.0	10.3	6.6	-5.1	10
CGE	4.5	4.7	-4.3	9.9	5.4	5.4	-4.3	6
CNE	8.2	8.0	-8.2	17.9	12.8	9.1	-2.9	10
BLK	6.8	1.9	3.9	9.7	8.2	6.2	3.9	10
HYD	7.6	6.0	-1.2	16.5	11.9	6.6	1.2	10
HGM	7.0	4.9	-4.1	13.2	10.7	6.6	1.7	11
CHV	9.5	10.7	-3.9	22.4	17.7	4.1	-3.7	11
HAR	6.0	9.5	-7.2	21.2	11.5	1.9	-6.2	11
WLF	12.4	4.1	5.8	17.5	15.0	11.1	5.8	6
MIL	.4	2.9	-2.5	6.4	.8	-1.0	-2.5	11
STW	1.9	4.5	-3.7	9.9	4.5	.2	-3.1	11
RAD	1.7	3.3	-.4	11.3	2.1	.0	.0	11
BUR	5.8	3.5	1.2	11.5	7.0	5.2	1.2	6
STP	6.0	8.0	-4.5	19.6	5.2	3.9	-1.0	8
DLK	2.5	1.7	.0	5.6	2.3	1.9	.0	5
PIC	M	M	M	M	M	M	M	M
FTP	3.5	1.9	.0	8.2	3.7	2.7	2.5	11
HYC	4.7	2.5	1.2	9.7	6.2	3.9	1.4	11
COL	1.9	1.7	-1.2	4.7	2.5	1.0	.0	11
HEB	1.7	12.2	-19.4	15.7	10.9	3.1	-15.2	11

Table A-10. Statistical summary of west to east component winds for all days in which synoptic Category #1 was present at 2200 MST. Units are knots. For each PROBE station the average (AVG), standard deviation (STD), minimum value (MIN), maximum value (MAX), 75th percentile value (75%), median value (50%), 25th percentile value (25%) and number of observations (# OBS) are listed.

STN	AVG	STD	MIN	MAX	75%	50%	25%	# OBS
SUN	3.3	6.6	-3.7	18.7	4.1	.0	-.4	12
DIV	2.5	5.1	-4.9	11.5	7.2	.8	-3.1	12
LAY	2.5	5.6	-6.0	12.1	6.8	-.4	-2.5	13
CSW	1.4	7.4	-9.1	11.5	8.0	-4.5	-5.6	10
CGN	4.9	8.0	-6.8	19.8	7.2	.8	-2.3	11
CGE	5.6	4.9	-3.1	12.6	5.4	5.2	-3.1	6
CNE	5.4	8.7	-8.7	20.0	10.7	3.7	-4.7	13
BLK	6.8	2.7	1.0	11.3	7.8	7.4	3.5	11
HYD	3.5	4.9	-2.3	12.6	6.2	1.0	-1.4	12
HGM	6.8	5.8	.8	20.2	7.4	5.2	1.2	12
CHV	7.8	8.2	-8.7	19.6	15.0	6.2	1.2	12
HAR	3.5	7.8	-5.4	15.2	8.4	-1.0	-4.5	13
WLF	8.0	6.2	-1.9	15.2	10.9	8.4	-1.9	6
MIL	.6	1.9	-2.9	4.7	1.2	.4	-1.0	13
STW	.0	2.1	-3.9	5.1	1.0	.0	-1.0	12
RAD	.0	1.4	-2.5	1.9	.8	.0	-1.0	12
BUR	4.1	2.9	1.4	8.0	2.1	1.6	1.4	5
STP	6.2	4.7	-4.1	11.9	9.1	6.0	-4.1	7
DLK	1.9	3.3	-2.7	5.8	5.4	.0	-2.7	7
PIC	M	M	M	M	M	M	M	M
FTP	3.1	2.7	-.6	8.0	2.9	1.7	.6	13
HYC	4.1	3.1	.0	13.0	3.7	3.1	2.9	13
COL	1.7	1.2	.4	3.9	1.7	1.2	.8	13
HEB	.0	10.1	-14.8	16.9	6.0	-2.5	-11.1	13

Table A-11. Statistical summary of west to east component winds for all days in which synoptic Category #3 was present at 0700 MST. Units are knots. For each PROBE station the average (AVG), standard deviation (STD), minimum value (MIN), maximum value (MAX), 75th percentile value (75%), median value (50%), 25th percentile value (25%) and number of observations (# OBS) are listed.

STN	AVG	STD	MIN	MAX	75%	50%	25%	# OBS
SUN	3.9	4.9	-5.1	13.6	6.0	2.1	.0	18
DIV	5.6	4.9	-1.0	16.9	7.4	4.5	1.9	17
LAY	1.6	6.0	-4.5	19.2	1.4	-.4	-3.3	18
CSW	4.7	6.8	-8.9	15.4	9.1	3.7	-2.9	15
CGN	5.8	7.8	-4.5	28.6	8.4	2.9	-.6	17
CGE	5.1	7.8	-5.6	20.6	8.6	6.8	-3.9	14
CNE	6.4	6.0	-7.2	16.5	9.9	5.4	2.3	18
BLK	4.9	2.9	.0	12.2	6.0	4.9	3.3	16
HYD	3.5	4.7	-1.9	13.2	4.3	1.9	.0	17
HGM	7.2	5.2	-3.3	15.4	10.5	6.4	3.3	17
CHV	10.5	7.4	-5.4	26.2	11.3	9.7	2.5	15
HAR	6.6	7.4	-10.5	18.7	10.1	8.4	-1.9	18
WLF	11.1	4.7	2.1	17.3	13.2	11.7	6.4	10
MIL	1.6	3.1	-2.1	9.5	1.2	.0	-.6	18
STW	1.2	5.1	-8.4	11.1	2.1	.0	-2.3	17
RAD	1.2	3.1	-2.9	8.2	1.0	.0	-1.7	17
BUR	2.7	2.1	.0	7.0	3.5	1.7	.4	11
STP	9.3	3.9	.0	14.4	10.7	9.9	6.0	11
DLK	1.6	1.9	-1.4	4.5	3.1	.4	-1.0	10
PIC	M	M	M	M	M	M	M	M
FTP	3.5	1.9	.2	6.8	4.5	3.3	1.9	17
HYC	4.1	1.7	-1.4	7.4	4.7	3.9	3.1	18
COL	1.2	1.4	-1.2	2.9	2.3	1.0	.0	18
HEB	7.6	6.0	-3.7	19.4	9.9	6.4	1.7	18

Table A-12. Statistical summary of west to east component winds for all days in which synoptic Category #3 was present at 1100 MST. Units are knots. For each PROBE station the average (AVG), standard deviation (STD), minimum value (MIN), maximum value (MAX), 75th percentile value (75%), median value (50%), 25th percentile value (25%) and number of observations (# OBS) are listed.

STN	AVG	STD	MIN	MAX	75%	50%	25%	# OBS
SUN	3.9	6.0	-5.6	17.9	6.6	4.1	-2.5	18
DIV	6.6	6.6	-6.8	17.3	9.7	7.0	3.7	16
LAY	4.5	4.9	-3.1	15.6	8.0	2.7	.0	16
CSW	5.2	6.8	-11.7	15.2	8.4	6.0	.0	15
CGN	6.2	7.2	-4.3	22.4	9.5	5.6	-1.0	17
CGE	3.9	8.7	-7.6	16.9	10.5	-2.7	-7.2	11
CNE	5.6	7.2	-5.6	17.1	10.9	7.4	-1.6	16
BLK	5.2	2.9	.6	10.7	7.0	4.3	2.5	14
HYD	5.8	5.4	-.4	14.8	9.9	5.4	.4	16
HGM	8.4	5.4	-.8	17.1	10.5	8.6	5.1	16
CHV	9.5	9.3	-6.0	27.2	14.2	11.9	-4.5	15
HAR	6.4	8.2	-8.2	19.8	10.9	6.6	-4.1	17
WLF	10.9	4.7	2.3	17.3	13.8	10.3	7.0	8
MIL	2.5	4.1	-3.1	8.9	4.9	.0	-.4	17
STW	3.1	4.3	-2.9	9.9	6.6	.8	-1.0	16
RAD	1.4	3.3	-1.7	11.9	1.2	.0	-.6	16
BUR	3.3	1.7	1.0	6.4	4.3	2.7	1.2	11
STP	10.3	6.2	.0	20.6	15.2	6.6	4.1	11
DLK	3.1	1.2	1.4	5.1	3.5	3.1	1.9	11
PIC	M	M	M	M	M	M	M	M
FTP	3.9	1.4	1.2	6.4	4.9	4.1	2.5	16
HYC	5.4	1.7	2.9	9.1	5.8	5.2	3.7	17
COL	1.9	1.0	.0	3.5	2.3	1.7	1.0	17
HEB	8.2	8.2	-12.1	23.1	11.7	9.3	4.3	16

Table A-13. Statistical summary of west to east component winds for all days in which synoptic Category #3 was present at 1400 MST. Units are knots. For each PROBE station the average (AVG), standard deviation (STD), minimum value (MIN), maximum value (MAX), 75th percentile value (75%), median value (50%), 25th percentile value (25%) and number of observations (# OBS) are listed.

STN	AVG	STD	MIN	MAX	75%	50%	25%	# OBS
SUN	7.4	7.6	-6.8	22.7	12.6	6.4	.0	18
DIV	8.6	7.2	-5.2	20.8	10.9	9.5	-2.5	14
LAY	8.2	5.6	.6	22.4	9.1	7.8	2.5	18
CSW	8.2	8.2	-12.1	20.8	12.8	8.6	3.7	16
CGN	8.2	9.1	-9.1	27.8	11.1	8.4	1.7	17
CGE	6.4	11.9	-10.7	23.5	13.4	5.2	-6.2	13
CNE	8.2	8.6	-8.2	25.3	10.3	8.4	2.9	18
BLK	6.2	2.1	1.9	11.7	7.2	5.8	5.1	16
HYD	7.0	6.2	-3.1	18.9	11.3	7.8	-.4	16
HGM	8.0	5.6	-1.9	18.5	11.3	7.2	2.5	17
CHV	11.7	9.3	-5.2	29.2	15.4	10.3	4.3	15
HAR	8.0	7.6	-7.4	21.2	12.6	8.4	1.0	17
WLF	12.4	3.7	6.8	19.1	14.0	10.7	8.4	10
MIL	2.5	4.3	-2.9	12.1	5.8	.4	-2.1	17
STW	3.3	5.2	-4.7	14.6	5.6	.6	.0	17
RAD	1.0	3.1	-3.5	8.9	1.9	.0	-1.4	17
BUR	4.3	2.3	1.7	9.1	4.1	2.9	1.7	9
STP	10.5	6.4	-.4	20.8	14.4	10.3	.0	11
DLK	3.5	1.0	1.6	4.7	3.9	3.7	2.5	11
PIC	M	M	M	M	M	M	M	M
FTP	4.7	1.4	.8	7.2	5.4	4.7	4.1	16
HYC	5.4	1.6	1.7	9.5	5.8	5.6	4.5	17
COL	1.9	1.0	.0	3.5	2.7	1.7	1.2	17
HEB	10.7	9.7	-12.2	35.2	14.4	9.3	5.6	17

Table A-14. Statistical summary of west to east component winds for all days in which synoptic Category #3 was present at 1700 MST. Units are knots. For each PROBE station the average (AVG), standard deviation (STD), minimum value (MIN), maximum value (MAX), 75th percentile value (75%), median value (50%), 25th percentile value (25%) and number of observations (# OBS) are listed.

STN	AVG	STD	MIN	MAX	75%	50%	25%	# OBS
SUN	5.6	5.4	-1.0	16.9	9.3	4.7	.0	12
DIV	10.3	5.8	2.7	19.8	10.1	7.4	5.2	10
LAY	7.2	6.4	-2.7	16.1	11.1	7.8	.0	13
CSW	7.8	7.0	-8.6	16.7	12.6	6.8	1.9	11
CGN	9.7	5.4	-2.7	18.7	13.8	8.4	6.4	12
CGE	7.0	9.3	-9.1	19.6	10.7	5.2	-6.6	9
CNE	8.6	6.6	-4.7	17.9	11.3	8.4	5.4	13
BLK	5.4	3.7	1.4	12.6	6.0	3.7	1.7	11
HYD	8.2	5.6	-1.0	15.2	12.6	8.7	.0	12
HGM	9.1	4.1	3.5	16.5	12.4	7.2	5.6	12
CHV	12.6	7.4	-5.1	19.6	16.3	15.6	5.2	10
HAR	10.7	7.8	-5.6	19.2	15.7	12.2	4.5	13
WLF	11.7	3.5	6.8	16.9	12.6	11.9	6.8	6
MIL	3.1	3.3	-.8	10.1	4.3	.8	.0	13
STW	2.7	4.3	-3.3	9.5	5.6	.4	.0	12
RAD	1.6	3.3	-3.3	10.9	1.9	.0	.0	13
BUR	5.1	2.7	1.4	9.1	4.9	3.3	1.4	5
STP	15.4	5.1	8.4	21.4	20.6	14.8	8.4	8
DLK	2.3	1.9	-.8	4.7	3.7	1.7	-.8	7
PIC	M	M	M	M	M	M	M	M
FTP	3.5	1.4	.4	6.0	4.3	3.3	2.7	12
HYC	4.9	1.9	1.9	8.7	5.1	4.1	3.3	13
COL	1.9	1.2	.0	3.7	2.7	1.7	.6	13
HEB	11.5	11.1	.6	42.2	12.6	6.2	4.1	13

Table A-15. Statistical summary of west to east component winds for all days in which synoptic Category #3 was present at 2200 MST. Units are knots. For each PROBE station the average (AVG), standard deviation (STD), minimum value (MIN), maximum value (MAX), 75th percentile value (75%), median value (50%), 25th percentile value (25%) and number of observations (# OBS) are listed.

STN	AVG	STD	MIN	MAX	75%	50%	25%	# OBS
SUN	5.6	5.8	-6.4	14.4	9.9	4.9	.2	13
DIV	5.2	4.1	-2.7	11.7	7.6	5.8	-.8	10
LAY	2.5	6.4	-6.0	15.2	5.2	-1.2	-1.7	13
CSW	5.8	4.9	-5.4	10.7	9.1	6.0	1.0	11
CGN	7.4	6.0	-2.5	16.7	11.7	7.0	-.4	11
CGE	7.0	8.7	-12.2	16.9	11.3	8.4	-6.8	10
CNE	8.9	6.6	-3.3	17.1	13.4	11.1	3.1	13
BLK	4.7	3.7	-.4	12.1	5.8	2.5	.0	11
HYD	6.8	6.2	-1.6	17.5	11.7	5.8	.0	13
HGM	9.5	4.1	1.7	15.4	13.6	8.0	6.4	12
CHV	10.1	6.0	-3.9	21.0	12.6	9.7	6.8	10
HAR	7.8	6.2	-9.1	13.8	11.5	7.8	5.1	13
WLF	13.2	4.7	4.3	16.7	15.9	13.0	4.3	5
MIL	2.9	3.7	-3.7	11.5	3.5	2.5	.0	13
STW	1.2	3.1	-5.6	6.8	3.9	.6	-.6	12
RAD	1.9	3.1	-1.0	10.1	2.5	.0	-.8	13
BUR	6.0	1.0	5.1	7.0	5.1	5.1	5.1	2
STP	15.4	5.2	8.4	24.3	16.5	14.6	8.4	7
DLK	1.6	1.4	-.6	3.3	2.1	.8	-.6	7
PIC	M	M	M	M	M	M	M	M
FTP	3.5	1.7	.6	7.6	3.7	3.3	1.9	12
HYC	4.9	1.9	.8	7.4	6.0	4.5	3.1	13
COL	1.7	.8	.6	3.1	2.3	1.6	1.2	13
HEB	5.1	6.4	-7.4	15.6	9.5	4.1	-1.7	13

Table A-16. Statistical summary of west to east component winds for all days in which synoptic Category #4 was present at 0700 MST. Units are knots. For each PROBE station the average (AVG), standard deviation (STD), minimum value (MIN), maximum value (MAX), 75th percentile value (75%), median value (50%), 25th percentile value (25%) and number of observations (# OBS) are listed.

STN	AVG	STD	MIN	MAX	75%	50%	25%	# OBS
SUN	-.2	3.5	-7.6	5.2	1.6	.8	-1.4	20
DIV	-3.5	3.3	-8.6	4.7	-2.7	-4.5	-5.2	20
LAY	-.8	2.1	-8.0	1.9	.6	-.6	-1.9	18
CSW	-2.7	1.6	-4.5	.4	-2.1	-3.5	-4.3	11
CGN	-.6	2.3	-5.4	3.9	.0	-1.0	-2.9	11
CGE	-5.6	1.9	-8.4	-2.1	-4.7	-6.0	-8.0	8
CNE	-6.2	4.1	-12.6	3.9	-4.9	-7.6	-9.1	21
BLK	5.2	3.3	.6	13.4	5.8	5.1	2.5	14
HYD	.0	1.7	-2.7	3.7	.8	.0	-1.6	19
HGM	2.3	2.7	-1.2	8.2	3.1	1.2	-.8	15
CHV	-1.9	6.0	-9.9	8.0	1.6	-5.4	-9.3	11
HAR	-6.4	5.6	-13.8	5.1	-3.7	-8.4	-11.7	18
WLF	9.7	6.4	3.3	20.4	9.1	6.2	3.3	4
MIL	-.2	1.0	-1.6	1.4	.4	-.8	-1.2	21
STW	-.4	2.7	-2.7	8.4	.0	-1.0	-2.5	13
RAD	-.4	1.0	-1.7	2.3	.0	-.6	-1.0	20
BUR	1.0	2.5	-2.1	6.0	1.7	1.0	-1.6	8
STP	13.2	4.1	6.2	18.7	16.1	11.5	6.2	7
DLK	-1.6	2.1	-3.9	2.9	.0	-2.7	-3.3	18
PIC	M	M	M	M	M	M	M	M
FTP	1.0	1.6	-2.1	3.7	1.6	1.2	.0	21
HYC	2.1	2.3	-1.4	6.6	3.5	2.1	-.2	21
COL	.8	1.0	-1.7	2.5	1.6	.8	.0	19
HEB	4.1	8.2	-12.2	27.0	7.2	2.3	.0	21

Table A-17. Statistical summary of west to east component winds for all days in which synoptic Category #4 was present at 1100 MST. Units are knots. For each PROBE station the average (AVG), standard deviation (STD), minimum value (MIN), maximum value (MAX), 75th percentile value (75%), median value (50%), 25th percentile value (25%) and number of observations (# OBS) are listed.

STN	AVG	STD	MIN	MAX	75%	50%	25%	# OBS
SUN	1.7	2.9	-6.0	8.4	2.7	1.2	.0	19
DIV	-.8	6.6	-10.1	14.4	1.4	-1.0	-7.4	21
LAY	1.0	1.6	-2.3	3.7	1.4	.6	.0	21
CSW	-4.7	3.7	-11.3	2.7	-3.3	-5.8	-8.4	15
CGN	.2	4.3	-4.5	14.4	.6	.0	-3.3	15
CGE	-4.9	6.4	-8.7	14.6	-6.4	-7.8	-8.7	11
CNE	-3.5	5.1	-9.7	11.5	-2.1	-4.5	-8.4	21
BLK	4.9	3.5	.0	11.5	7.2	5.2	.0	15
HYD	1.0	2.3	-3.3	9.7	1.6	1.0	-.6	21
HGM	2.5	4.5	-6.0	11.3	4.7	1.0	.0	16
CHV	-1.4	8.4	-12.2	17.7	-1.6	-3.9	-8.0	13
HAR	-5.6	6.6	-12.8	16.3	-6.0	-7.4	-9.5	20
WLF	5.4	5.6	-8.0	13.8	8.4	4.1	2.3	11
MIL	-.2	1.6	-2.3	5.2	.0	-.8	-1.6	22
STW	.4	2.5	-2.5	8.7	.2	.0	-1.7	14
RAD	.4	1.9	-2.3	8.0	.6	.4	.0	20
BUR	1.2	4.1	-5.8	11.7	1.0	.6	-1.2	11
STP	7.4	6.6	-5.8	21.4	11.1	5.1	2.3	11
DLK	1.2	1.7	-2.5	4.9	2.1	.6	-.4	18
PIC	M	M	M	M	M	M	M	M
FTP	2.7	1.7	-.8	5.4	3.7	3.1	1.2	22
HYC	4.1	3.5	-3.3	11.9	5.8	5.1	.0	22
COL	.8	1.7	-1.9	4.1	1.9	.4	-1.0	21
HEB	2.3	8.7	-16.1	14.4	7.4	3.7	-1.4	22

Table A-18. Statistical summary of west to east component winds for all days in which synoptic Category #4 was present at 1400 MST. Units are knots. For each PROBE station the average (AVG), standard deviation (STD), minimum value (MIN), maximum value (MAX), 75th percentile value (75%), median value (50%), 25th percentile value (25%) and number of observations (# OBS) are listed.

STN	AVG	STD	MIN	MAX	75%	50%	25%	# OBS
SUN	2.5	3.5	-5.1	9.1	5.1	2.9	.0	20
DIV	4.1	5.4	-5.1	15.7	7.6	3.5	-1.4	19
LAY	1.6	3.1	-1.6	11.1	1.9	.6	-.8	20
CSW	-.8	5.1	-8.2	13.4	1.0	-2.7	-5.1	15
CGN	1.7	3.7	-2.7	10.9	1.4	.4	-1.0	15
CGE	-.6	7.6	-8.4	15.6	.8	-5.1	-7.4	10
CNE	.6	4.7	-6.8	14.0	1.6	.0	-3.3	22
BLK	7.4	2.1	3.7	11.5	8.9	6.8	5.8	16
HYD	.8	2.7	-1.9	9.5	1.2	-.4	-.8	21
HGM	2.1	3.9	-1.9	12.8	2.7	1.4	-1.6	17
CHV	2.7	5.1	-4.9	14.2	6.2	1.0	-1.7	12
HAR	-1.6	6.8	-9.7	16.3	-.8	-4.3	-6.6	20
WLF	9.5	2.5	6.0	16.7	10.3	8.7	7.6	11
MIL	.0	1.7	-2.9	3.9	.8	.0	-1.6	21
STW	1.0	2.1	-2.1	6.6	.6	.0	-.4	14
RAD	.0	1.9	-3.5	7.8	.0	.0	-.8	21
BUR	2.9	2.7	.0	9.3	3.3	1.7	.4	10
STP	11.1	5.2	1.9	20.8	13.6	10.5	6.6	13
DLK	2.1	1.4	-.8	3.9	3.1	1.9	1.0	17
PIC	M	M	M	M	M	M	M	M
FTP	3.7	1.7	.8	8.7	4.9	3.3	2.3	21
HYC	5.6	2.5	.0	13.6	6.4	5.4	4.3	21
COL	2.1	2.1	-1.7	6.8	3.5	2.3	.0	21
HEB	4.5	10.9	-16.7	28.0	9.7	6.4	1.2	21

Table A-19. Statistical summary of west to east component winds for all days in which synoptic Category #4 was present at 1700 MST. Units are knots. For each PROBE station the average (AVG), standard deviation (STD), minimum value (MIN), maximum value (MAX), 75th percentile value (75%), median value (50%), 25th percentile value (25%) and number of observations (# OBS) are listed.

STN	AVG	STD	MIN	MAX	75%	50%	25%	# OBS
SUN	1.7	3.7	-6.6	9.9	3.7	1.4	.0	24
DIV	1.2	4.1	-5.6	12.2	2.5	1.0	-1.9	22
LAY	.6	5.1	-6.8	15.2	1.0	-1.0	-2.7	22
CSW	-.4	6.2	-9.3	14.8	.4	-1.2	-4.3	16
CGN	.8	5.6	-7.6	17.1	1.6	-.2	-3.3	17
CGE	-.4	7.4	-8.0	16.9	-1.9	-4.7	-5.4	13
CNE	.0	7.2	-7.4	21.6	.6	-3.3	-4.7	24
BLK	5.6	4.1	-1.9	14.2	8.2	5.4	1.6	17
HYD	2.5	5.1	-3.5	16.5	2.1	1.2	-.6	23
HGM	3.5	6.0	-2.9	16.3	5.8	1.7	-1.6	18
CHV	2.5	5.4	-8.0	11.5	5.8	.6	-1.4	12
HAR	-.2	6.4	-9.1	15.0	1.4	-1.7	-5.1	21
WLF	11.3	4.9	1.6	20.4	13.2	10.7	7.0	11
MIL	.8	2.7	-2.9	8.0	1.2	.0	-1.0	24
STW	-.4	3.1	-6.0	9.9	.0	-.8	-1.9	16
RAD	1.2	3.9	-1.9	14.4	.0	.0	-.6	23
BUR	1.9	2.3	-1.6	8.2	2.1	1.7	.0	12
STP	11.7	8.9	-5.8	27.0	17.5	7.8	2.5	11
DLK	-.4	2.3	-3.7	4.9	1.2	-1.0	-2.3	21
PIC	M	M	M	M	M	M	M	M
FTP	1.9	1.7	-1.4	5.8	2.5	1.6	1.0	24
HYC	3.1	1.6	-.8	6.0	4.1	3.3	1.9	23
COL	1.4	1.0	.0	3.9	1.9	1.4	.8	24
HEB	3.3	6.0	-11.3	15.9	5.2	3.9	-1.0	24

Table A-20. Statistical summary of west to east component winds for all days in which synoptic Category #4 was present at 2200 MST. Units are knots. For each PROBE station the average (AVG), standard deviation (STD), minimum value (MIN), maximum value (MAX), 75th percentile value (75%), median value (50%), 25th percentile value (25%) and number of observations (# OBS) are listed.

STN	AVG	STD	MIN	MAX	75%	50%	25%	# OBS
SUN	.4	3.1	-7.8	5.8	2.3	.4	-2.3	21
DIV	-1.0	3.7	-5.2	8.2	-.6	-2.3	-3.5	19
LAY	.4	3.7	-3.5	13.2	.4	-.8	-1.9	19
CSW	-2.1	4.5	-9.1	11.1	-2.1	-3.5	-4.5	13
CGN	.0	5.6	-5.1	19.1	.8	-1.7	-3.9	15
CGE	-2.5	6.0	-8.0	14.0	-1.9	-5.2	-6.8	12
CNE	-2.3	8.6	-12.2	23.9	-2.7	-4.7	-8.2	20
BLK	6.2	2.1	1.9	9.3	7.6	5.8	4.3	15
HYD	1.9	5.1	-2.1	17.1	1.2	.6	-.4	20
HGM	4.5	5.2	-2.9	18.1	6.8	3.7	.4	16
CHV	1.7	7.6	-9.5	14.2	6.0	-2.5	-8.6	11
HAR	-3.7	7.4	-11.1	14.2	-4.5	-7.4	-9.1	18
WLF	8.2	8.9	-6.8	19.8	13.0	5.6	-5.4	9
MIL	.0	1.9	-2.5	8.4	.4	.0	-.8	21
STW	-.4	1.7	-3.3	4.9	.0	.0	-1.6	14
RAD	.8	3.5	-1.6	15.4	.6	.0	-.8	21
BJR	1.7	3.1	-2.1	7.8	2.3	.0	-1.2	11
STP	9.7	10.1	-4.1	29.2	12.1	3.7	.6	9
DLK	-1.2	2.5	-4.3	5.4	.4	-1.9	-3.5	19
FIC	M	M	M	M	M	M	M	M
FTP	1.2	1.7	-1.0	5.8	1.9	.4	.0	21
HYC	2.7	2.5	-1.9	8.4	4.1	2.3	.4	21
COL	1.2	.8	-.8	2.5	1.9	1.2	1.0	19
HEB	2.5	7.2	-14.6	20.6	3.5	1.4	-2.7	21